

NPS-67-84-016

NAVAL POSTGRADUATE SCHOOL
Monterey, California

AD-A151 476



THESIS

SUPersonic MISSILE SEEKER LENS SYSTEM
USING GRADIENT INDEX MATERIAL
FOR FIRST ELEMENT LENS

by

David S. Davidson

September 1984

DTIC FILE COPY

Thesis Advisor:

Allen E. Fuhs

DTIC
ELECT

MAR 22 1985

D

Approved for public release; distribution unlimited.

Prepared for: Defense Advanced Research Projects Agency
1400 Wilson Boulevard
Arlington, VA 22209

85 03 11 113

NAVAL POSTGRADUATE SCHOOL
Monterey, California

Commodore R. H. Schumaker
Superintendent

David A. Schrady
Provost

This thesis prepared in conjunction with research
supported in part by Defense Advanced Research Projects
Agency under DARPA Order 4035.

Reproduction of all or part of this report is authorized.

Released as a
Technical Report by:

J. N. Dyer
J. N. DYER
Dean of Science and Engineering

UNCLASSIFIED

SECURITY CLASSIFICATION OF THIS PAGE (When Data Entered)

REPORT DOCUMENTATION PAGE		READ INSTRUCTIONS BEFORE COMPLETING FORM																				
1. REPORT NUMBER NPS-67-84-016	2. GOVT ACCESSION NO. A151476	3. RECIPIENT'S CATALOG NUMBER																				
4. TITLE (and Subtitle) Supersonic Missile Seeker Lens System Using Gradient Index Material for First Element Lens	5. TYPE OF REPORT & PERIOD COVERED Master's Thesis; September 1984																					
7. AUTHOR(s) David S. Davidson	6. PERFORMING ORG. REPORT NUMBER NPS-67-84-016																					
9. PERFORMING ORGANIZATION NAME AND ADDRESS Naval Postgraduate School Monterey, California 93943	10. PROGRAM ELEMENT, PROJECT, TASK AREA & WORK UNIT NUMBERS N62271&WE40007																					
11. CONTROLLING OFFICE NAME AND ADDRESS Naval Postgraduate School Monterey, California 93943	12. REPORT DATE September 1984																					
14. MONITORING AGENCY NAME & ADDRESS (if different from Controlling Office) COL Rene Larriva, USMC Defense Advanced Research Projects Agency 1400 Wilson Boulevard Arlington, Virginia 22209	13. NUMBER OF PAGES 119																					
16. DISTRIBUTION STATEMENT (of this Report) Approved for public release; distribution unlimited.	15. SECURITY CLASS. (of this report) Unclassified																					
17. DISTRIBUTION STATEMENT (of the abstract entered in Block 20, if different from Report)	15a. DECLASSIFICATION/DOWNGRADING SCHEDULE																					
18. SUPPLEMENTARY NOTES <i>cont'd p 4)</i> <i>Include:</i>	<table border="1"> <tr> <td colspan="2">Accession For</td> </tr> <tr> <td>NTIS</td> <td>GRANT <input checked="" type="checkbox"/></td> </tr> <tr> <td colspan="2">DTIC TAB</td> </tr> <tr> <td colspan="2">Unannounced</td> </tr> <tr> <td colspan="2">Justification</td> </tr> <tr> <td colspan="2">By</td> </tr> <tr> <td colspan="2">Distribution/</td> </tr> <tr> <td colspan="2">Availability Codes</td> </tr> <tr> <td>Dist</td> <td>Avail and/or Special</td> </tr> <tr> <td colspan="2">A-1</td> </tr> </table>		Accession For		NTIS	GRANT <input checked="" type="checkbox"/>	DTIC TAB		Unannounced		Justification		By		Distribution/		Availability Codes		Dist	Avail and/or Special	A-1	
Accession For																						
NTIS	GRANT <input checked="" type="checkbox"/>																					
DTIC TAB																						
Unannounced																						
Justification																						
By																						
Distribution/																						
Availability Codes																						
Dist	Avail and/or Special																					
A-1																						
19. KEY WORDS (Continue on reverse side if necessary and identify by block number) Missile Sensors, Conical Optics, Missile Aerodynamics, Conical Lens, Projectile Aerodynamics, Guided Projectile, Gradient Refractive Index, and Ray Tracing. Lens Design.																						
20. ABSTRACT (Continue on reverse side if necessary and identify by block number) The design of a supersonic missile seeker lens system using an aerodynamically efficient lens, a scanning mirror and detector was accomplished through the use of ray-tracing routines. The design of the first element lens uses a gradient in refractive index to overcome the severe handicap that the pointed shape imposes. This problem has been previously solved for positive orientations of the center of symmetry of the Gradient Refractive Index (GRIN) material with respect to the lens. In this study the negative																						

UNCLASSIFIED

SECURITY CLASSIFICATION OF THIS PAGE (When Data Entered)

20. Abstract continued

orientations are resolved and the lens studies for a range of orientations and strengths of gradient. The best lens is then used in conjunction with the mirror and detector in a ray-tracing scheme. Such a system was found to be feasible and worthy of further study.

S N 0102-LF-014-6601

UNCLASSIFIED

SECURITY CLASSIFICATION OF THIS PAGE (When Data Entered)

Approved for public release; distribution unlimited.

SUPersonic MISSILE SEEKER LENS SYSTEM
USING GRADIENT INDEX MATERIAL
FOR FIRST ELEMENT LENS

by

David S. Davidson

Captain, Canadian Forces

B. Eng (Engineering Physics), Royal Military College, 1976

Submitted in partial fulfillment of the
requirements for the degree of

MASTER OF SCIENCE IN PHYSICS

and

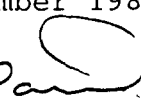
MASTER OF SCIENCE IN ENGINEERING SCIENCE

from the

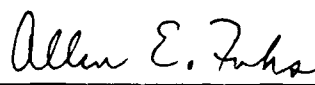
NAVAL POSTGRADUATE SCHOOL

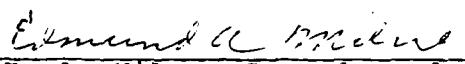
September 1984

Author:


David S. Davidson

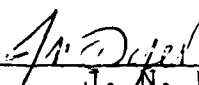
Approved by:


Allen E. Fuhs, Thesis Advisor


E. A. Milne, Second Reader


G. E. Schacher, Chairman
Department of Physics


M. F. Platzer, Chairman
Department of Aeronautics


J. N. Dyer

Dean of Science and Engineering

ABSTRACT

The design of a supersonic missile seeker lens system using an aerodynamically efficient lens, a scanning mirror and detector was accomplished through the use of ray-tracing routines. The design of the first element lens uses a gradient in refractive index to overcome the severe handicap that the pointed shape imposes. This problem has been previously solved for positive orientations of the center of symmetry of the Gradient Refractive Index (GRIN) material with respect to the lens. In this study the negative orientations are resolved and the lens studies for a range of orientations and strengths of gradient. The best lens is then used in conjunction with the mirror and detector in a ray-tracing scheme. Such a system was found to be feasible and worthy of further study.

TABLE OF CONTENTS

I.	INTRODUCTION15
A.	OUTLINE OF LENS DESIGN TO DATE15
B.	GRADIENT REFRACTIVE INDEX (GRIN)15
C.	AIM AND INTENT OF THIS STUDY16
II.	GRIN LENS DESIGN18
A.	GRIN LENS DESIGN METHODOLOGY18
B.	GRIN RAY PATH DESCRIPTION19
C.	GRIN LENS GEOMETRY22
D.	RAY MATCHING24
III.	NEAR-RADIAL LINES30
A.	DESCRIPTION OF DIFFICULTY30
B.	PRELIMINARY WORK - IMPROVING THE ITERATION SCHEME31
C.	PRELIMINARY WORK - DOUBLE PRECISION36
D.	PRELIMINARY WORK - CHECKING ACCURACY36
E.	FIRST PROPOSED SOLUTION - STRAIGHT LINES38
F.	SECOND PROPOSED SOLUTION - REDUCED EQUATION38
G.	THIRD PROPOSED SOLUTION - MARCHAND METHOD45
H.	FOURTH PROPOSED SOLUTION - ANGLE IN TERMS OF RADIUS46
IV.	GRADIENT INDEX SEEKER LENS RAY TRACE RESULTS53
A.	FRONT SURFACE ACCURACY53
B.	SPOT SIZE RESULTS53

C.	SELECTION OF A BEST LENS	53
V.	MIRROR AND DETECTOR SYSTEM	57
A.	DESCRIPTION OF SYSTEM	57
B.	LENS TO DETECTOR RAY TRACE	58
1.	Ray Direction Exiting Lens	58
2.	Point of Intersection on Mirror	58
3.	Ray Direction Exiting Mirror	61
4.	Ray Count on Detector	64
C.	MIRROR AND DETECTOR SYSTEM RESULTS	65
VI.	CONCLUSIONS AND RECOMMENDATIONS	68
A.	CONCLUSIONS	68
B.	RECOMMENDATIONS	69
APPENDIX A:	PROGRAM GISL LISTING	70
APPENDIX B:	PROGRAM CHECK LISTING	93
APPENDIX C:	PROGRAM DETPLOT LISTING	103
APPENDIX D:	DETECTOR SIGNAL	107
LIST OF REFERENCES		117
INITIAL DISTRIBUTION LIST		118

LIST OF TABLES

LIST OF FIGURES

2.1	GRIN Lens Coordinate System and Parameters (from Carr)	20
2.2	GRIN Lens and Ray Geometry	23
2.3	Ray Path Showing Improper Matching and Minimum Radius	26
2.4	Ray Path Radius and Angle	27
2.5	Ray Matching Regions	29
3.1	Ray Trace Showing Region of Radial Lines . . .	32
3.2	Newton-Raphson Iteration Geometry	34
3.3	Newton-Raphson Logic Flowchart	35
3.4	Geometry of Accuracy Check - Forward Ray Trace	39
3.5	Expanded View of Front Surface - Straight Line Method	41
3.6	Reduced Equation Implementation	44
3.7	Radius and Angle Relation	48
3.8	Angle in Terms of Radius Iteration Logic Flowchart	50
3.9	Angle in Terms of Radius Iteration Geometry . .	51
3.10	Diverging Iteration - Forward Ray Trace	52
4.1	Spot Size Results - ALFAP = 0.3 Radians	56
5.1	Lens, Mirror and Detector System	59
5.2	Detector Signal	60
5.3	Reflection of Ray on Mirror	63

LIST OF SYMBOLS

SYMBOL	FORTRAN EQUIVALENT	DEFINITION	UNITS
a	A	index function parameter	nondimensional
arg	ARG	argument of arcsine function in GRIN ray equation	nondimensional
\arg_0	-	argument of initial arcsine function in GRIN ray equation	nondimensional
b	B	index function parameter	nondimensional
c	C	ray matching constant	radians
D_{lm}	D1	ray geometrical distance from lens to mirror	nondimensional
D_{nd}	D2	ray geometrical distance from mirror to detector	nondimensional
DT	DETP	position of detector along x-axis	nondimensional
e	E	GRIN ray trace constant	nondimensional
K	CK	x-direction cosine of ray from lens to mirror	nondimensional
K'	CKK	x-direction cosine of ray from mirror to detector	nondimensional
ℓ_0	-	z-direction cosine of ray at initial point	nondimensional
L	CL	y-direction cosine of ray from lens to mirror	nondimensional
L'	CLL	y-direction cosine of ray from mirror to detector	nondimensional

M	CM	z-direction cosine of ray from lens to mirror	nondimensional
M'	CMM	z-direction cosine of ray from mirror to detector	nondimensional
M_0	-	Marchand reduced integral expression	-
MP	MIRP	position of mirror pivot point on x-axis	nondimensional
n	-	index of refraction	nondimensional
n_0	-	index of refraction at initial point of GRIN ray	nondimensional
\vec{n}	-	vector normal to mirror plane	-
n_x	-	x-component of vector normal to mirror plane	nondimensional
n_y	-	y-component of vector normal to mirror plane	nondimensional
p_0	-	x-direction cosine of GRIN ray at initial point	nondimensional
q_0	-	y-direction cosine of GRIN ray at initial point	nondimensional
r	RAD	radius to ray from center of symmetry	nondimensional
r_0	RO	radius to ray at initial point	nondimensional
r'	RP	first guess radius in iteration scheme	nondimensional
r''	-	second guess radius in iteration scheme	nondimensional
r'''	-	third guess radius in iteration scheme	nondimensional
r_{fs}	-	radius to front surface	nondimensional

\dot{r}_{fs}	-	derivative with respect to nondimensional angle of radius to front surface	
r_{gr}	-	radius to GRIN ray	nondimensional
\dot{r}_{gr}	-	derivative with respect to angle of radius to GRIN ray	nondimensional
\vec{r}_i	-	ray vector incident to mirror	nondimensional
r_{xi}, r_{yi}	-	components of ray vector incident to mirror	nondimensional
\vec{r}_r	-	ray vector reflected off mirror	-
r_{xr}, r_{yr}	-	components of ray reflected off mirror	nondimensional
R	R	radius from x-axis to outermost point of inner surface	nondimensional
R_z	Rzero	radius to edge of GRIN material	nondimensional
U	U	angle of incident radiation for lens construction	radians
x_d	XD	x-component of ray at detector	nondimensional
x_m	XM	x-component of ray at mirror	nondimensional
x_0	XO	x-component of ray at lens inner surface	nondimensional
y_d	YD	y-component of ray at detector	nondimensional
y_m	YM	y-component of ray at mirror	nondimensional

y_0	YO	y-component of ray at lens inner surface	nondimensional
z_d	ZD	z-component of ray at detector	nondimensional
z_m	ZM	z-component of ray at mirror	nondimensional
z_0	ZO	z-component of ray lens inner surface	nondimensional
ϵ	EPSILON	sign function of GRIN ray equation	-
ψ	PSI	angle between GRIN ray and radians radial arm from center of symmetry	
ψ_0	PSIO	angle between GRIN ray and radians radial arm at initial point	
θ	THETA	angle from x-axis to radius	radians
θ_0	THETO	angle from x-axis to initial point	radians
θ_L	-	angle for GRIN ray part to left of part of minimum radius	radians
θ_R	-	angle for GRIN ray part to right of point of minimum radius	radians
θ'	THETAP	angle of first guess in iteration scheme	radians
θ''	-	angle to second guess in iteration scheme	radians
θ'''	-	angle of third guess in iteration scheme	radians
θ_m	THETM	angle from x-axis to plane of mirror	radians

ACKNOWLEDGEMENTS

The author would like to thank Distinguished Professor Allen E. Fuhs for his guidance and perserverance during the writing of this thesis.

The author would also like to express his gratitude to his wife Johanne for her support during this period.

I. INTRODUCTION

A. OUTLINE OF LENS DESIGN TO DATE

The design of a 'pointed' aerodynamically efficient missile seeker lens has been the topic of a number of studies. Frazier [Ref. 1], and Terrell [Ref. 2], first studied the idea of using a pointed lens as a means of obtaining some degree of aerodynamic efficiency. They also introduced the idea of using Gradient Refractive Index (GRIN) material in order to overcome the difficulties in imaging imposed by the odd shape. Amichai [Ref. 3], and Carr [Ref. 4], studied the GRIN concept in more detail, Amichai by defining the outer surface as a cone and solving for the inner surface and Carr by defining the inner surface as a cone and solving for the outer. The main reference for this author's study was drawn from Carr's work and a review of that thesis would be helpful if the reader seeks a more detailed background from that given in the next few pages.

B. GRADIENT REFRACTIVE INDEX (GRIN)

Although the theory for GRIN has been developed and known for some time it was not until fairly recently that materials have become available that allow the theory to be put into practice. A gradient in index will cause light rays to bend in an otherwise homogeneous material. Thus,

the lens designer now has a new dimension of flexibility which will allow him to solve problems that could not be formerly solved. A proper selection of the manner in which the gradient varies is also important. The designer would normally select certain degrees of symmetry. Three are most common; axial, radial or spherical gradients.

GRIN material in the shape of rods now commonly use axial and radial gradients in such devices as fiber-optic cables and photocopying machines. Spherical gradients are not available because spherical gradient material has not yet been produced. Spherical gradients do offer an advantage in that they lend themselves more easily to mathematical description since closed form solutions for the ray paths can be obtained.

A good introduction to gradients and the materials currently available for production of large scale GRIN lens systems is provided by Moore [Ref. 6], and Light [Ref. 7]. These also give the reader an idea of the advantages that may be realized along with the problems associated with the design and production of such items.

C. AIM AND INTENT OF THIS STUDY

The aim of this study is to complete the design of the Gradient Index Seeker Lens (GISL) initiated by Carr. This design uses a spherical gradient and 'pointed' lens shape. This study does not determine the aerodynamic efficiency of

the design but rather ensures that the lens has a generally pointed character that will also allow some degree of imaging for off-axis objects. The spherical gradient is chosen since it seems to fit the geometrical shape of the lens and also since the three-dimensional analysis of rays is much simpler.

This design is accomplished through the use of ray tracing techniques. Thus, no actual study of the lens material nor the manner in which such a lens could be manufactured is intended. It is the hope of the author that studies of this nature will provide the impetus for the development of suitable GRIN material with spherical gradients.

Once the lens design was completed a 'best' lens was chosen and a simple detector system applied to it to see if precise definition of off-axis targets is possible.

II. GRIN LENS DESIGN

A. GRIN LENS DESIGN METHODOLOGY

The method by which the GRIN Lens was designed in Carr's thesis [Ref. 4], is the subject of this section. A cross-section view of the top half of the lens is shown in Figure 2.1.

As can be seen, the lens is designed by defining the inner surface as a cone and then constructing the outer surface so that a backwards ray trace from a point source will result in parallel lines emerging. This is done by tracing rays from the back edge of the lens towards the front surface and finding the point of intersection of the ray and front surface line. The front surface line is found by using the previous ray solution as described below. The intersection of the ray and the line is determined using an iteration procedure. Once a solution is found the front surface line that will cause the ray to emerge parallel with all other rays is determined. This front surface line is then used to find a point solution for the next ray. About 1000 rays are traced starting at the outside edge of the inner cone and working inwards towards the center. Details of the iteration process is included in later sections.

Once the lens outside surface has been constructed the lens is then studied to see how well it will image three dimensional skew rays that enter the lens at varying degrees of incidence. To accomplish this, a grid is placed in front of the lens and then rays are traced from the intersection points of the grid through the lens and onto the image plane. The grid is then tilted at successive angles and the resulting 'spots' on the image plane recorded for each case. The manner in which these spots move on the image plane and their size are the major performance characteristics of the lens.

B. GRIN RAY PATH DESCRIPTION

Following Marchand [Ref. 5], GRIN ray paths in spherical gradients are found through the solution of the appropriate line integral:

$$= r_0 + e \frac{r}{r_0} \frac{dr}{r(n^2 r^2 - e^2)^{1/2}} \quad (2.1)$$

where

$$e = n r \sin \theta = n_0 r_0 \sin \theta \quad (2.2)$$

and

$$\theta = 1$$

It should be noted that the value of θ is -1.0 if the radius is decreasing with angle and +1.0 if the radius is increasing with angle.

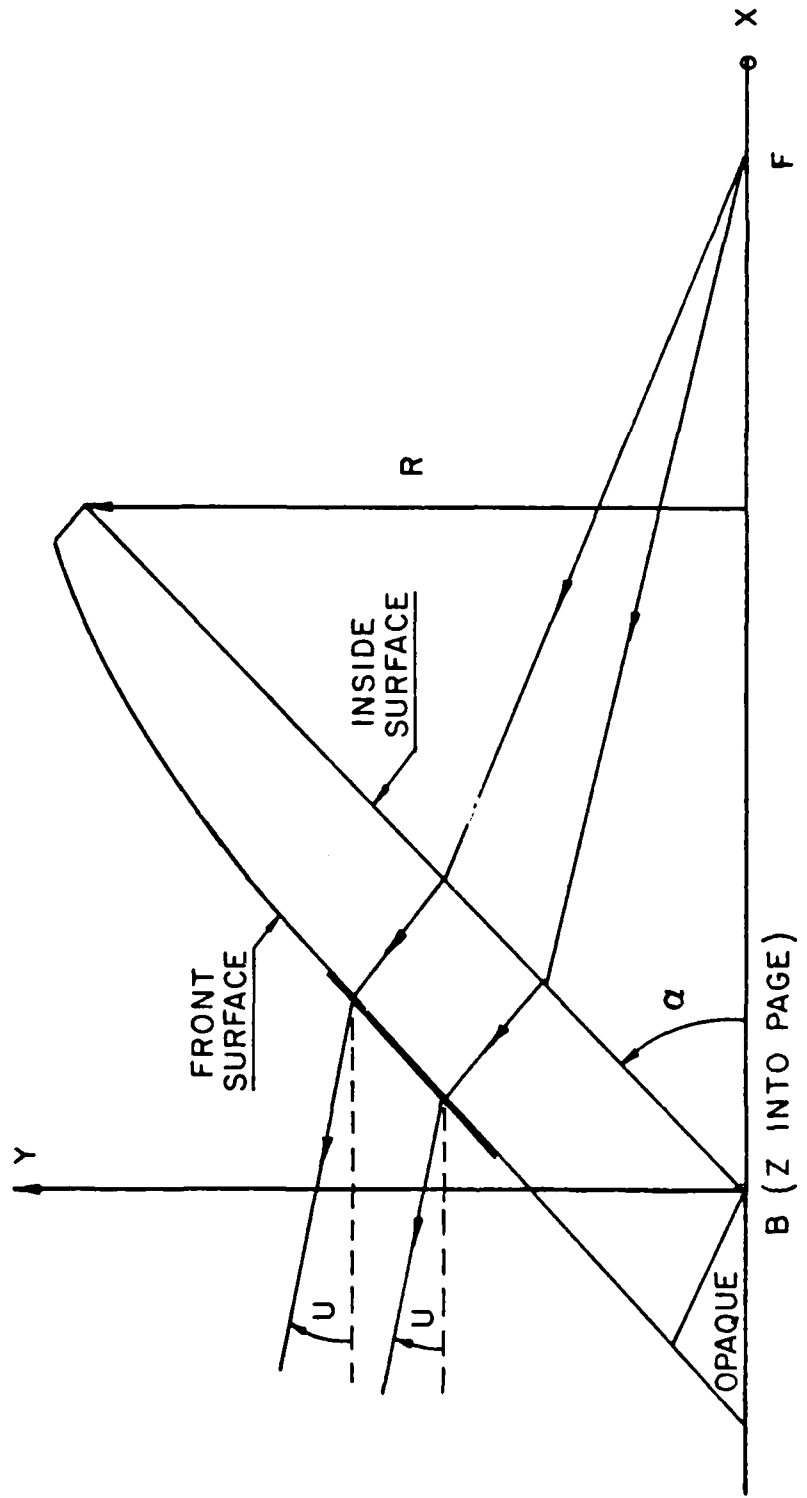


Figure 2.1 GRIN Lens Coordinate System and Parameters (from Carr).

The choice of index gradient is instrumental in allowing the integral to be solved in closed form. In this study the index is defined as:

$$n^2 = (a + br^2/R_z^2)$$

The constant a defines the strength of the index at the origin and the constant b defines the strength of the gradient and whether it is negative or positive.

As can be seen in Figure 2.2, the ray path is described by the constant e in conjunction with the parameter θ , the angle between the radial arm of the coordinate system and the direction of the ray at any point.

The solution of the integral in equation 2.1 results in the following expression:

$$\theta = \theta_0 - \frac{\epsilon}{2} \{ \sin^{-1}(\arg_0) - \sin^{-1}(\arg) \} \quad (2.3)$$

where

$$\arg_0 = \frac{a - 2e/r_0^2}{(a^2 + 4be^2/R_z^2)^{1/2}}$$

and

$$\arg = \frac{a - 2e/r^2}{(a^2 + 4be^2/R_z^2)^{1/2}}$$

or, expressed in terms of the radius,

$$r = \frac{\sqrt{2} |e|}{\{a + (a^2 + 4be^2/R_z^2) \sin [-2\varepsilon(\arg_0 - \varepsilon_0)] - \sin^{-1}(\arg_0)\}}^{1/2} \quad (2.4)$$

C. GRIN LENS GEOMETRY

A factor which must be considered is the manner in which the lens is cut out of the GRIN material. Figure 2.2 shows an orientation of the material with respect to the lens such that the center of symmetry of the material is inside the lens. Carr has defined this as a negative value of OB, the distance from the point O to the point B. Carr was able to work out the lens problem for positive values of this parameter only, thus the major portion of this study is to develop methods that enable solutions for negative values of OB. In so doing, two factors have to be overcome:

- a) ray matching - When the ray path radius initially decreases and then increases with change in angle the ray path equation must be matched at the point of minimum radius.
- b) near-radial lines - Rays that show very little curvature are difficult to describe in terms of radius and angle and these cause problems in the iterative solution scheme.

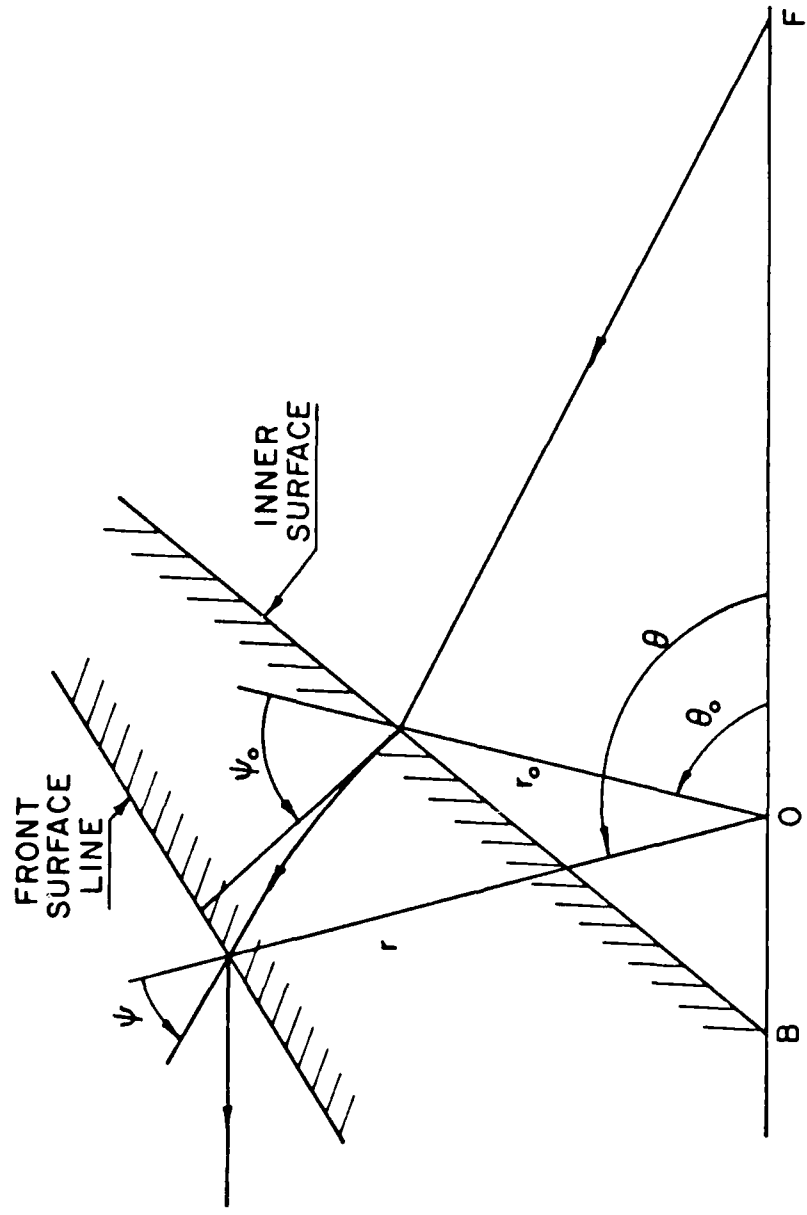


Figure 2.2 GRIN Lens and Ray Geometry.

The solution to the ray matching problem is relatively simple and is discussed in the next section. The resolution of near-radial lines is a more complex task and is covered in the following chapter.

D. RAY MATCHING

As stated previously the ray path equation changes signs as the radius of the path decreases and then increases. Such a path is shown in Figure 2.3. Simply changing sign in the equation as the point of minimum radius is passed does not produce the desired result, but rather has the effect shown in Figures 2.3 and 2.4.

The resolution of this problem is fairly simple. At the point of minimum radius the arcsine function in equation 2.3 containing this radius (\arg) reduces to $- \pi/2$. This is due to the fact that at this point the value of $\sin \varphi$ is -1 . Thus:

$$\sin \varphi = -1$$

and

$$e^2 = n^2 r^2$$

Thus:

$$\arg = \frac{a - 2n^2}{(a^2 + 4bn^2 r^2 / R_z^2)^{1/2}} = \frac{a - 2(a + br^2 / R_z^2)^2}{(a^2 + 4b(a + br^2 / R_z^2)r^2 / R_z^2)^{1/2}} = 1$$

and

$$\sin^{-1}(\arg) = -\pi/2$$

If the radius is initially decreasing as shown in Figure 2.3, we can find the angle of the minimum radius. We call this the critical angle or θ_L :

$$\theta_L = \theta_0 - \frac{\epsilon}{2} \{ \sin^{-1}(\arg_0) + \pi/2 \}$$

The positive and the negative forms of the equation should both contain the point of minimum radius, in other words, by approaching the point from the left or the right the same result should be obtained. The fact that this does not happen is shown in Figure 2.3 and reveals the need to match the rays at the point of minimum radius.

This matching is achieved by simply adding a constant to either the positive or the negative form of equation 2.3 and then matching at the point of minimum radius in the following manner:

$$\theta_R = \theta_L + c$$

thus

$$-\frac{\epsilon}{2} \{ \pi/2 + \sin^{-1}(\arg_0) \} = +\frac{\epsilon}{2} \{ \pi/2 + \sin^{-1}(\arg_0) \} + c$$

The constant c can then be found:

$$c = -\epsilon \{ \pi/2 + \sin^{-1}(\arg_0) \}$$

This constant must now be applied for all points past the point of minimum radius; in our example all points in

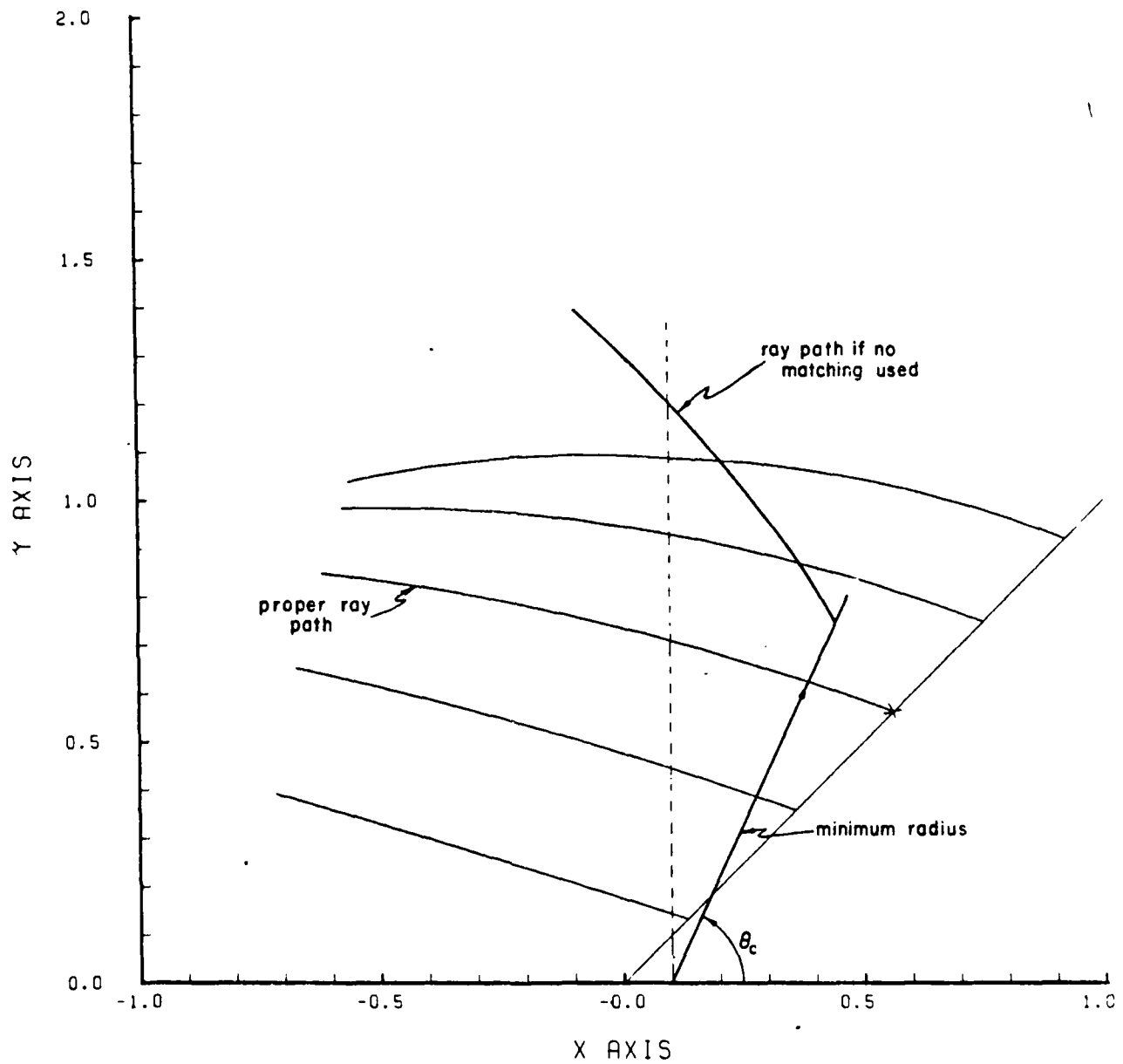


Figure 2.3 Ray Path Showing Improper Matching and Minimum Radius.

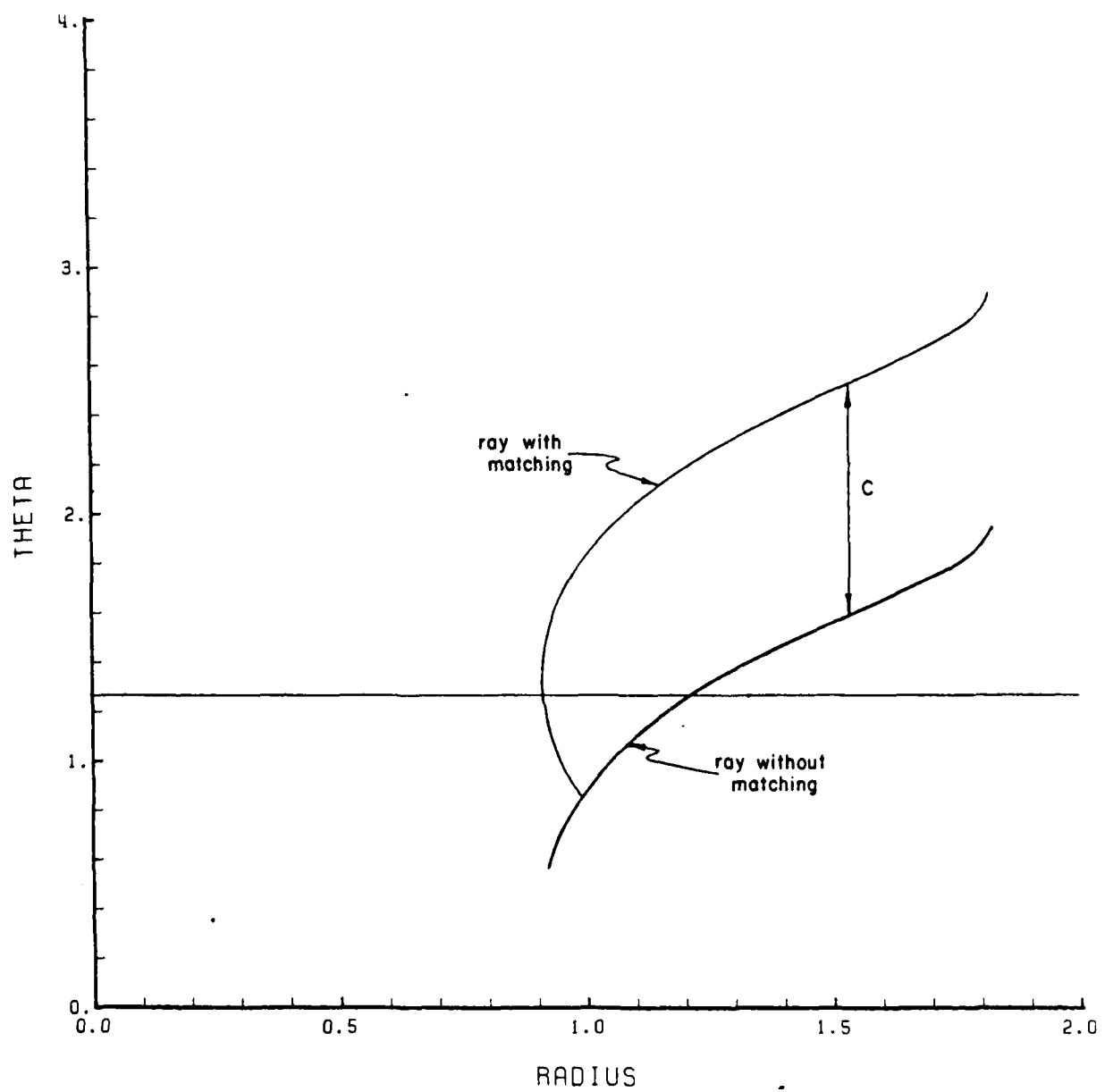


Figure 2.4 Ray Path Radius and Angle.

the increasing radius portion of the ray must be found using the form:

$$\theta = \theta_0 + \frac{\epsilon}{2} [\sin^{-1}(\arg_0) - \sin^{-1}(\arg)] + c$$

In the iteration scheme the ray path equation must be more carefully handled. First, the critical angle and the constant c must be found. Second, the angle of the ray must be checked to see if it has passed the critical angle. If it has then the constant c is added to equation 2.3 and the point recalculated. The details of the iteration methods will be described in the following chapter.

For further clarification Figure 2.5 shows the regions in which ray matching is required for a certain position of the center of symmetry. Note also that were the value of OB positive then all rays in the lens would never reach a minimum radius point. Thus ray matching is a problem unique to the negative OB case.

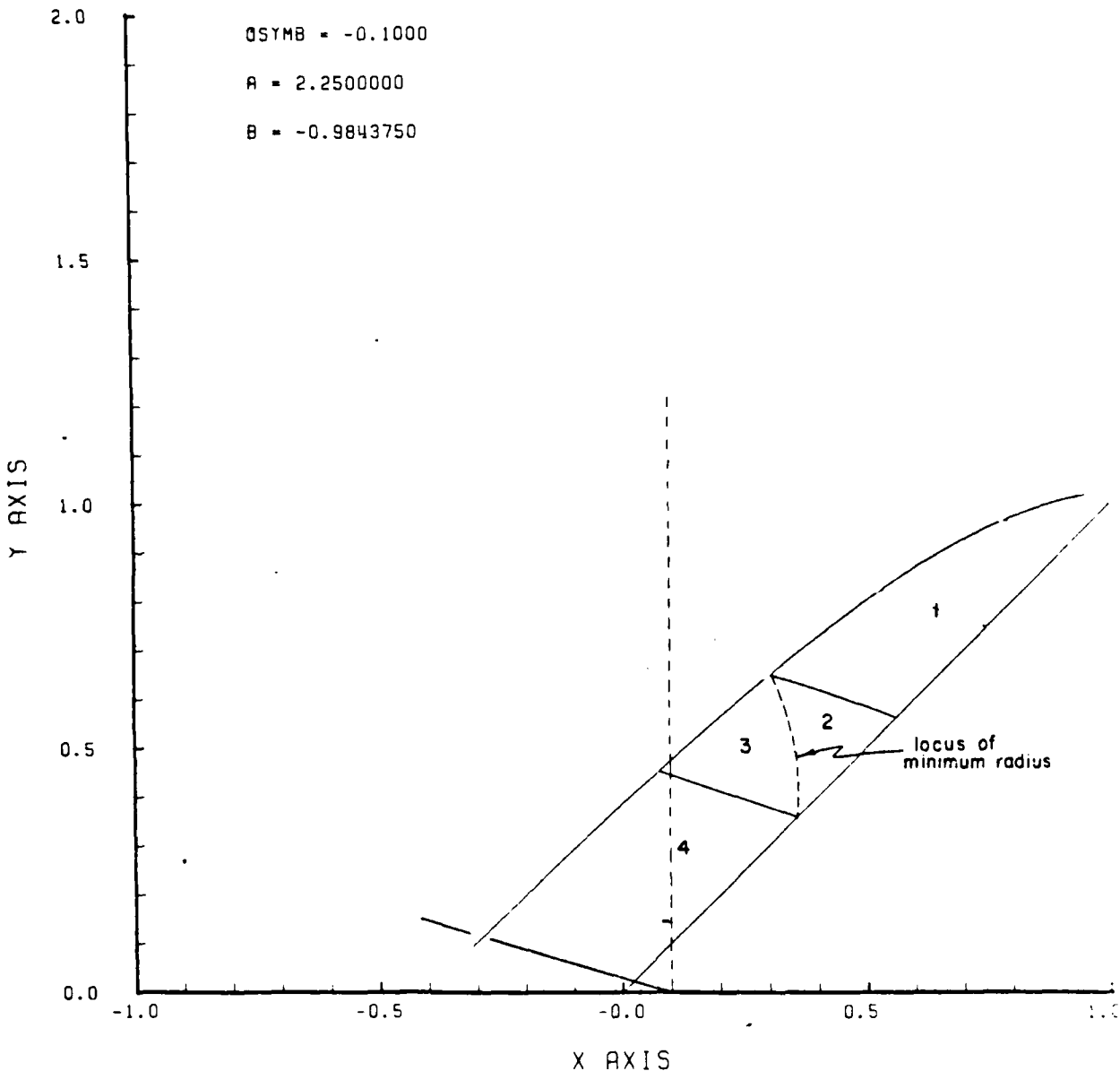


Figure 2.5 Ray Matching Regions.

III. NEAR-RADIAL LINES

A. DESCRIPTION OF DIFFICULTY

As mentioned previously, the ray paths that are nearly radial are difficult to describe mathematically in terms of radius and angle. This is due to the simple reason that a straight line originating from the center of the coordinate system has no change in angle and an undefinable change in radius.

The region in which this problem occurs in the lens design is shown in Figure 3.1. As can be seen, near-radial lines mean that the angle ψ and thus the constant e will be very small, so small as to cause equation 2.4 to approach a singularity and thus break down. In the iterative scheme, as the front surface solutions are found from the outside edge of the lens inwards, the values of ψ and e become increasingly smaller if the center of symmetry is inside the lens (OB negative). When this region is reached, equation 2.4 reduces the r_0 for all angles and further construction of the front surface is rendered impossible. This effect is shown in Figure 3.1.

Of note is the fact that if the radial line region is passed successfully, the rays begin to curve in the opposite sense, that is they are always convex to the

radial lines in the case of a negative gradient and concave to the radial lines if a positive gradient is used.

The resolution of the near-radial lines proved to be a difficult task and became a major portion of this study. The manner in which it was overcome is the subject of the following sections.

B. PRELIMINARY WORK - IMPROVING THE ITERATION SCHEME

The first step in the resolution of the problem was to simplify the iteration scheme. In his work Carr developed a scheme based on the geometry of the rays and coordinate system [Ref. 4], which worked well for all positive values of OB (that is, for all orientations of the center of symmetry to the left of the inside surface cone. See Figure 2.2). It was decided instead to use the Newton-Raphson approach, which is simpler in concept and not dependent on geometry.

Carr used the Newton-Raphson method in the second portion of the design involving the skew ray trace, but he did not use it for the lens construction.

The manner in which this scheme works is now described so that the reader will be able to better understand the concept of how all iterative methods work for this design, as well as how the ray matching previously described fits in.

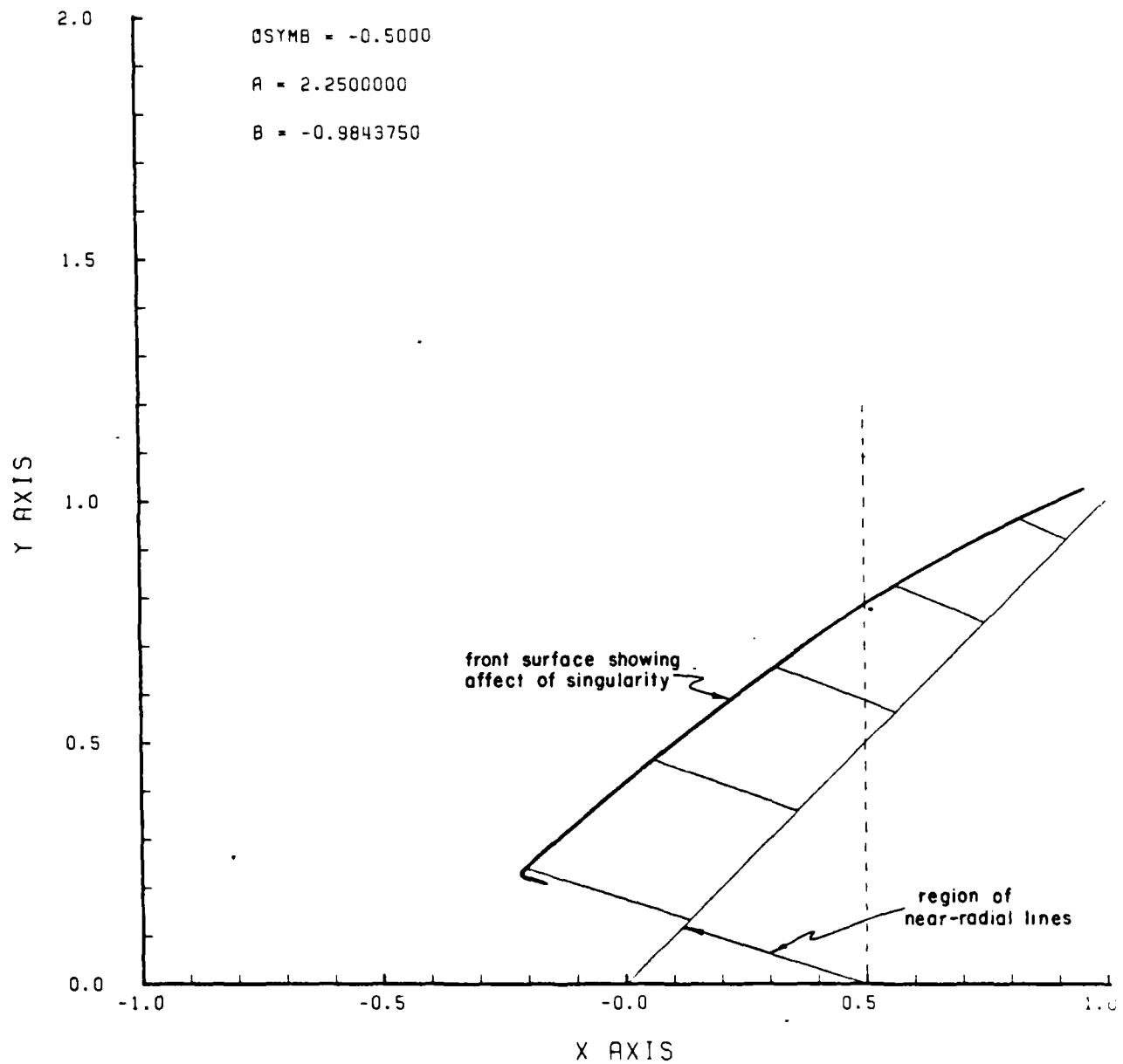


Figure 3.1 Ray Trace Showing Region of Radial Lines and Effect of Singularity.

The geometry associated with this plan is shown in Figure 3.2 and a flowchart outlining the iteration logic is shown as Figure 3.3. As can be seen with reference to the two figures, an initial point is first chosen by drawing a straight line from the inside surface intercept to the slope of the front surface obtained from a previous ray path solution. Newton-Raphson seeks to find the intercept of this front surface line with the curved ray path. This is done by using the initial angle to find the radius and derivative with respect to angle for each line and then calculating a new angle according to the relation:

$$\theta'' = \theta' - \frac{r_{fs} - r_{gr}}{\dot{r}_{fs} - \dot{r}_{gr}}$$

This new angle is then used to recalculate the radii and derivatives and thus an iterative loop is formed. Once the difference in angle is small enough the iteration is stopped and the solution considered to be found.

Ray matching is also employed in this scheme. As each new angle is calculated, it is checked to see if the critical angle has been passed. If it has, the constant c of equation 2.5 is added to the angle and thus the proper radius and derivative will be then found.

Once a solution has been found it is used to find a new front surface slope by determining that slope which will

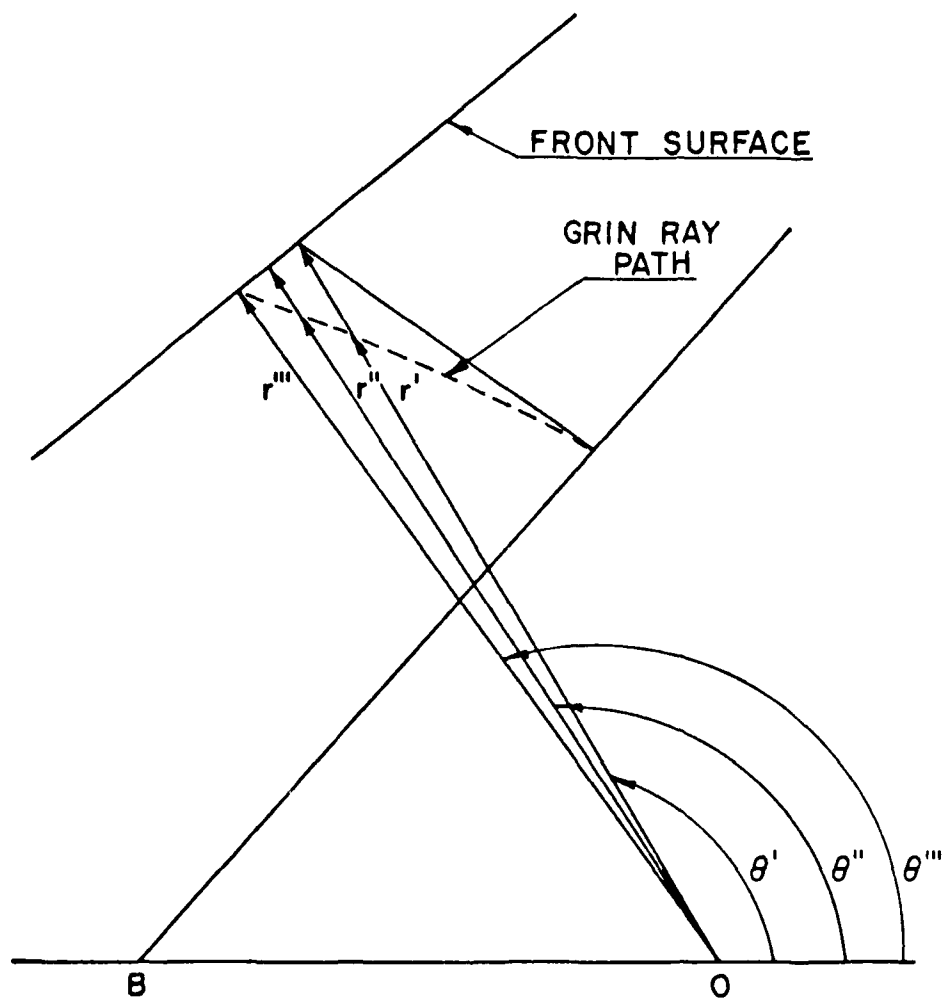


Figure 3.2 Newton-Raphson Iteration Geometry.

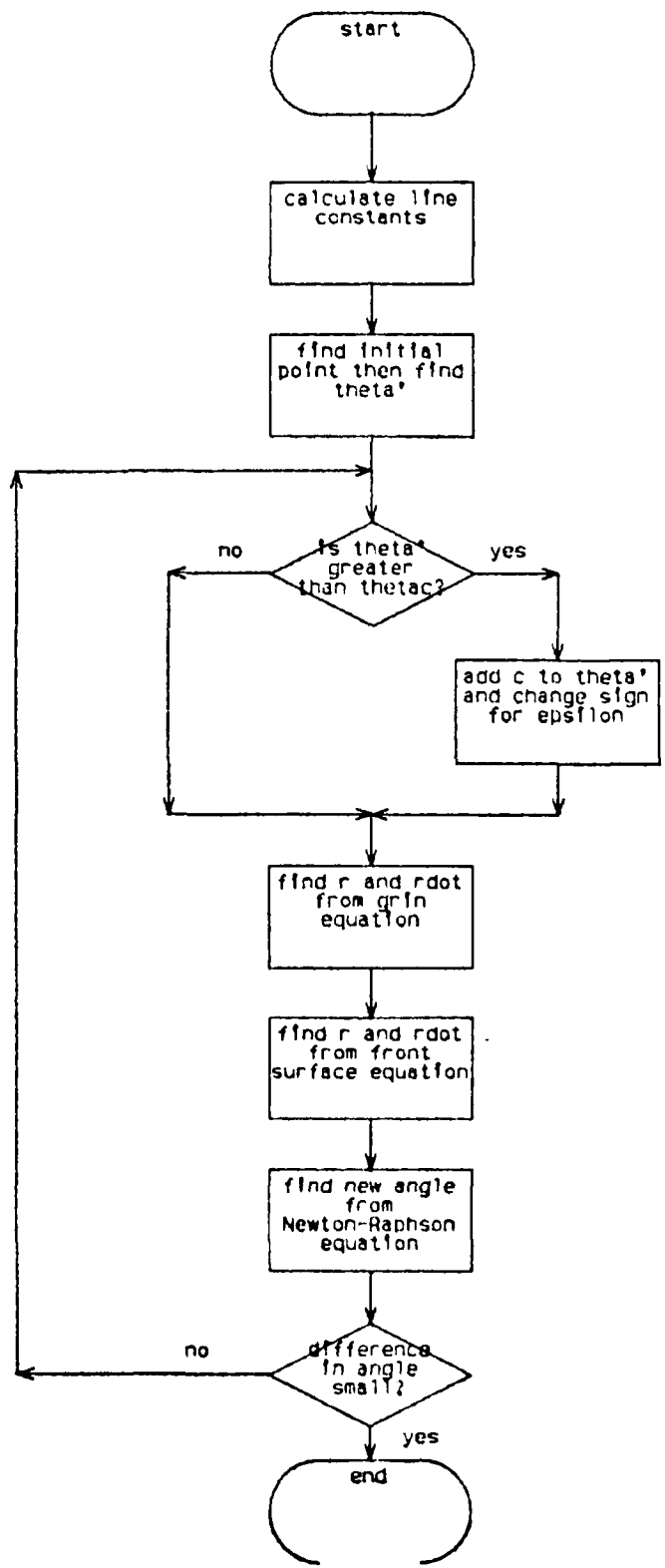


Figure 3.3 Newton-Raphson Logic flowchart.

cause the refracted ray to emerge parallel to the axis. It is this slope that is used to find the solution for the next ray in the scheme.

When this new iterative procedure was implemented it was found to work efficiently for both the positive and negative gradients, but it did not resolve the problem of near-radial lines.

The reader should refer to Appendix A for a listing of program GISL, which is the ray tracing program originally written by Carr and modified by the author.

C. PRELIMINARY WORK - DOUBLE PRECISION

The next avenue that was explored was to place the ray tracing scheme in double precision. This was considered necessary since very small differences in angle were required in the region of the radial lines.

Once this was installed in the routine it was found to improve significantly the accuracy of the calculations and succeeded in delaying the point at which the iterations broke down. It did not solve the crux of the difficulty however.

D. PRELIMINARY WORK - CHECKING ACCURACY

At this point it was decided to develop a scheme to check the accuracy of the front surface solution. The manner in which this was done is shown in Figure 3.4

The ray trace was completed in a forward direction from the front surface to the focal point in a two-dimensional fashion. These rays were caused to originate from the mid point of each set of points that define the front surface. The slope of the front surface for each of these rays was taken to be the line drawn between the two adjacent points on the front surface. In this fashion the worst case was chosen since the skew ray trace used to determine the performance of the lens uses incident rays that can hit the front surface at any point.

These rays were then traced through the lens and back towards the focal point. The x-coordinate of the focal point was defined and the y-coordinate calculated from the ray trace to see how close it would come to the y-coordinate of the focal point originally used to start construction of the front surface. A listing of this routine is shown as Appendix B.

Another benefit of this two-dimensional ray trace was that it allowed the author to confirm the methods by which a forwards ray trace is done. In this manner ray matching and sign convention in angles was checked. Also this ray trace is different in that a solution between the ray path in the lens and the back surface, rather than the front surface, was now required in the iterative solution scheme and this could now be verified to ensure that it was properly done.

Another method of checking the accuracy of the solution would be to study the front surface smoothness in the region of near-radial lines. Although not as precise as the above method this idea allowed the author to confirm that the front surface was sufficiently smooth. By this means it was also possible to see a physical representation of the lens in the region of the singularity.

E. FIRST PROPOSED SOLUTION - STRAIGHT LINES

The first proposed method of solving the mathematical difficulty was to simply replace the near-radial lines with completely straight lines just before the singularity was reached. This could be done by following the decrease of the parameter ψ_0 until it became small enough to ensure that the lines were nearly straight.

This idea was implemented but it was found not to be sufficiently accurate. It must be emphasized that an inaccuracy in even a single point could not be tolerated since this would mean that all succeeding points in the iterative solution scheme would carry that error as well.

For these reasons the straight line solution was rejected and other means of solving the difficulty were sought.

F. SECOND PROPOSED SOLUTION - REDUCED EQUATIONS

The second method that was used to resolve the problem of near-radial lines was to reduce equation 2.4 by

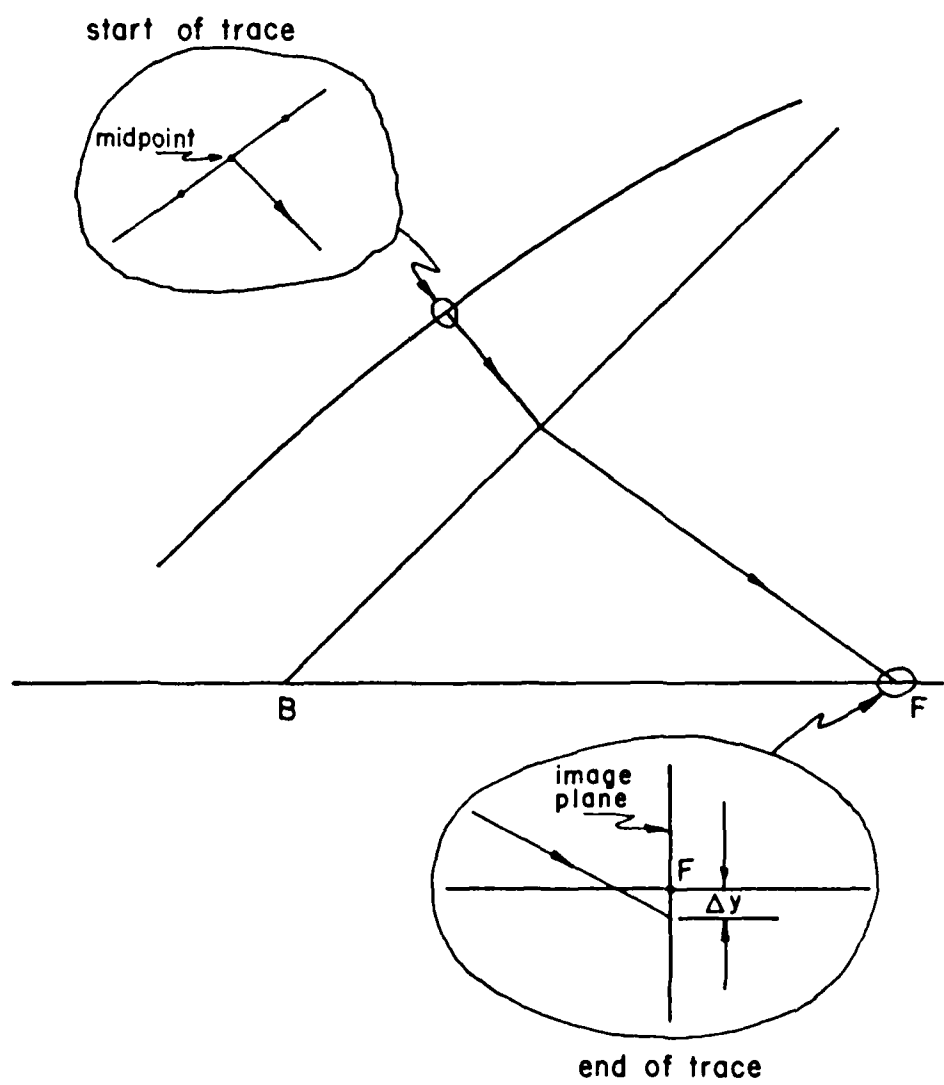


Figure 3.4 Geometry of Accuracy Check - Forwards Ray Trace.

employing small angle approximations, binomial expansions and curve fitting. The details of how this was done follows.

Recalling equation 2.3:

$$\alpha = \psi_0 - \frac{r}{2} \{ \sin^{-1}(\arg_0) - \sin^{-1}(\arg) \}$$

The arguments of these arcsine functions were reworked as follows:

$$\arg_0 = \frac{a - 2(a+b')\psi_0^2}{(a^2 + 4b'(a+b')\psi_0^2)^{1/2}}$$

and

$$\arg = \frac{a - 2(a+b')\psi_0^2 r_0^2 / r^2}{(a^2 + 4b'(a+b')\psi_0^2)^{1/2}}$$

where

$$\psi_0 \approx \sin \psi_0$$

$$b' = b r_0^2 / R_z^2$$

Note the angle ψ_0 is very small.

These arguments were then reduced using a binomial expansion:

$$\arg_0 = 1 - \frac{2(a+b')^2 \psi_0^2}{a^2}$$

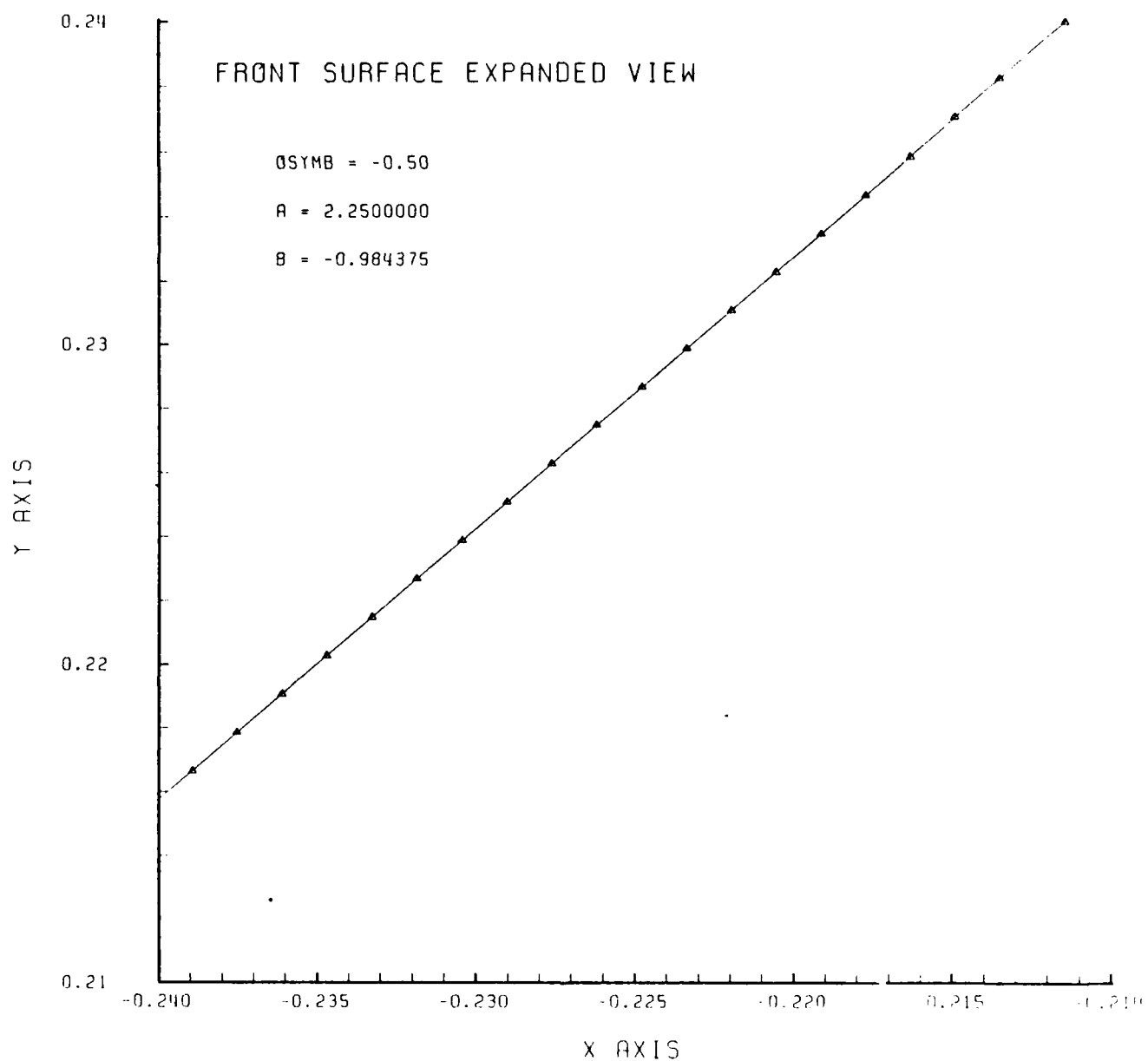


Figure 3.5 Expanded View of Front Surface .. Straight Line Method.

and

$$\arg = 1 - \frac{2(a+b')\psi_0^2 \left(\frac{r_0}{r^2} a+b'\right)}{a^2}$$

Again the ψ_0^2 term ensures that the expansion is valid.

A function of the type $\arcsin(x)$ where x is known to be close to the value 1 can be curve fitted into the form:

$$\sin^{-1}(x) = \pi/2 - [2(1-x)]^{1/2}$$

This equation applies to both arcsine functions as the ψ_0^2 term ensures that the argument is close to 1.

When placed in the equation the arguments result in the following final expression:

$$\theta = \theta_0 + \frac{\epsilon \psi_0}{2} \left\{ (a+b') - \left[(a+b') \left(\frac{r_0}{r^2} a+b' \right) \right]^{1/2} \right\}$$

In terms of radius:

$$r = r \frac{(a(a+b'))^{1/2}}{\left\{ \left[\frac{a}{\epsilon \psi_0} (\theta - \theta_0) - (a+b') \right]^2 - b'(a+b') \right\}^{1/2}}$$

The reduced equation was then implemented in the iterative front surface solution scheme by constantly checking it against the complete equation. When the

difference between the two became small, the reduced equation was subsequently used in solving for the front surface. The reduced equation was then turned off when the rays had progressed an equal distance on the other side of the singularity. See Figure 3.2 for clarification.

The equation worked well in resolving the front surface for the lens construction and did produce a smooth surface similar to that shown in Figure 3.5.

It did not do well when the accuracy program check was applied. One reason is that although it was easy to implement the equation for the lens construction it was not so easy to complete the forwards trace since these rays hit the front surface randomly making it difficult to know when to use the reduced equation. In practice the reduced equation could be implemented when the absolute value of the parameter ψ_0 became smaller than that used in the lens construction phase during the time that the reduced equation was used. There was then no way of telling how accurate the front surface was, in other words, there was no method to show how the rays would physically react in the region of the singularity. Thus the reduced equation method would work but it is not an entirely satisfactory solution.

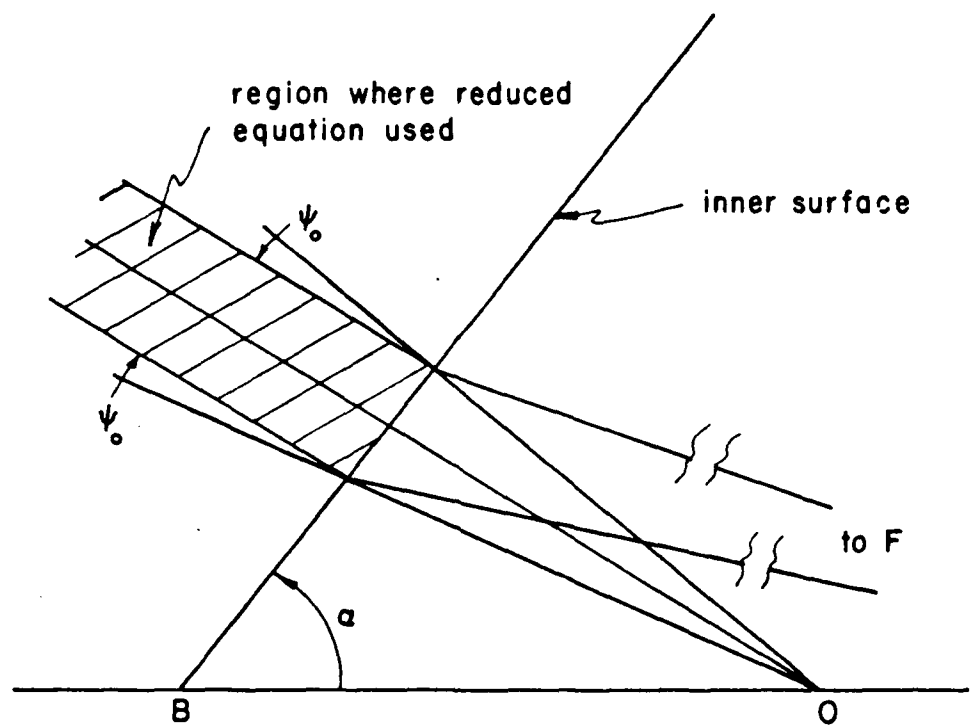


Figure 3.6 Reduced Equation Implementation.

Program CHECK was tried without using the reduced equation but disastrous results were obtained for those points in the region of the singularity.

For these reasons it was decided that another means of resolving the problem was required.

G. THIRD PROPOSED SOLUTION - MARCHAND METHOD

The third proposed solution is drawn from Marchand [Ref. 5] p. 27, in which he proposes a means of improving the ray trace formula so that nearly radial lines will be more easily described.

The method is based on redefining variables as follows:

$$\theta = eM_0 \quad (3.1)$$

where

$$M_0 = \int_{r_0}^r \frac{dr}{r(n^2 r^2 - e^2)^{1/2}}$$

Marchand describes the ray path using the parameters α and β such that:

$$\beta = \sin\theta / \sin\theta_0 \quad (3.2)$$

$$\alpha = \cos\theta - \beta \cos\theta_0$$

This enables the coordinates of the ray to be described as:

$$x = r \left(\frac{x_0}{r_0} + \beta \frac{p_0}{n_0} \right)$$

$$y = r \left(\frac{y_0}{r_0} + \frac{q_0}{n_0} \right)$$

$$z = r \left(\frac{z_0}{r_0} + \frac{0}{n_0} \right)$$

Upon substitution of equations 2.2 and 3.2, equation 3.1 becomes:

$$= n_0 r_0 M_0 \operatorname{sinc}$$

The parameter can now be more accurately solved for small angles of using a Maclaurin series for the sinc function.

This method was then implemented in program GISL using an iteration scheme based on Cartesian rather than polar coordinates.

This method was not found to improve the accuracy of the ray trace in the region of near radial lines and was not adopted.

One reason for this may lie in the fact that in our solution to the integral in equation 2.1 the value e no longer appears at the front of the expression. Thus there is no advantage to redefining the variable as shown in equation 3.1.

H. FOURTH PROPOSED SOLUTION - ANGLE IN TERMS OF RADIUS

The fourth method and the one that proved successful involved the solution of the front surface slope and the

GRIN ray using the form of the ray trace equation shown in equation 2.3 rather than that of equation 2.4.

The reason for this choice is shown in Figure 3.7. This figure shows that when the rays are nearly radial a small change in angle will result in a huge change in radius. Thus the form of the ray trace equation using $r()$ is inherently unstable. Previously we have used this form in order to make use of the Newton-Raphson technique. It was thought that if the iteration scheme could be reworked so that the form $\psi(r)$ of the equation could be used then better results might be obtained.

A suitable iteration method was found and is illustrated in Figures 3.8 and 3.9.

The figures show that an initial point was chosen in the same manner as before, that is by drawing a straight line from the ray refracted at the inner surface out to the front surface slope. This point provides the radius for equation 2.4 so that a new angle can be calculated. This angle is then used to find the corresponding radius out to the front surface slope. This new radius is then used in equation 2.4 to find the next angle and thus an iterative loop is formed.

Thus a simple scheme was found. It should be noted however that this method will only converge when the initial angle is greater than 90 degrees. The reason for this lies in the geometry and is shown in Figure 3.10.

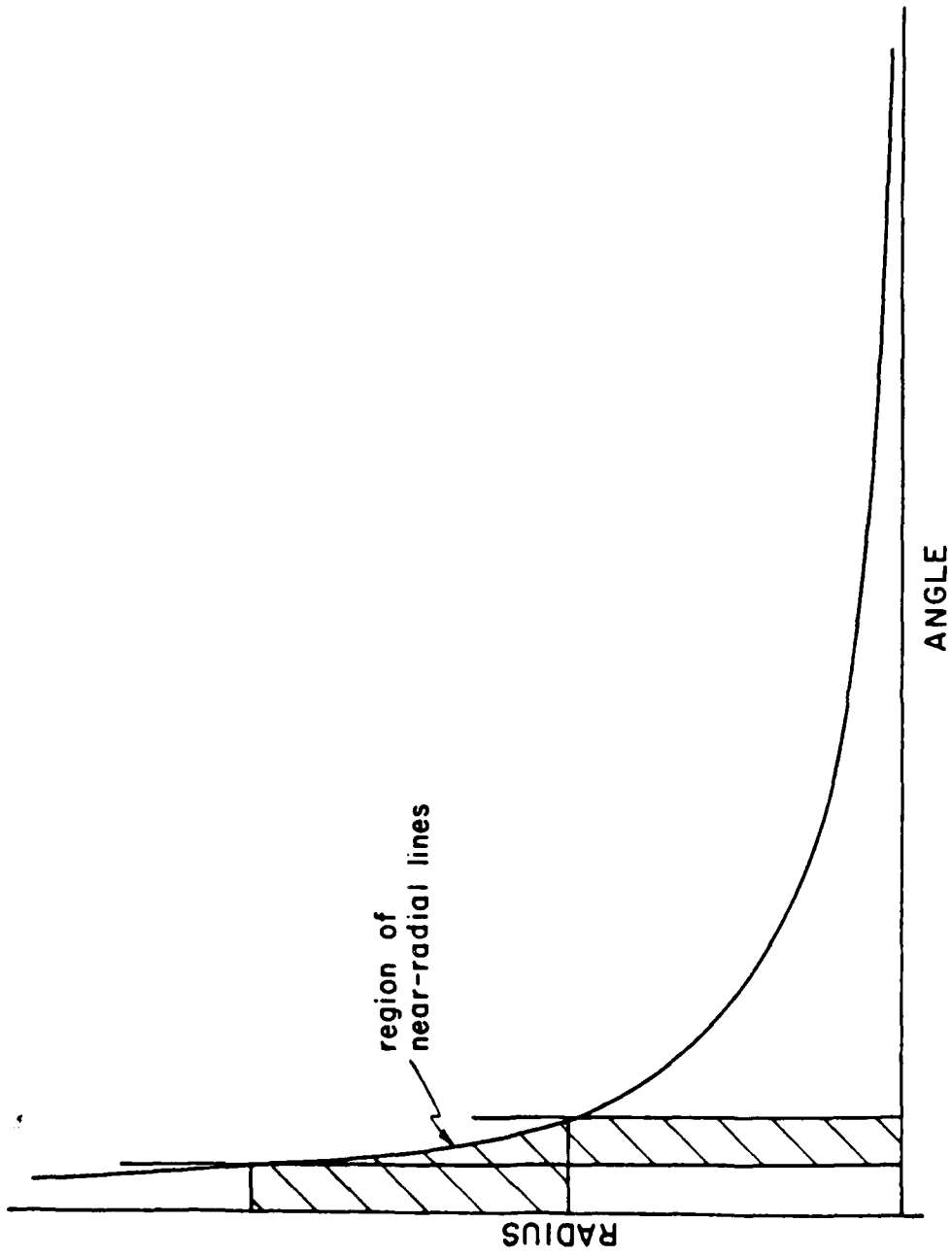


Figure 3.7 Radius and Angle Relation.

Thus the iteration will only converge when the rays are in the region of the nearly radial lines. This does not cause a difficulty since the Newton-Raphson method, modified to include ray matching, can find solutions efficiently in the region where the initial angle is less than 90 degrees.

Figure 3.10 is also drawn to show the reader an example of a forward ray trace.

This simple scheme was implemented and found to work successfully for both the lens construction and the skew ray trace; see [Ref. 8].

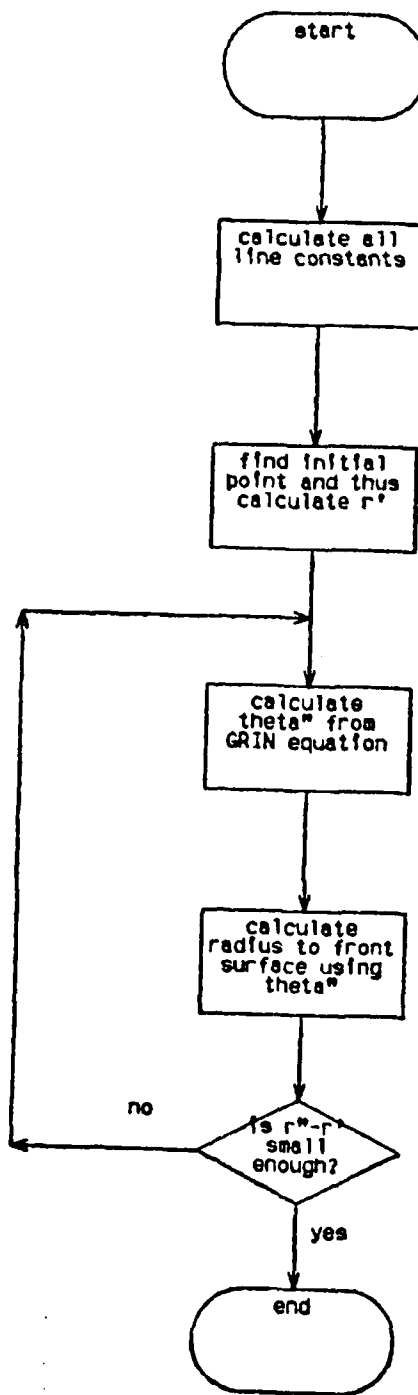


Figure 3.8 Angle in Terms of Radius Iteration Logic
Flowchart.

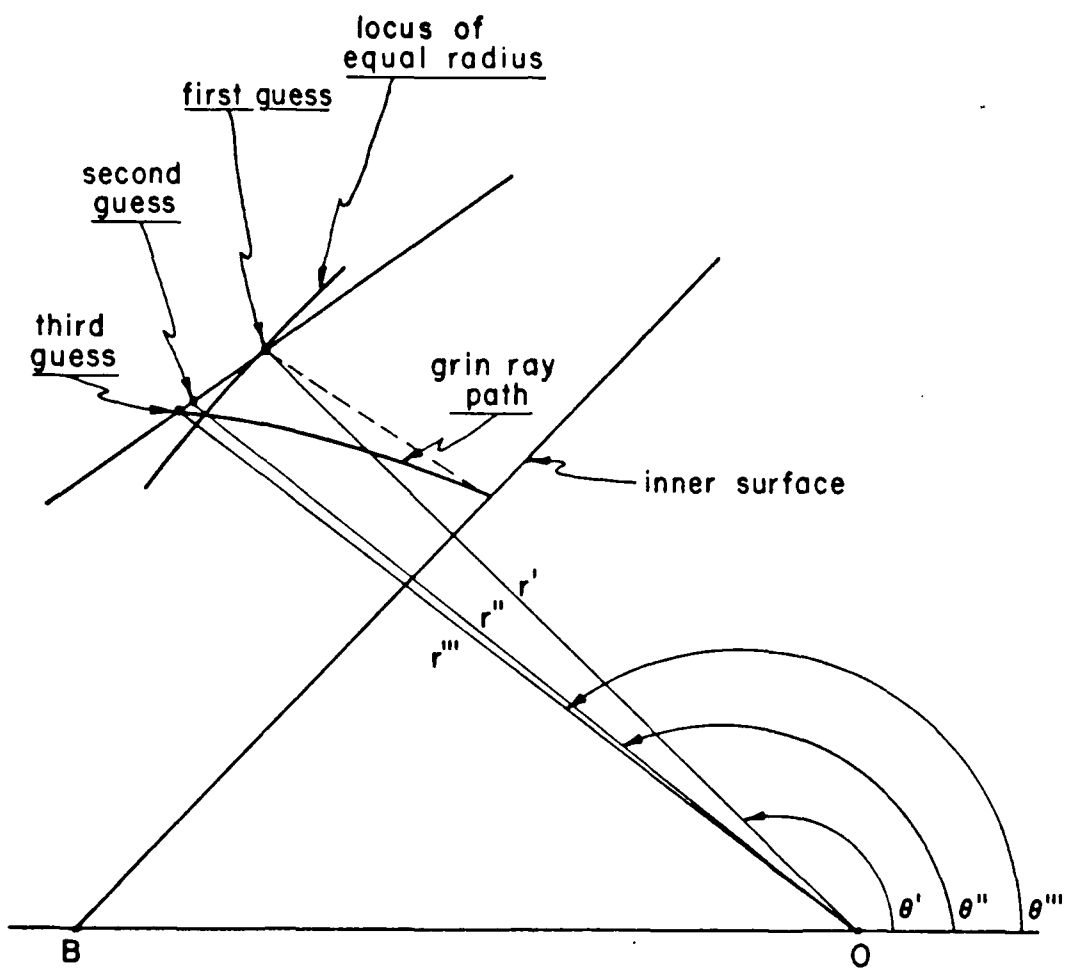


Figure 3.9 Angle in Terms of Radius Iteration Geometry.

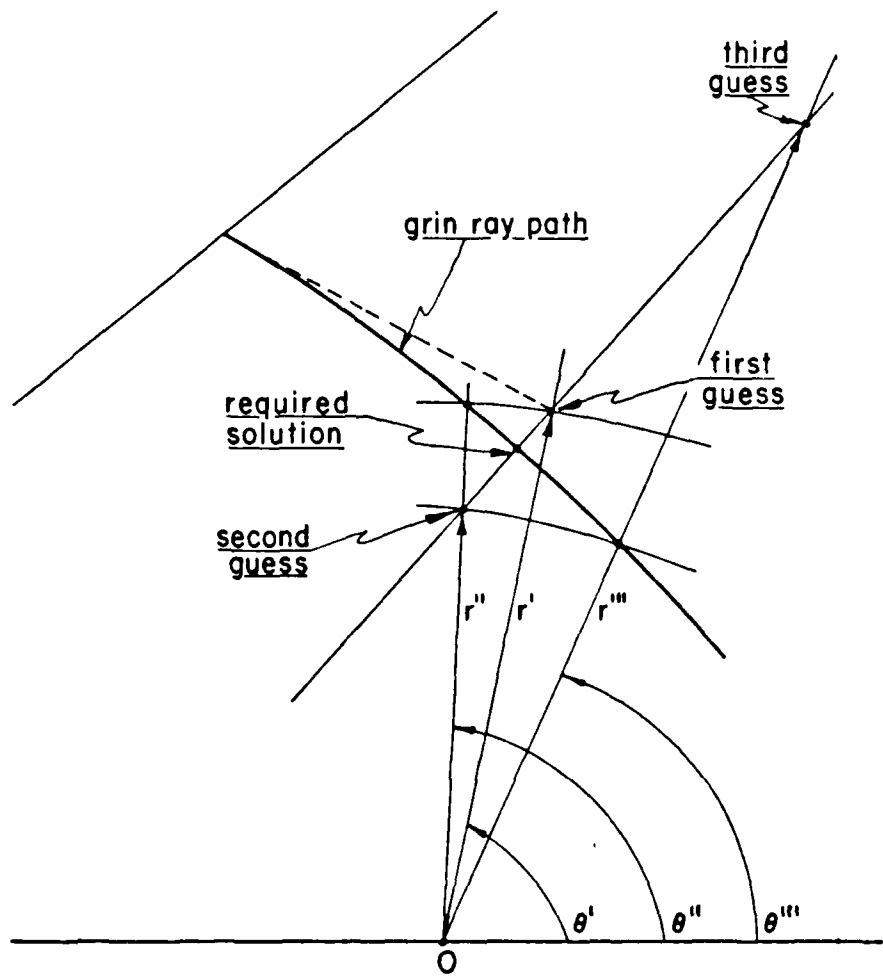


Figure 3.10 Diverging Iteration - Forward Ray Trace.

IV. GRADIENT INDEX SEEKER LENS RAY TRACE RESULTS

A. FRONT SURFACE ACCURACY

As mentioned previously, the front surface of the Gradient Index Seeker Lens was checked for accuracy by completing a ray trace from the midpoint of each set of solutions. A sample of the output from program Check is shown in Table I so that the reader will have an indication of the accuracy of the ray trace in the region of near-radial lines. Note that the most radial lines occur when the absolute value of the angle ψ_0 is smallest.

B. SPOT SIZE RESULTS

The results of program GISL showing the variation of spot size are shown in Figure 4.1. This figure shows how the spot size varies as gradient strengths and orientations of the center of symmetry are changed for a median angle of incidence of 0.3 radians.

Note that all orientations of the center of symmetry are now included. The studious reader should refer to Carr's work [Ref. 4], to compare results.

C. SELECTION OF A BEST LENS

The best lens was selected by determining those parameters that would result in a small spot size and also cause the least number of rays to be reflected or refracted

outside the missile diameter. Figure 4.1 shows that these criterion were not easily discernable and a judgemental decision was required.

The reader should note that a value of 2.25 was chosen for the parameter a . This was done since the resulting value of 1.5 for the index of refraction at the center of symmetry is common to a large number of possible lens materials. Also of note is the fact that the focal point was chosen to be 2.0 units along the x -axis from the inner surface cone. This was done since this value resulted in smaller spot sizes generally.

With these criterion in mind a value of -0.2 for α_B and a 5% negative gradient were chosen as parameters for the best lens design.

A more detailed study of the lens parameters could be accomplished with use of an optimization program in which a large number of parameters could be varied in order to find the best lens. This would achieve a more satisfactory result than the one shown.

TABLE I
FRONT SURFACE ACCURACY

Line Number	Angle θ_0 (Radians)	Error in y- coordinate	number of iterations
895	0.0411	0.0008	4
896	0.0390	0.0007	4
897	0.0369	0.0008	4
898	0.0349	0.0009	4
899	0.0328	0.0007	4
900	0.0308	0.0009	4
901	0.0288	0.0008	4
902	0.0268	0.0008	4
903	0.0247	0.0009	4
904	0.0227	0.0009	3
905	0.0207	0.0008	3
906	0.0187	0.0009	3
907	0.0167	0.0008	3
908	0.0147	0.0008	3
909	0.0127	0.0010	3
910	0.0107	0.0009	3
911	0.0087	0.0008	3
912	0.0067	0.0010	3
913	0.0048	0.0009	3
914	0.0028	0.0010	2
915	0.0008	0.0010	2
916	-0.0010	0.0010	2
917	-0.0030	0.0010	3
918	-0.0050	0.0010	3
919	-0.0069	0.0009	3
920	-0.0089	0.0011	3
921	-0.0108	0.0010	3
922	-0.0127	0.0010	3
923	-0.0147	0.0009	3
924	-0.0166	0.0011	3
925	-0.0185	0.0010	3
926	-0.0204	0.0011	4
927	-0.0223	0.0011	4
928	-0.0243	0.0010	4
929	-0.0261	0.0012	4
930	-0.0281	0.0011	4
931	-0.0300	0.0012	4
932	-0.0318	0.0012	4
933	-0.0337	0.0012	4
934	-0.0356	0.0011	4
935	-0.0375	0.0013	4

Figure 4.1 Spot Size Results - ALFAP = 0.3 Radians. Each Box Contains Spot Size, Number of Rays OSYMB

Outside Missle Diameter, Number of Rays on Image Plane. Total Number of Incident Rays is 135.

V. MIRROR AND DETECTOR SYSTEM

A. DESCRIPTION OF SYSTEM

A scanning mirror and a detector were added to the GRIN best lens in order to determine if precise definition of off-axis targets would be possible. The design of these two new elements is shown in Figure 5.1.

The mirror is made to 'nod' at a high rate and thus scans the spot across the detector. The detector consists of two sections, as shown in Figure 5.1. Thus, when the spot is scanned across the two plates a signal from each detector will be generated and will result in the form shown in Figure 5.2. This arrangement will allow an accurate measurement of the mirror angle for which the spot crosses the axis. The electronics of the detector signal processor could then be arranged to relate the mirror angle to the angle of incident radiation so that the precise line-of-sight angle of an off-axis target will be known.

Note that this is a simple detector system that will only resolve angles in one plane. A more sophisticated system along the same lines could be designed with a four-element detector and a more intricate method of scanning the spot across the detector. It was decided to keep the mirror and detector system as simple as possible since the

aim of this work is only to show that a precise angle measuring device is feasible.

B. LENS TO DETECTOR RAY TRACE

This section describes the mathematics of the ray trace from the lens to the mirror and then to the detector. A listing of program DETPLOT which accomplishes this task is included as Appendix C.

The ray trace consists of the following parts:

- a. ray direction exiting lens
- b. point of intersection on mirror
- c. ray direction exiting mirror
- d. detector ray count
1. Ray Direction Exiting Lens

The ray direction exiting the lens is derived from the direction cosines of the ray as calculated by program GISL. This data is used as an input to program DETPLOT along with the coordinates of the point at which the ray left the lens.

2. Point of Intersection on Mirror

The point of intersection of the ray and mirror may be described by the following expressions:

$$x_m = D_m K + x_0 \quad (5.1)$$

$$y_m = D_m L + y_0 \quad (5.2)$$

$$z_m = D_m M + z_0 \quad (5.3)$$

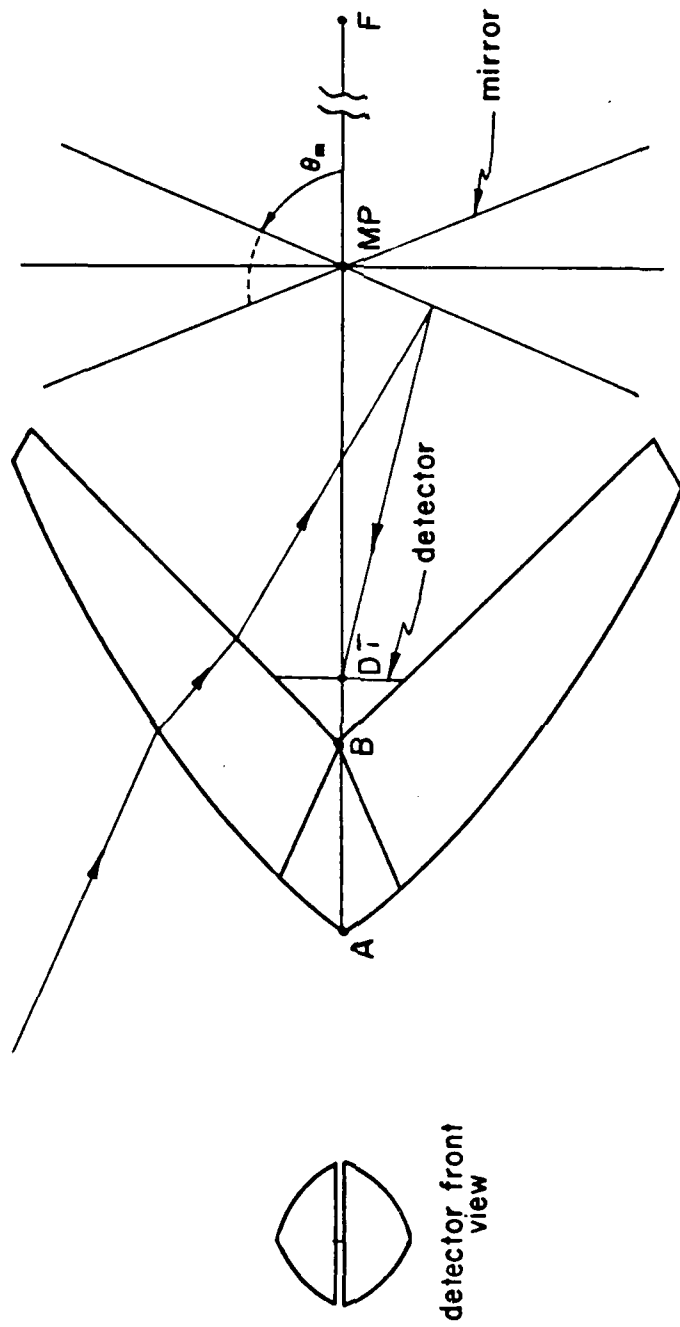


Figure 5.1 Lens, Mirror and Detector System.

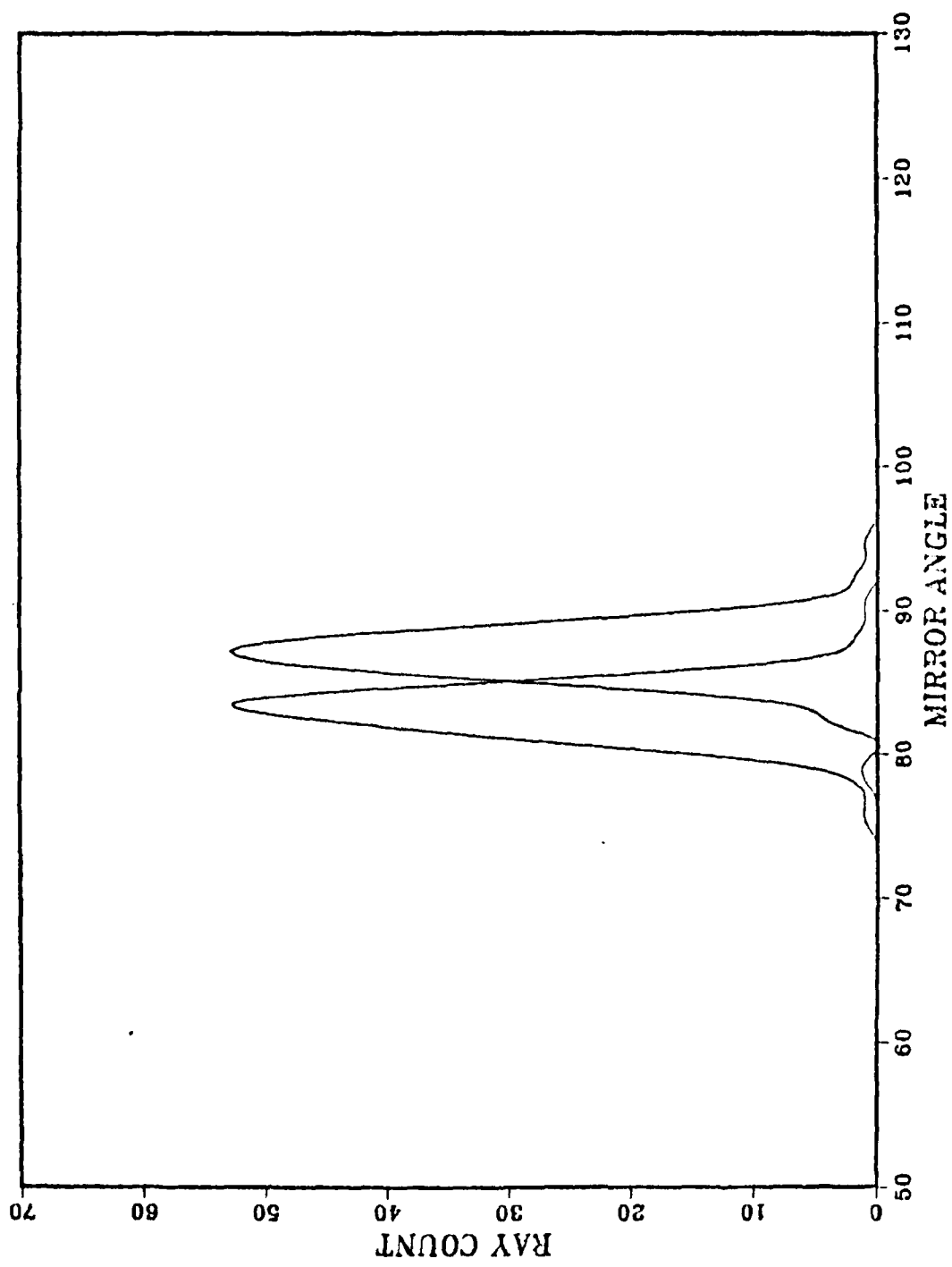


Figure 5.2 Detector Signal.

Since the surface of the mirror is tilted along the z-axis it can be described by the equations:

$$y_m = \tan \theta_m (x_m - MP) \quad (5.4)$$

$$y_m^2 \cos^2 \theta_m + z_m^2 < R \quad (5.5)$$

Where equation 5.4 describes a tilted plane and equation 5.5 limits the plane to the mirror diameter.

Neglecting equation 5.5 for a moment, equations 5.1, 5.2 and 5.4 may be combined to solve for D_{em} . The result is:

$$D_{em} = \frac{\tan \theta_m (x_0 - MP) - y_0}{L - K \tan \theta_m}$$

Now that D_{em} is known, equations 5.1, 5.2 and 5.3 may be used to find the coordinates of the mirror intersection point. These are then checked with equation 5.5 to make sure they are not outside the mirror diameter.

3. Ray Direction Exiting Mirror

The solution of the ray direction leaving the mirror is best understood vectorially. See Figure 5.3.

Reflection off a mirror is governed by two factors. Firstly, the angles of incidence and reflection must equal. Using vectors this is expressed as:

$$\hat{n} \cdot \vec{r}_i = - \hat{n} \cdot \vec{r}_r$$

In component form:

$$n_x r_{xi} + n_y r_{yi} = - n_x r_{xr} - n_y r_{yr} \quad (5.6)$$

Secondly, the ray is reflected in the same plane as the incident ray. This may be expressed vectorially by using the cross product to generate the vector \vec{n}_p as shown in Figure 5.3. Thus:

$$\vec{n}_p = \vec{r}_i \times \vec{n} = \vec{r}_r \times \vec{n}$$

In component form:

$$\vec{e}_x(-n_y r_{zi}) + \vec{e}_y(-n_x r_{zi}) + \vec{e}_z(n_y r_{xi} - n_x r_{yi}) =$$

$$\vec{e}_x(-n_y r_{zr}) + \vec{e}_y(-n_x r_{zr}) + \vec{e}_z(n_y r_{xr} - n_x r_{yr})$$

Three equations result:

$$-n_y r_{zi} = -n_y r_{zr}$$

$$-n_x r_{zi} = -n_x r_{zr}$$

$$n_y r_{xi} - n_x r_{yi} = n_y r_{xr} - n_x r_{yr} \quad (5.7)$$

The first two results are not unexpected as the mirror should not effect the z-component of the ray.

Equations 5.6 and 5.7 may now be combined to find the x- and y-components of the ray. When this is done the two following expressions result:

$$r_{xr} = \frac{(n_y^2 - n_x^2)}{(n_x^2 + n_y^2)} r_{xi} - \frac{2n_x n_y}{(n_x^2 + n_y^2)} r_{yi}$$

$$r_{yr} = \frac{(n_x^2 - n_y^2)}{(n_x^2 + n_y^2)} r_{yi} - \frac{2n_x n_y}{(n_x^2 + n_y^2)} r_{xi}$$

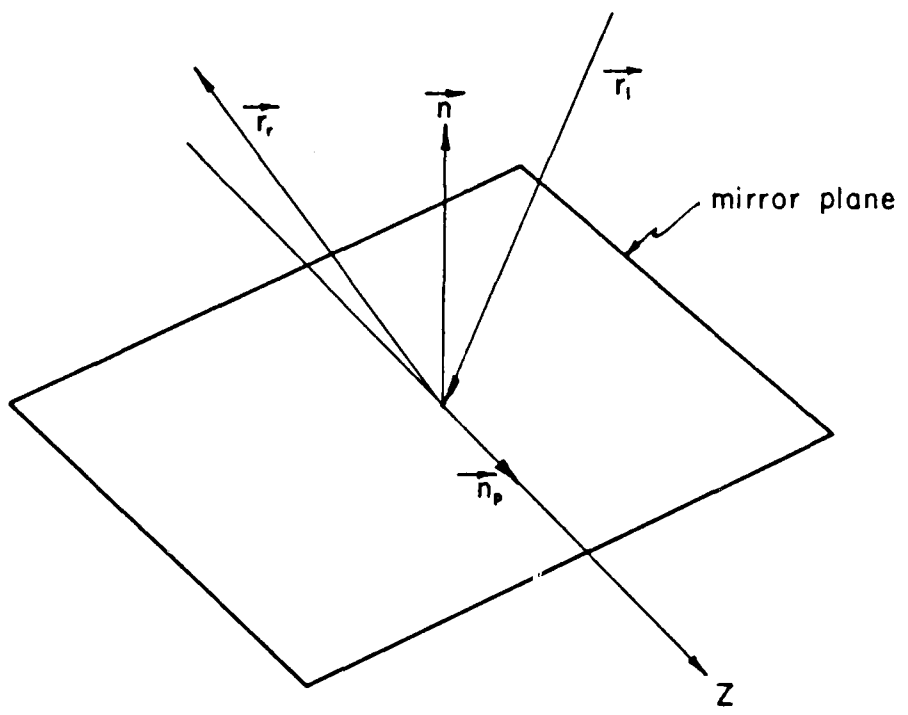


Figure 5.3 Reflection of Ray on Mirror.

Since the vector \vec{n} is entirely in the x-y plane, its components may be related to mirror angle as follows:

$$n_x = -\sin m$$

$$n_y = \cos m$$

When the above equations, along with well known trigonometric identities are used the following expressions will be found.

$$r_{xr} = \cos(2m)r_{xi} + \sin(2m)r_{yi}$$

$$r_{yr} = -\cos(2m)r_{yi} + \sin(2m)r_{xi}$$

Thus these equations represent the change in direction for the exiting ray and form two of its direction cosines, the third being r_{zr} .

4. Ray Count on Detector

The coordinates of the ray at the detector are described by the expressions:

$$x_d = D_{nd} K' + x_m$$

$$y_d = D_{nd} L' + y_m$$

$$z_d = D_{nd} M' + z_m$$

Since x_d is used to define the position of the detector, it is known. Thus the value D_{nd} may be solved and the corresponding y and z-components may be found.

The ray is then checked to make sure it is within the detector diameter. If it is the y-coordinate is checked to find out if it is negative or positive, and thus

whether the ray has struck the upper or lower half of the detector. The ray count is then incremented accordingly.

Program DETPLOT traces all rays for each increment of mirror angle and thus generates plots such as that shown in Figure 5.2.

C. MIRROR AND DETECTOR SYSTEM RESULTS

Appendix D shows the results of the detector signals as a function of mirror angle at angles of incidence from 0 to 40 degrees. For these the mirror pivot point was placed at 1.4 units along the x-axis from the inner surface cone since this was the smallest distance that would still allow full movement of the scanning mirror. The focal length was adjusted to 2.8 units for the lens design calculations so that the spot would be imaged as small as possible on the detector. Figure 5.4 summarizes the results shown in Appendix D. As can be seen, the smaller angles of incidence (those in the range 0 to 16 degrees) result in a linear relation between angle of incidence and mirror tilt angle, corresponding to an on-axis spot. The larger values of the angle of incidence resulted in a more random relation between these two quantities.

Appendix D also shows that the error in determining mirror angle increases as the angle of incidence increases. This is due to the fact that each successive plot is less distinct and thus a precise measure of the angle becomes

more difficult. Although this effect shows a deterioration in the lens system performance, it is not harmful since, as the missile corrects itself, the measurement of angle will become more accurate.

For these reasons this simple system is considered to be a viable means of target detection and shows that the GISL can be a successful missile seeker lens.

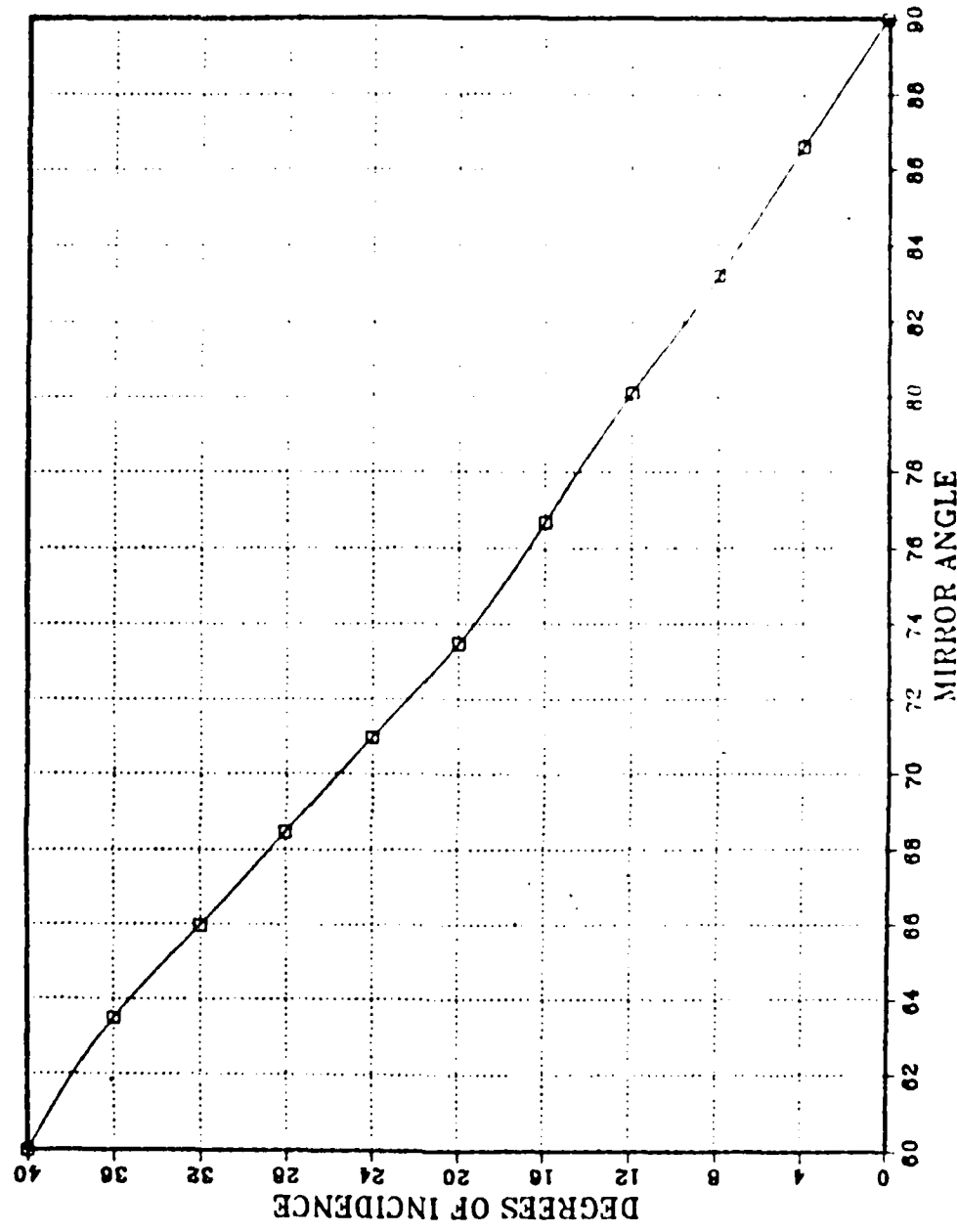


Figure 5.4 Mirror Tilt for On-Axis Spot and Angle of Incidence.

VI. CONCLUSIONS AND RECOMMENDATIONS

A. CONCLUSIONS

Two objectives were accomplished in the course of this study. Firstly, the Gradient Index Seeker Lens design, as initiated by Carr [Ref. 4], was completed in that all orientations of the center of symmetry with respect to the lens were made possible to describe mathematically. The results obtained for the spot size on the image plane showed trends that indicated the parameters that would produce a 'best' lens, but precise definition of these values was not possible.

Secondly, it was shown that a scanning mirror and detector system applied to the lens could be described using ray-trace techniques and also that such a system could be used to provide precise angle measurements of off-axis targets at angles less than 16 degrees. For larger values of angle, error in definition became increasingly greater.

Specifically, then, the following conclusions are made:

- a) The Gradient Index Seeker Lens can be described using ray-trace techniques and can be shown to provide adequate imaging of off-axis objects.
- b) A scanning mirror and detector system can be used to provide precise angle measurements.

B. RECOMMENDATIONS

The following recommendations for further study are made:

- a) An optimization program should be applied to program GISL to study the variations of all important parameters.
- b) A detector system capable of detection in all directions should be designed.
- c) The manner in which signal processing of the detector signals can be carried out should be studied.
- d) A study of Gradient Index material and the methods by which a lens could be manufactured should be undertaken.

APPENDIX A

```

***** GRADIENT INDEX SEEKER / LENS *****

THIS PROGRAM DESIGNS THE GRADIENT INDEX SEEKER LENS
IN TWO STAGES FROM THE FRONT SURFACE IS CONSTRUCTED
BY TRACING RAYS FROM THE FOCAL POINT BACK THROUGH THE
LENS DEFINING THE FRONT SURFACE SO THAT THE RAYS EMERGE
PARALLEL. DIRECTING A SKewed RAY TRACE IS COMPLETED IN A
FORWARD DIRECTION FOR ANY ANGLES OF INCIDENCE. THAT
OFF THE RESUME MEASUREMENTS MAY BE MADE.
THIS PROGRAM WAS INITIALLY WRITTEN BY H. CARR AND
THEN MODIFIED BY D. DAVIDSON
*****
```

SPECIFICATION STATEMENTS

```

INTEGER I,J,K,L,M,N,P,FLAG(1000),U,RAYS,SITDRAY,SELLNUM,
1NUMBER,CCORD,NUMB,IANGLE,THICK,CG,H,COUNT,SHAPES,UGT,
1CUCR(800),NUMBT,ELLIPS,SQURAY,TRIP,FILTER,CCORT,
1FACE,FLLG,CCUNT2,DYDXT(1010),LIP(1010),GAMMA,ABUNP,
1REAL,DYEXN(1010),DYRAY(1000),RAYZ(1000),CEN,TURBL,BUT,TOPL,
1T,ALFAF,GRIL,RAY(1000),DELTA,X,DELTAX,TURB,ST,RAIU,DYDXNP,LK,LL
1RADIANF,INC,TUP,BCT,TURB,DU,EC,DPAR1,PAE2,NINCY(1000),
1REAL,NF1,JP,VPAU,B0,CUDU,ECL,EL2(7,1000),EL2(7,1000),
1ELL,ELY(7,1000),EL2(7,1000),EL2(7,1000),
1IPAR3,XLIAP(1000),YLIA(1000),SUM1,
1ISUM2,SUM3,SUM4(1000),SIGMA(1000),IRMSRAD(1000),
1REAL,RCCE(500),SUM4(500),FRACTN(500),SDRAD(1000),YCENTK(20,800),
1THETAE,VEPSLCN,PSI,XIP,YIP,XIP,YIP,ERRCR,XF,YP,ZP,RH,D2T,ABS,X1PP
1REAL,LY1FP,ZETA,P,BASE,BASL,ROOO,N2X1K,N2X2K,SLINC,ARKLOS,CHEKRO,CALIBK,
1PRCANT,IFRCNT,PRCNIC,SURFL,TSURFL,
1SIGN,DIFFOR,XMAVET,XMAVET
1DOUELE,PRECISION,A,E,U,F,R,ALPHA,BETA,P1,P12(1010),Y2(1010),X1H,
1XI(1010),Y1(1010),I1(1010),I2(1010),CSYMBX2(1010),Y2(1010),X1H,
1Y1H,I2P(1010),UP(1010),UUP(1010),N2,N20,N3,E,BF,RO,RZERO,
1IDLUDP,ARG,RSINOC,DIFF,PSI0,PSI4,ZEIA,EXIT,I,TAO,THEIAH,
1RAD,RAE,RDG,RCF,RDT,EUNR,THEIA,TCRIT,I,TAO,THEIA,RSIN,
1BE,SLRF,RPF,CHECK1,CHECK2,KADH,ROCTS,RF,THIAP,BEF,F,SSKE,N2X2I,
1XX,AR
1CLLP,CMP,ROX,ROY,ROZ,NOX,NPOY,NOZ,NUM5,NUM6,NUM7,NUM8,CSYMPH,
1THETA2,NUM,NUM1,NUM2,NUM3,NUM4,NUM5,NUM6,NUM7,NUM8,CSYMPH,
1C1500420,1C1500430,1C1500440,1C1500450,1C1500460,1C1500470,1C1500480,1C1500490,1C1500500,1C1500510,1C1500520,1C1500530,1C1500540,1C1500550,1C1500560,1C1500570,1C1500580,1C1500590,1C1500600,1C1500610,1C1500620,1C1500630,1C1500640,1C1500650,1C1500660,1C1500670,1C1500680,1C1500690,1C1500700,1C1500710,1C1500720,1C1500730,1C1500740,1C1500750,1C1500760,1C1500770,1C1500780,1C1500790,1C1500800,1C1500810,1C1500820,1C1500830,1C1500840,1C1500850,1C1500860,1C1500870,1C1500880,1C1500890,1C1500900,1C1500910,1C1500920,1C1500930,1C1500940,1C1500950,1C1500960,1C1500970,1C1500980,1C1500990,1C1500100,1C1500101,1C1500102,1C1500103,1C1500104,1C1500105,1C1500106,1C1500107,1C1500108,1C1500109,1C1500110,1C1500111,1C1500112,1C1500113,1C1500114,1C1500115,1C1500116,1C1500117,1C1500118,1C1500119,1C1500120,1C1500121,1C1500122,1C1500123,1C1500124,1C1500125,1C1500126,1C1500127,1C1500128,1C1500129,1C1500130,1C1500131,1C1500132,1C1500133,1C1500134,1C1500135,1C1500136,1C1500137,1C1500138,1C1500139,1C1500140,1C1500141,1C1500142,1C1500143,1C1500144,1C1500145,1C1500146,1C1500147,1C1500148,1C1500149,1C1500150,1C1500151,1C1500152,1C1500153,1C1500154,1C1500155,1C1500156,1C1500157,1C1500158,1C1500159,1C1500160,1C1500161,1C1500162,1C1500163,1C1500164,1C1500165,1C1500166,1C1500167,1C1500168,1C1500169,1C1500170,1C1500171,1C1500172,1C1500173,1C1500174,1C1500175,1C1500176,1C1500177,1C1500178,1C1500179,1C1500180,1C1500181,1C1500182,1C1500183,1C1500184,1C1500185,1C1500186,1C1500187,1C1500188,1C1500189,1C1500190,1C1500191,1C1500192,1C1500193,1C1500194,1C1500195,1C1500196,1C1500197,1C1500198,1C1500199,1C1500200,1C1500201,1C1500202,1C1500203,1C1500204,1C1500205,1C1500206,1C1500207,1C1500208,1C1500209,1C1500210,1C1500211,1C1500212,1C1500213,1C1500214,1C1500215,1C1500216,1C1500217,1C1500218,1C1500219,1C1500220,1C1500221,1C1500222,1C1500223,1C1500224,1C1500225,1C1500226,1C1500227,1C1500228,1C1500229,1C1500230,1C1500231,1C1500232,1C1500233,1C1500234,1C1500235,1C1500236,1C1500237,1C1500238,1C1500239,1C1500240,1C1500241,1C1500242,1C1500243,1C1500244,1C1500245,1C1500246,1C1500247,1C1500248,1C1500249,1C1500250,1C1500251,1C1500252,1C1500253,1C1500254,1C1500255,1C1500256,1C1500257,1C1500258,1C1500259,1C1500260,1C1500261,1C1500262,1C1500263,1C1500264,1C1500265,1C1500266,1C1500267,1C1500268,1C1500269,1C1500270,1C1500271,1C1500272,1C1500273,1C1500274,1C1500275,1C1500276,1C1500277,1C1500278,1C1500279,1C1500280,1C1500281,1C1500282,1C1500283,1C1500284,1C1500285,1C1500286,1C1500287,1C1500288,1C1500289,1C1500290,1C1500291,1C1500292,1C1500293,1C1500294,1C1500295,1C1500296,1C1500297,1C1500298,1C1500299,1C1500300,1C1500301,1C1500302,1C1500303,1C1500304,1C1500305,1C1500306,1C1500307,1C1500308,1C1500309,1C1500310,1C1500311,1C1500312,1C1500313,1C1500314,1C1500315,1C1500316,1C1500317,1C1500318,1C1500319,1C1500320,1C1500321,1C1500322,1C1500323,1C1500324,1C1500325,1C1500326,1C1500327,1C1500328,1C1500329,1C1500330,1C1500331,1C1500332,1C1500333,1C1500334,1C1500335,1C1500336,1C1500337,1C1500338,1C1500339,1C1500340,1C1500341,1C1500342,1C1500343,1C1500344,1C1500345,1C1500346,1C1500347,1C1500348,1C1500349,1C1500350,1C1500351,1C1500352,1C1500353,1C1500354,1C1500355,1C1500356,1C1500357,1C1500358,1C1500359,1C1500360,1C1500361,1C1500362,1C1500363,1C1500364,1C1500365,1C1500366,1C1500367,1C1500368,1C1500369,1C1500370,1C1500371,1C1500372,1C1500373,1C1500374,1C1500375,1C1500376,1C1500377,1C1500378,1C1500379,1C1500380,1C1500381,1C1500382,1C1500383,1C1500384,1C1500385,1C1500386,1C1500387,1C1500388,1C1500389,1C1500390,1C1500391,1C1500392,1C1500393,1C1500394,1C1500395,1C1500396,1C1500397,1C1500398,1C1500399,1C1500400,1C1500401,1C1500402,1C1500403,1C1500404,1C1500405,1C1500406,1C1500407,1C1500408,1C1500409,1C1500410,1C1500411,1C1500412,1C1500413,1C1500414,1C1500415,1C1500416,1C1500417,1C1500418,1C1500419,1C1500420,1C1500421,1C1500422,1C1500423,1C1500424,1C1500425,1C1500426,1C1500427,1C1500428,1C1500429,1C1500430,1C1500431,1C1500432,1C1500433,1C1500434,1C1500435,1C1500436,1C1500437,1C1500438,1C1500439,1C1500440,1C1500441,1C1500442,1C1500443,1C1500444,1C1500445,1C1500446,1C1500447,1C1500448,1C1500449,1C1500450,1C1500451,1C1500452,1C1500453,1C1500454,1C1500455,1C1500456,1C1500457,1C1500458,1C1500459,1C1500460,1C1500461,1C1500462,1C1500463,1C1500464,1C1500465,1C1500466,1C1500467,1C1500468,1C1500469,1C1500470,1C1500471,1C1500472,1C1500473,1C1500474,1C1500475,1C1500476,1C1500477,1C1500478,1C1500479,1C1500480,1C1500481,1C1500482,1C1500483,1C1500484,1C1500485,1C1500486,1C1500487,1C1500488,1C1500489,1C1500490,1C1500491,1C1500492,1C1500493,1C1500494,1C1500495,1C1500496,1C1500497,1C1500498,1C1500499,1C1500500,1C1500501,1C1500502,1C1500503,1C1500504,1C1500505,1C1500506,1C1500507,1C1500508,1C1500509,1C1500510,1C1500511,1C1500512,1C1500513,1C1500514,1C1500515,1C1500516,1C1500517,1C1500518,1C1500519,1C1500520,1C1500521,1C1500522,1C1500523,1C1500524,1C1500525,1C1500526,1C1500527,1C1500528,1C1500529,1C1500530,1C1500531,1C1500532,1C1500533,1C1500534,1C1500535,1C1500536,1C1500537,1C1500538,1C1500539,1C1500540,1C1500541,1C1500542,1C1500543,1C1500544,1C1500545,1C1500546,1C1500547,1C1500548,1C1500549,1C1500550,1C1500551,1C1500552,1C1500553,1C1500554,1C1500555,1C1500556,1C1500557,1C1500558,1C1500559,1C1500560,1C1500561,1C1500562,1C1500563,1C1500564,1C1500565,1C1500566,1C1500567,1C1500568,1C1500569,1C1500570,1C1500571,1C1500572,1C1500573,1C1500574,1C1500575,1C1500576,1C1500577,1C1500578,1C1500579,1C1500580,1C1500581,1C1500582,1C1500583,1C1500584,1C1500585,1C1500586,1C1500587,1C1500588,1C1500589,1C1500590,1C1500591,1C1500592,1C1500593,1C1500594,1C1500595,1C1500596,1C1500597,1C1500598,1C1500599,1C1500600,1C1500601,1C1500602,1C1500603,1C1500604,1C1500605,1C1500606,1C1500607,1C1500608,1C1500609,1C1500610,1C1500611,1C1500612,1C1500613,1C1500614,1C1500615,1C1500616,1C1500617,1C1500618,1C1500619,1C1500620,1C1500621,1C1500622,1C1500623,1C1500624,1C1500625,1C1500626,1C1500627,1C1500628,1C1500629,1C1500630,1C1500631,1C1500632,1C1500633,1C1500634,1C1500635,1C1500636,1C1500637,1C1500638,1C1500639,1C1500640,1C1500641,1C1500642,1C1500643,1C1500644,1C1500645,1C1500646,1C1500647,1C1500648,1C1500649,1C1500650,1C1500651,1C1500652,1C1500653,1C1500654,1C1500655,1C1500656,1C1500657,1C1500658,1C1500659,1C1500660,1C1500661,1C1500662,1C1500663,1C1500664,1C1500665,1C1500666,1C1500667,1C1500668,1C1500669,1C1500670,1C1500671,1C1500672,1C1500673,1C1500674,1C1500675,1C1500676,1C1500677,1C1500678,1C1500679,1C1500680,1C1500681,1C1500682,1C1500683,1C1500684,1C1500685,1C1500686,1C1500687,1C1500688,1C1500689,1C1500690,1C1500691,1C1500692,1C1500693,1C1500694,1C1500695,1C1500696,1C1500697,1C1500698,1C1500699,1C1500700,1C1500701,1C1500702,1C1500703,1C1500704,1C1500705,1C1500706,1C1500707,1C1500708,1C1500709,1C1500710,1C1500711,1C1500712,1C1500713,1C1500714,1C1500715,1C1500716,1C1500717,1C1500718,1C1500719,1C1500720,1C1500721,1C1500722,1C1500723,1C1500724,1C1500725,1C1500726,1C1500727,1C1500728,1C1500729,1C1500730,1C1500731,1C1500732,1C1500733,1C1500734,1C1500735,1C1500736,1C1500737,1C1500738,1C1500739,1C1500740,1C1500741,1C1500742,1C1500743,1C1500744,1C1500745,1C1500746,1C1500747,1C1500748,1C1500749,1C1500750,1C1500751,1C1500752,1C1500753,1C1500754,1C1500755,1C1500756,1C1500757,1C1500758,1C1500759,1C1500760,1C1500761,1C1500762,1C1500763,1C1500764,1C1500765,1C1500766,1C1500767,1C1500768,1C1500769,1C1500770,1C1500771,1C1500772,1C1500773,1C1500774,1C1500775,1C1500776,1C1500777,1C1500778,1C1500779,1C1500780,1C1500781,1C1500782,1C1500783,1C1500784,1C1500785,1C1500786,1C1500787,1C1500788,1C1500789,1C1500790,1C1500791,1C1500792,1C1500793,1C1500794,1C1500795,1C1500796,1C1500797,1C1500798,1C1500799,1C1500800,1C1500801,1C1500802,1C1500803,1C1500804,1C1500805,1C1500806,1C1500807,1C1500808,1C1500809,1C1500810,1C1500811,1C1500812,1C1500813,1C1500814,1C1500815,1C1500816,1C1500817,1C1500818,1C1500819,1C1500820,1C1500821,1C1500822,1C1500823,1C1500824,1C1500825,1C1500826,1C1500827,1C1500828,1C1500829,1C1500830,1C1500831,1C1500832,1C1500833,1C1500834,1C1500835,1C1500836,1C1500837,1C1500838,1C1500839,1C1500840,1C1500841,1C1500842,1C1500843,1C1500844,1C1500845,1C1500846,1C1500847,1C1500848,1C1500849,1C1500850,1C1500851,1C1500852,1C1500853,1C1500854,1C1500855,1C1500856,1C1500857,1C1500858,1C1500859,1C1500860,1C1500861,1C1500862,1C1500863,1C1500864,1C1500865,1C1500866,1C1500867,1C1500868,1C1500869,1C1500870,1C1500871,1C1500872,1C1500873,1C1500874,1C1500875,1C1500876,1C1500877,1C1500878,1C1500879,1C1500880,1C1500881,1C1500882,1C1500883,1C1500884,1C1500885,1C1500886,1C1500887,1C1500888,1C1500889,1C1500890,1C1500891,1C1500892,1C1500893,1C1500894,1C1500895,1C1500896,1C1500897,1C1500898,1C1500899,1C1500900,1C1500901,1C1500902,1C1500903,1C1500904,1C1500905,1C1500906,1C1500907,1C1500908,1C1500909,1C1500910,1C1500911,1C1500912,1C1500913,1C1500914,1C1500915,1C1500916,1C1500917,1C1500918,1C1500919,1C1500920,1C1500921,1C1500922,1C1500923,1C1500924,1C1500925,1C1500926,1C1500927,1C1500928,1C1500929,1C1500930,1C1500931,1C1500932,1C1500933,1C1500934,1C1500935,1C1500936,1C1500937,1C1500938,1C1500939,1C1500940,1C1500941,1C1500942,1C1500943,1C1500944,1C1500945,1C1500946,1C1500947,1C1500948,1C1500949,1C1500950,1C1500951,1C1500952,1C1500953,1C1500954,1C1500955,1C1500956,1C1500957,1C1500958,1C1500959,1C1500950,1C1500951,1C1500952,1C1500953,1C1500954,1C1500955,1C1500956,1C1500957,1C1500958,1C1500959,1C1500960,1C1500961,1C1500962,1C1500963,1C1500964,1C1500965,1C1500966,1C1500967,1C1500968,1C1500969,1C1500970,1C1500971,1C1500972,1C1500973,1C1500974,1C1500975,1C1500976,1C1500977,1C1500978,1C1500979,1C1500980,1C1500981,1C1500982,1C1500983,1C1500984,1C1500985,1C1500986,1C1500987,1C1500988,1C1500989,1C1500990,1C1500991,1C1500992,1C1500993,1C1500994,1C1500995,1C1500996,1C1500997,1C1500998,1C1500999,1C15001000,1C15001001,1C15001002,1C15001003,1C15001004,1C15001005,1C15001006,1C15001007,1C15001008,1C15001009,1C15001000,1C15001001,1C15001002,1C15001003,1C15001004,1C15001005,1C15001006,1C15001007,1C15001008,1C15001009,1C15001010,1C15001011,1C15001012,1C15001013,1C15001014,1C15001015,1C15001016,1C15001017,1C15001018,1C15001019,1C15001010,1C15001011,1C15001012,1C15001013,1C15001014,1C15001015,1C15001016,1C15001017,1C15001018,1C15001019,1C15001020,1C15001021,1C15001022,1C15001023,1C15001024,1C15001025,1C15001026,1C15001027,1C15001028,1C15001029,1C15001020,1C1
```

LCP(HX, OFFY, CPHZ, X INT XINTD, BETA0, ALPRAO, XI, YI, ZI, AL, BL, CL, DP,
 LKP, LL, P, LMP, KKLMM, THETA1, PHI1, PHIP, T, RA, CKPP, CLP, P, CMPP
 ID1, C2, C3, X1R, Y1R, Z1R, QPL(1000), YIM(1000), ZIM(1000), DIM(1000),

MAJOR VARIABLE DEFINITIONS

A	:: STRENGTH OF INDEX CONSTANT
B	:: FOCAL LENGTH OF INDEX GRADIENT
F	:: INSIDE SURFACE CONE HALF-ANGLE
AL PR A	:: INCIDENT RAY OFFSET ANGLE
U	:: NUMBER OF ITERATIONS IN LENS CONSTRUCTION
T	:: MAXIMUM INSIDE SURFACE RADII'S FROM X-AXIS
R	:: NOTE THAT ALL DIMENSIONS REFERENCED TO THIS VALUE
N1, N3	:: THICKNESS OF LENS AT EDGE
CSYM B	:: INDICES OF REFRACTION OUTSIDE LENS
X	:: DISTANCE FROM CENTRE OF SYMMETRY TO INSIDE SURFACE
AL FAP	:: ALONG X-AXIS POSITION IF OPTIC LEFT OF B
GRID	:: ANGLE OF INCIDENT RADIATION FOR SKEW RAY TRACE
ENUM	:: GRID INCREMENT. DEFINES NUMBER OF SKEW RAYS
ELL	:: NUMBER OF ELLIPSSES MUST BE INTEGER AND ODD
	:: Z-COORDINATE INCREMENT FOR ELLIPSE PLUTS

OUTPUT OPTIONS:

TO HAVE LENS SHAPE DATA PRINTED SET "SHAPE" TO 1. OTHERWISE	SET "SHAPE"=0.
SET SHAPE=C	SET SHAPE=C
TO HAVE SKEW RAY AND MIRROR IMAGE SKEW RAY DATA PRINTED SET	"SQRAY" TO 1. ELSE SET "SQRAY" TO 0. (INTEGER)
SQRAY=C	SQRAY=C
TO HAVE ELLIPSE SHAPE DATA PRINTED SET "ELLIIPS" TO 1. OTHERWISE	SET "ELLIIPS"=0.
ELLIIPS=C	ELLIIPS=C
SET CONSTANTS	SET CONSTANTS
F=4.0	F=4.0
ALPRA=C	ALPRA=C
U=0.00000	U=0.00000
I=1C08	I=1C08
R=1.0	R=1.0
T=0.05	T=0.05
N1=1.0	N1=1.0
N3=1.0	N3=1.0

```

A=2.25
B=-C*5E4275
CSYB=-C550
P1=2.14592653589793
P12=P1/2.0
ALFAP=C0000
GRIL=0.150
ENUW=5
ELL=GRIC/7.5

C *****
C SECTION 1. FRONT SURFACE CONSTRUCTION
C *****
C BE TA=DATAN(F/(F-R*CCUTAN(ALPHA)))
C DL UDP=BETA/1
C BF=F/R
C WRITE(4,125)BF,ALPHA,ALFAP
C FFORMAT(4,125)
C 125 WRITE(6,100) ALPHA,BETA,R,L,I,T,NL,
C IF(SHAPE2C. 1) WRITE(6,100) ALPHA,BETA,R,L,I,T,NL,
C IN3,EF,CLUDP
C START LENS CONSTRUCTION BY TRACING OUTERMOST RAY
C FILTER=C
C J=1
C FIND OUTERMOST INSIDE SURFACE POINT
C UDP(J)=EETA
C X2(J)=(EF*D SIN(UDP(J)))/(DSIN(UDP(J))+CTAN(ALPHA))*DCOS(UDP(J))
C Y2(J)=(X2(J)*DTAN(ALPHA))
C CALCULATE ALL LINE CONSTANTS
C I2P(J)=ALPHA+DATAN((BF-X2(J))/Y2(J))
C R0=CSQRT((X2(J)+CSYMB)*Z2+Y2(J)**2)
C RZERO=R0
C IF(CSYMELT>0.6) RZERO=DSQRT(R**2+CSYME**2)
C CALL INCLEX(R0,N20,A,B,RZERO)
C I2(J)=CARSIN((N3/N20)*CSIN(I2P(J)))
C UP(J)=P12-ALPHA-I2(J)
C EA(1)=X2(J)+CSYMB
C IF(EA(X2(J)+CSYMB)=1.0000001*CSYME
C BASE=X2(J)+CSYMB

```

```

THEIAO=LATAN(Y2(J)/BASE)
IF(THETA0 .LT. 0.0) THETA0=PI+THETA0
ED=T/R
X1=X2(J)-ED*D COS(LP(J))
Y1=Y2(J)+ED*D SIN(LP(J))
BAS1=X1+CSYMB
IF(EAS1.EQ.0.0) SYMB=1.0000001*OSYMB
BAS1=X1+CSYMB
THEIAE=DATAN(Y1/BAS1)
IF(THETAE.LT.0.0) THETAE=PI+THETA0
PSIO=PI-LP(J)-THETA0
EPSION=+1.0
IF(PSI0.GT.PI2*OR.PS10.LT.0.0) EPSLCN=-1.0
E=N20*RC*D SIN(PS10)
ARG=ESGR(A**2+4*B*(E**2)/(RZERO**2))
ASIN=(2*(E**2)/(R0**2)-A)/ARG
C=P12-RSINO
IF(PS10.LT.PI2) C=0.0
TCRIT=THETA0-(EPSLN/2)*(PI2-RSINO)
IF(THETAE.GE.TCRIT) THETE=THETAE-C
IF(THETAE.LT.TCRIT) THETE=THETAE
IF(THETAE.GE.TCRIT) EPSLCN=+1.0
THETE=THETA-THETA0

C FIND RADIUS CORRESPONDING TO ANGLE SPECIFIED BY EDGE THICKNESS
NOTE THAT NO ITERATION REQUIRED FOR FIRST RAY
CALL RAYUSIA,E,ARG,R SINO,THETE,RAD,RDCTG,FILTER,EP SLUN
IF(FILTER.EQ.1) WRITE(6,1800)
IF(FILTER.EQ.1) GC1TG 82

C CALCULATE COORDINATES, ANGLE AND SLCFE FOR FRONT SURFACE SOLUTION
X1(J)=RAD*CCS(THETAE)-CSYMB
Y1(J)=RAD*SIN(THETAE)
CALL INCEX(RAD,N2,A,B,RZERG)
PSI=DARSIN(E/(N2*RAD))
IF(THETAE.LT.TCRIT) PSI=PI-PSI
ZETIA=PI-PSI-THETAE
II(SIN(ZETA-U))**2)/((DCCS(ZETA-U))**2+G1501640
1(U SIN(ZETA-U))**2)
IIPC(J)=CARSIN((N1/N2)*CSIN(II(J)))
DYCXN(J)=-DTAN((II(J)+U))
DYCXT(J)=DCUTAN((II(J)+U))
IF(SHAPE.EQ.0) GCTG5
MRIT(6200),DX1(J),Y1(J),X2(J),Y2(J),UP(J),IZ(J),UP(J),
IIIP(J),II(J),DYDX(J),CONTINUE

```

```

C END CF TRACE FOR 1ST RAY
C START ITERATIVE SOLUTION SCHEME
      K=I+1
      SURFL=C*J
      DO 10 I=P=0,K
      TRIP=1
      L=J-1

C CALCULATE INNER SURFACE COORDINATES
      UDP(J)=BETA-(L)*DLUDP
      X2(J)=(BF*D SIN(UDP(J)))/(DSIN(UDP(J))+DTAN(ALPHA))
      1   DCOS(UDP(J))
      Y2(J)=(X2(J)*DTAN(ALPHA)

C CALCULATE ALL LINE CONSTANTS
      RO=CSQRT((X2(J)+CSYMB)*#2+Y2(J)*#2)
      IF(J.EQ.K)R00=R0
      12 P(J)=ALPHA+DATAN((BF-X2(J))/Y2(J))
      CALL INDEX(R0,N20,A,B,RZERO)
      I2(J)=DARSIN((N3/N20)*DSIN(I2P(J)))
      LP(J)=PI/2-ALPHA-I2(J)
      THETAC=DATAN(Y2(J)/(X2(J)+OSYMB))
      IF(THETAO>0)THETAO=PI+THETAO
      PSIO=PI-LP(J)-THETAO
      EPSLCN=1.0
      IF(PSIO.GT.PI/2.OR.PSIO.LT.0.0)EPSLUN=-1.0
      E=N2C*R0*DSIN(PSIO)
      Y1H=((DCOTAN(L)+U)*DCOTAN(LP(J))*Y2(J))+(Y2(J))*
      X2(J)*DTAN(UP(J))+Y1H*(L)-X1H*(DCOTAN(UP(J))-
      1   (DCCTAN(L)+U)*DCOTAN(UP(J)))*(Y1H+Y2(J)+X2(J)*DTAN(UP(J)))
      X1H=((CCOTAN(UP(J)))*((L)-X1H+Y2(J)+X2(J)*DTAN(UP(J)))
      IF(B.EQ.0)GC1TC8
      ARG=CSQRT(A*#2+4*B*(E*#2)/(R0*#2)-A)/ARG
      RSINC=CSRSIN((2*(E*#2)/(R0*#2)-A)/ARG)
      C=PI/2-RSINO
      IF(PSIO.LT.P12)C=0
      TCRIT=THETAO-(EPSLCN/2.)*((P12-RSINO)
      THETAP=DATAN(Y1H/(X1HTSYMB))
      IF(THETAP.LT.0.C)THETAP=P1+THETAP
      RP=CSQRT((X1H+OSYMB)*#2+Y1H*#2)
      SL=CCCTAN((L)+L)
      EE=Y1H-SL*(X1H+CSYMB)

```

```

C IF ANGLE LARGE ENOUGH GO TO ANGLE IN TERMS OF RADIUS ITERATION
C IF( TETA0.GT.PI2 ) GO TO 106
C NEWTON-RAPHSON ITERATION

```

```

7
X1(J)=RAD*D COS( THETAP)-OSYMB
Y1(J)=RAD*D SIN( THETAP)
CALL INDEX(RAD,N2,A,B,RZERO)
EONR=E/(N2*RAD) WRITE(6,978) EONR
IF(ECNR.GT.0) WRITE(6,978) ECNR
9978 FORNAT(1,CGT,EONR=0,F19.16)
PSIP=DARSIN(EONR) ECNR=1.0
IF(TTETAP.LT.TCRITAND.PS10.GT.0.0) PSIP=PI-PSIP
ZETA=PI-PSI-TTHETAP
GO TO 9
C   CONTINUE
C   X1(J)=X1H
C   Y1(J)=Y1H
C   ZETA=LF(J)
C
C   CONTINUE
1  I F(Y1(J).LE.0.0) GO TO 11
    I I (D SIN(ZETA-U))**2/(DCOS(ZETA-U)-(N1/N2))**2
    I I P(J)=DARSIN((N1/N2)*DSIN(I1(J)))
    CYDX1(J)=(-DTAN((I1(J)+U))
    DYDX1(J)=DCOTAN((I1(J)+U))
    SLINCF=LSQRT((X1(J)-X1(L))*2+(Y1(L)-Y1(J))*2)
    SURFL=SURFL+SLINCR
    IF(STAPE.EQ.0) GO TO 10
    WRITE(6,200) J,X1(J),X2(J),Y1(J),Y2(J),UDF(J),I2P(J),I2I(J),
    10 CONTINUE
    GO TO 12
C
C   END OF TRACE FOR FRONT SURFACE CONSTRUCTION
C
C   opaque nse section calculations
11 CONTINUE
12 K=J-1
    AB=(-X1(K)+(Y1(K))/DYEXT(K))
    STATNA=-AE
    GAMMA=ATAN(DYEXT(K))
    CNP=(Y1(K))/SIN(GAMMA)
    TSURFL=(CNP*SURFL)
    WRITE(6,200) GAMMA,STATNA,CNP,SURFL,TSURFL
C
C   WRITE CINPUT FILE FOR PROGRAM CHECK

```



```

1 IF I=CEN+TORBI GO TO 20
1 IF RAYZ(G)=RAYZ(G)+GRID
1 GO TO 20
C 30 CONTINUE
N=N/2
IF(Y1(N)*LT. RAYZ(G)) GO TO 32
IF(RAYZ(G).GT. 1.15) GO TO 32
31 CONTINUE
IF(Y1(N).GT. RAYZ(G)) GO TO 36
IF(N=1) EQ. 0) GC TC 34
32 CONTINUE
N=N-1
33 CONTINUE
IF(Y1(N).GT. RAYZ(G)) GO TO 36
IF(N=1) EQ. 0) GO TO 34
GC TC 33
34 CONTINUE
RAYZ(G)=0.0
IF(RAYY(G)=RAYY(G)+GRID
GC TC 20
35 CONTINUE
RAYY(G)=RAYY(G)-GRID
GO TO 25
36 CONTINUE
RADIAS=SQR((RAYZ(G)**2+((RAYY(G)/CCS(ALFAP))-((X1(N)+AB)*
1 TAN(ALFAP))**2)
IF(Y1(N).GT. RADIAS) GO TC 40
IF(RADIUS .GT.Y1(N)) GO TO 37
N=N-1
GC TC 36
37 CONTINUE
IF(N = C1(i) + AB)*SIN(ALFAP)
CEN=(X1(i)*COS(ALFAP)
TURB=Y1(i)*COS(ALFAP)
RAYZ(G)=0.0
IF(RAYY(G)=RAYY(G)+GRID
ECT=CEN-TCR
CHECKFLR BOTTOM EDGE OF LENS, GO TO MIRROR IMAGE RAYS
IF(RAYY(G).LT. ECT) GO TO 60

```

```

      GO TO 2C
      38 CONTINUE
      RAY(G)=RAYY(G)+GRIC
      TU=CEM*TORE
      IF (RAYY(G) .GT. TOP) GC TO 39
      GO TO 20
      39 CONTINUE
      RAY(G)=-GRID
      GU TO 2C
      40 CONTINUE
      P=N+1

C   CALCULATE INTERCEPT POINT ON OUTER SURFACE
      AU=RAYY(G)/COS(ALFAP)
      BU=TAN(ALFAP)
      CD=(Y1(N)-Y1(P))/(X1(N)-X1(P))
      DO=X1(F)
      EU=Y1(F)
      PAR1=(AC*BO+CO*EO-(CU**2)*DU-AB*(BC**2))
      PAR2=(EC**2-CD**2)
      PAR3=(AC**2+AB*(BO**2)*AB-2.0*AC*BC*AB+
      1RAYZ(G)**2-(EO-CG*CO)**2)
      X0=(PAR1/PAR2)+SQR((PAR1/PAR2)**2-PAR3)
      IF ((PAR1/PAR2)<0) X0=X0-2.0*SQR((PAR1/PAR2)**2-PAR3)
      Y0=RAY(G)/COS(ALFAP)-(X0+AB)*TAN(ALFAP)
      ZD=RAYZ(G)

C   CALCULATE THE DIRECTION COSINES OF CUT SITE SURFACE NORMAL
      DELTAX=X1(N)-X1(P)
      DELTAY=Y1(N)-Y1(P)
      SP=DSUR1((RAD1US-Y1(P))**2+(X0-X1(P))**2)
      ST=SQRT(DELTA**2+DELTAY**2)
      RATIO=S/ST
      DYDXNP=DYDXN(N)-DYDXN(P)+DYDXN(F)
      NP=1.0/LDXNP
      IF (YO .EQ. 0.0) GO TO 41
      2YC=(ZCYC*GE-8235000)/8235000
      IF (ZCYC*LE. NPJ=LCSC(DATAN(ZC/YC))
      NPK=DSIN(DATAN(ZC/YC))
      GO TO 42
      41 CONTINUE
      NPJ=0
      NPK=1.0
      GU TO 42

```

```

42 CONTINUE
NPJ=0.0
NPK=-1.0
CONTINUE
DIRECTION COSINES OF EXTERNAL RAY
CK=COS(ALFAPI)
CL=-SIN(ALFAPI)

DIRECTION COSINES OF OUTSIDE SURFACE NORMAL
LK=NPI/(SQR(NPJ**2+NPJ**2+NPK**2))
LL=(NPJ*LK)/NPJ
LM=(NPK*LK)/NPJ
IF(YO-LI<0.0) GO TO 44
GO TO 45
CONTINUE
LL=-LL
LM=-LM
CONTINUE
THETA=ACOS(CK*LK+CL*LL)

ANGLES OF INCIDENCE AND REFRACTION OUTSIDE SURFACE
PHI=PI-IT-ETA
RO=DSQR((XL+0.0*SYMB)**2+YO**2+ZC**2)
CALL TANCE(XR0,N20,A'BRZERG)
AR=(N1/N20)*DSIN(PHI)
IF(ART<1.0) ART=1.0
IF(ART>1.0) ART=-1.0
PHIF=DASIN(ART)
IF(ART<-1.0) ART=-1.0

CALCULATION OF TRANSMITED INTENSITY AT CUTSIDE SURFACE
FACE=1
CALL XPLI(PH1,N20,XMTNC,FACE,XM,N1,N3)
IF(FACE=EQ.3) GO TO 53
NU=M=DCCSIPH1)-(N1/N20)*DCOS(PH1)

INITIAL DIRECTION COSINES OF INTERNAL REFRACTED RAY
CKP=(N1/N20)*CK-NU*KL
CMF=-NU*LN*CL-NU*KL
CKP=CKF
CLF=CLF
CMF=CMF

```

```

C INTERNAL RAY LENGTH AND INSIDE SURFACE INTERCEPT
C
C RO X=(XC+DSYMB)/RO
C RO Y=YC/FC
C RO Z=ZO/FC
C NP CX=RC1*CMR-R0Z*CLP
C NP CY=RC2*CKP-R0X*CMR
C NP CZ=RC3*CLP-R0Y*CKP
C NP Q=DSCRT(NFOX**2+NPOY**2+NPOZ**2)
C NP QX=NFCX/NPO
C NP QY=NFCY/NPO
C NP QZ=NFCZ/NPO

C CALCULATE FSIO AND THEN DETERMINE ITS SIGN
C
C PS10=UARCCOS(ROX*CKP+ROY*CLP+ROZ*CMR)
C IF (NPOZ*EC=0.0) XX=CSYMB*R0Z/(ROX*NPOY)*((NPCY*ROY+ROZ+NPOZ))
C IF (NPOZ*EC=0.0) GO TO 121
C XX=DSYMB*(ROX*NPOZ)*(NPOZ*ROZ/R0Y+NP0Y)
C
C CONTINUE
121 CCK=DSYMB/D SQR(T(DS YMB**2+XX**2))
C CL=0.0
C CN=XX/C SQR((SYMB**2+XX**2))
C IF (NPOZ*EC=0.0) CCL=XX/DSQRT((SYMB**2+XX**2))
C IF (NPOZ*EC=0.0) CCN=0.0
C IF (ETA1=F1-DARCOS(CCK*CKP+CCL*CLP+CCN*CMF))
C THETA2=LARCUS(CCK*CKP+CCL*CLP+CCN*CMF)
C FLUG=0
C IF (THETA1.GT.THETA2.AND.DSYM.B.LT.0.0) FLUG=1
C IF (FLUG.EC.1) PSIO=-PS10

C CALCULATE LINE CONSTANTS
C
C EPSLON=+1.0
C IF (PS10*CLT*PI2).AND.PS10.GT.PI2) EPSLON=-1.0
C E=N20*RC*CSIN(PS10)
C ARG=DSGRI(LA**2+4*B*E**2/RZERO**2)
C RSINO=LARSIN((2*E**2/R0**2-A)/ARG)
C F12=LARSIN(0.0)
C IF (PS10*CLT*PI2) C=0.0
C TCRIT=-EPSLCN/2*(PI2-RSINO)
C NUM1=(CLP*YC+CMR*ZC-CKP*X0*(DTAN(ALPHA)**2))*
C NUM2=(CLP**2+CMR**2-(CKP**2)*(DTAN(ALPHA)**2))*
C NUM3=(YC**2+Z0**2-(X0**2)*(DTAN(ALPHA)**2))*
C NUM4=NUM1**2-NUM2*NUM3

C CHECK FOR INTERCEPT WITH INSIDE SURFACE

```

```

C IF (NUM4 .LT. 0.0) GC TC 50
C CALCULATE FIRST GUESS POINT
D = -ALM1/NUM2-DSQRT( NUM4 )/NUM2
X1H = C2*CKP+X0
Y1H = C2*CLP+YC
Z1H = C2*CMR+ZO
1F(Z1H,LTH,O,O) GC TO 50
OSYMFH=DSQRT((CSYMB+X1H)**2+Y1H**2+Z1H**2)
OPHX=(CSYMB+X1H)/CSYMPH
OPHY=Y1H/CSYMPH
OPHZ=Z1H/CSYMPH
THETAP=LARCOS(ROX*CPhX+ROY*OPHY+ROZ*OPHZ)
RF=CSYMPH
IF (E EQ .0) GC TO 124
SIGN=-1.0
IF (CSYME GT .0) SIGN=+1.0
IF (FS10 .LT. 0.0) THETAP=-THETAP

C INITIALIZE SURF ROUTINE TO FIND CORRECT VALUE OF SIGN
CALL SURF( THETAP ,RADU,RDOTS,SIGN,FILTER,NPOX,NPOY,NFOZ,PS10,
1X0,Y0,Z0,CSYMB,R0,CKKP,CLLP,CMMR,ALPHA)
IF (RADU .LT. 0.0) SIGN=-SIGN
THETP=PI-THETA+THETAP
IF (ABS(PS10) .GT. 3.0 AND OCSYMB .LT. 0.0) GO TO 118

C CALL NEWTON-RAPHSON ITERATION IF ANGLE LARGE ENOUGH
IF (ABS(PS10) .GT. 3.0 AND OCSYMB .LT. 0.0)
1 CALL INTERZ(RP,THETAP,RAU,THTAP,A,E,ORG,RSIND,EPSON,SIGN,
NPOX,NPOY,NPOZ,PS10,X0,Y0,ZC,OSYMB,R0,CKKP,CLLP,CMMR,
ALPHA,THTAP,FLUG)
1 IF (ABS(PS10) .GT. 3.0 AND OCSYMB .LT. 0.0) GO TO 118

C CALL ANGLE IN TERMS OF RADIUS ROUTINE IN ANGLE SMALL ENOUGH
1 EPSON,CSYMB,FLUG
1 CALL INTER1(SIGN,THETAP,RADU,THTAP,FILTER,A,E,ARG,RSIND,
1 ALPHAA,CSYMB,FLUG)
11 E CCAINIE

C CHECK FOR FAILED RAYS
IF (FILTER .EQ. 2) GC TO 51
IF (FILTER .EQ. 3) GC TO 50
IF (FILTER .EQ. 4) GC TO 50

```

```

C          GU 1C 123
C          TH1TAP=THETAP
C          RAC=FP
C          CALCULATE ALL REQUIRED PARAMETERS AT SOLUTION POINT
C123      BE1AO=D SIN(THETAP)/D SIN(PSI0)
C          ALFA0=DCOS(THETAP)-BETA0*D COS(PSI0)
C          XI=RAD*(ALFA0*((X0+USYMB)/R0)+BETA0*CKKP)-USYMB
C          YI=RAD*(ALFA0*((Y0/R0)+BETA0*CLLF))
C          ZI=RAC*(ALFA0*((Z0/R0)+BETA0*CMNP))
C          CALL INDEX(RAD,N2A,B,RZERG)
C          ECNR=DAES(E/(N2*RAD))
C          IF(ECNR.GT.1.0) WRITE(6,9978) ECNR
C          IF(ECNR.LT.1.0) ECNR=1.0
C          PSIP=DARSIN(ECNR)
C          IF(USYMB.LT.0.0.AND.TCRIT.GT.THETAP) PSIF=PI-PSIP
C          CALCULATE REFRACTION CF RAY AT INNER SURFACE
C
C          A1=(YI+USYMB)/RAD
C          B1=YI/RAD
C          C1=2*YI/RAD
C          CALL DIRECT(CKP*CLP*CMPPDIR,A1,B1,C1,NPCX,NPOY,NPOZ,PSIP)
C          IF(XI**LT**0.0*CR*X1**GT*X2**1.0) GOTO 51
C          NUM2=DSQRT((XI**2)*(DTAN(ALPHA)**4)+YI**2+ZI**2)
C          DIRECTION COSINES CF INSIDE NORMAL
C
C          LKF=-XI*(DTAN(ALPHA)**2)/NUM5
C          LMF=YI/NUM5
C          KKLPM=CKP*LKP+CLP*LLP+CMPP*LMP
C          IF(KKLPM.GE.1.0) THETAI=0.0
C          IF(KKLPM.LE.-1.0) THETAI=PI
C          IF(LABS(KKLPM).GE.1.0) GO TO 457
C          THETAI=CARCOS((CKP*LKP)+(CLP*LLP)+(CMPP*LMP))
C          CCAINLE
C
C          ANGLES CF INCIDENCE AND TOTAL INTERNAL REFLECTION
C          AT THE INSIDE SURFACE:
C          PHI1=PI-THETAI
C          IF(FLG.EQ.1) PHI1=THETAI
C          TKA=DARSIN(N3/N2)
C          CHECK FOR TOTAL INTERNAL REFLECTION:

```

```

C IF(FRIP.EQ.TIRA) GO TO 52
C IF(FRIP=DARSIN((N2/N3)*DSIN(PHI1))
C
C CALCULATION OF TRANSMITTED INTENSITY AT INSIDE SURFACE
C
C CALL XMINT(PHI1,N2,XMTNCP,FACE,XM,N1,N3)
C NTACTY(G)=XM*INC*XMTNCP
C XAVE1=XMAVE+NTACTY(G)
C XAVE=XMAVE/(G*1.0)
C NLP8=DCOS(PHI1P)-(N2/N3)*DCOS(PHI1)
C
C CALCULATE DIRECTION COSINES OF INSIDE EXTERNAL REFRACTED RAY
C CORRECTING FOR RAYS PAST REGION OF NEAR-RADIAL LINES
C
C IF(FLUG.EQ.1) CKP=-CKP
C IF(FLUG.EQ.1) CLP=-CLP
C IF(FLUG.EQ.1) CMP=-CMP
C CLPP=(N2/N3)*CKP-NUM8*LP
C CLPP=(N2/N3)*CLP-NUM8*LLP
C CPP=(N2/N3)*CMP-NUM8*LMP
C
C WRITE OUTFILE FOR PROGRAM DEFLOT
C
C 126 WRITE(4,126) X1,Y1,Z1,CKPP,CLPP,CMP
C
C LENGTH OF INSIDE EXTERNAL REFRACTED RAY
C
C L2=(BF-X1)/CKPP
C NUM6=((X0+AB)*CK+Y0*CL)
C NLP7=((X0+AB)*(-CL)+Y0*CK)
C
C LENGTH OF OUTSIDE INCIDENT RAY
C
C L1=DSQRT((X0-NUM6)**2+(Y-C-NUM7)**2)
C
C TOTAL OPTICAL PATHLENGTH:
C
C FL(G)=N1*D1+N2*D2+N3*D3
C
C INTERSECTION WITH THE IMAGE PLANE:
C
C YIM(G)=(BF-X1)/CKPP)*CLPP+Y1
C ZIM(G)=(BF-X1)/CKPP)*CMP+Z1
C LIN(G)=DSQRT(YIM(G)**2+ZIM(G)**2)
C IF(DAES(YIM(G)).GT.1.0.OR.DAES(YIM(G)).LT.-1.0)
C     CALL SQR(YIM(G))
C
C 130
C 131
C 132
C 133
C 134
C 135
C 136
C 137
C 138
C 139
C 140
C 141
C 142
C 143
C 144
C 145
C 146
C 147
C 148
C 149
C 150
C 151
C 152
C 153
C 154
C 155
C 156
C 157
C 158
C 159
C 160
C 161
C 162
C 163
C 164
C 165
C 166
C 167
C 168
C 169
C 170
C 171
C 172
C 173
C 174
C 175
C 176
C 177
C 178
C 179
C 180
C 181
C 182
C 183
C 184
C 185
C 186
C 187
C 188
C 189
C 190
C 191
C 192
C 193
C 194
C 195
C 196
C 197
C 198
C 199
C 200
C 201
C 202
C 203
C 204
C 205
C 206
C 207
C 208
C 209
C 210
C 211
C 212
C 213
C 214
C 215
C 216
C 217
C 218
C 219
C 220
C 221
C 222
C 223
C 224
C 225
C 226
C 227
C 228
C 229
C 230
C 231
C 232
C 233
C 234
C 235
C 236
C 237
C 238
C 239
C 240
C 241
C 242
C 243
C 244
C 245
C 246
C 247
C 248
C 249
C 250
C 251
C 252
C 253
C 254
C 255
C 256
C 257
C 258
C 259
C 260
C 261
C 262
C 263
C 264
C 265
C 266
C 267
C 268
C 269
C 270
C 271
C 272
C 273
C 274
C 275
C 276
C 277
C 278
C 279
C 280
C 281
C 282
C 283
C 284
C 285
C 286
C 287
C 288
C 289
C 290
C 291
C 292
C 293
C 294
C 295
C 296
C 297
C 298
C 299
C 300
C 301
C 302
C 303
C 304
C 305
C 306
C 307
C 308
C 309
C 310
C 311
C 312
C 313
C 314
C 315
C 316
C 317
C 318
C 319
C 320
C 321
C 322
C 323
C 324
C 325
C 326
C 327
C 328
C 329
C 330
C 331
C 332
C 333
C 334
C 335
C 336
C 337
C 338
C 339
C 340
C 341
C 342
C 343
C 344
C 345
C 346
C 347
C 348
C 349
C 350
C 351
C 352
C 353
C 354
C 355
C 356
C 357
C 358
C 359
C 360
C 361
C 362
C 363
C 364
C 365
C 366
C 367
C 368
C 369
C 370
C 371
C 372
C 373
C 374
C 375
C 376
C 377
C 378
C 379
C 380
C 381
C 382
C 383
C 384
C 385
C 386
C 387
C 388
C 389
C 390
C 391
C 392
C 393
C 394
C 395
C 396
C 397
C 398
C 399
C 400
C 401
C 402
C 403
C 404
C 405
C 406
C 407
C 408
C 409
C 410
C 411
C 412
C 413
C 414
C 415
C 416
C 417
C 418
C 419
C 420
C 421
C 422
C 423
C 424
C 425
C 426
C 427
C 428
C 429
C 430
C 431
C 432
C 433
C 434
C 435
C 436
C 437
C 438
C 439
C 440
C 441
C 442
C 443
C 444
C 445
C 446
C 447
C 448
C 449
C 450
C 451
C 452
C 453
C 454
C 455
C 456
C 457
C 458
C 459
C 460
C 461
C 462
C 463
C 464
C 465
C 466
C 467
C 468
C 469
C 470
C 471
C 472
C 473
C 474
C 475
C 476
C 477
C 478
C 479
C 480
C 481
C 482
C 483
C 484
C 485
C 486
C 487
C 488
C 489
C 490
C 491
C 492
C 493
C 494
C 495
C 496
C 497
C 498
C 499
C 500
C 501
C 502
C 503
C 504
C 505
C 506
C 507
C 508
C 509
C 510
C 511
C 512
C 513
C 514
C 515
C 516
C 517
C 518
C 519
C 520
C 521
C 522
C 523
C 524
C 525
C 526
C 527
C 528
C 529
C 530
C 531
C 532
C 533
C 534
C 535
C 536
C 537
C 538
C 539
C 540
C 541
C 542
C 543
C 544
C 545
C 546
C 547
C 548
C 549
C 550
C 551
C 552
C 553
C 554
C 555
C 556
C 557
C 558
C 559
C 560
C 561
C 562
C 563
C 564
C 565
C 566
C 567
C 568
C 569
C 570
C 571
C 572
C 573
C 574
C 575
C 576
C 577
C 578
C 579
C 580
C 581
C 582
C 583
C 584
C 585
C 586
C 587
C 588
C 589
C 590
C 591
C 592
C 593
C 594
C 595
C 596
C 597
C 598
C 599
C 600
C 601
C 602
C 603
C 604
C 605
C 606
C 607
C 608
C 609
C 610
C 611
C 612
C 613
C 614
C 615
C 616
C 617
C 618
C 619
C 620
C 621
C 622
C 623
C 624
C 625
C 626
C 627
C 628
C 629
C 630
C 631
C 632
C 633
C 634
C 635
C 636
C 637
C 638
C 639
C 640
C 641
C 642
C 643
C 644
C 645
C 646
C 647
C 648
C 649
C 650
C 651
C 652
C 653
C 654
C 655
C 656
C 657
C 658
C 659
C 660
C 661
C 662
C 663
C 664
C 665
C 666
C 667
C 668
C 669
C 670
C 671
C 672
C 673
C 674
C 675
C 676
C 677
C 678
C 679
C 680
C 681
C 682
C 683
C 684
C 685
C 686
C 687
C 688
C 689
C 690
C 691
C 692
C 693
C 694
C 695
C 696
C 697
C 698
C 699
C 700
C 701
C 702
C 703
C 704
C 705
C 706
C 707
C 708
C 709
C 710
C 711
C 712
C 713
C 714
C 715
C 716
C 717
C 718
C 719
C 720
C 721
C 722
C 723
C 724
C 725
C 726
C 727
C 728
C 729
C 730
C 731
C 732
C 733
C 734
C 735
C 736
C 737
C 738
C 739
C 740
C 741
C 742
C 743
C 744
C 745
C 746
C 747
C 748
C 749
C 750
C 751
C 752
C 753
C 754
C 755
C 756
C 757
C 758
C 759
C 760
C 761
C 762
C 763
C 764
C 765
C 766
C 767
C 768
C 769
C 770
C 771
C 772
C 773
C 774
C 775
C 776
C 777
C 778
C 779
C 780
C 781
C 782
C 783
C 784
C 785
C 786
C 787
C 788
C 789
C 790
C 791
C 792
C 793
C 794
C 795
C 796
C 797
C 798
C 799
C 800
C 801
C 802
C 803
C 804
C 805
C 806
C 807
C 808
C 809
C 8010
C 8011
C 8012
C 8013
C 8014
C 8015
C 8016
C 8017
C 8018
C 8019
C 8020
C 8021
C 8022
C 8023
C 8024
C 8025
C 8026
C 8027
C 8028
C 8029
C 8030
C 8031
C 8032
C 8033
C 8034
C 8035
C 8036
C 8037
C 8038
C 8039
C 8040
C 8041
C 8042
C 8043
C 8044
C 8045
C 8046
C 8047
C 8048
C 8049
C 8050
C 8051
C 8052
C 8053
C 8054
C 8055
C 8056
C 8057
C 8058
C 8059
C 8060
C 8061
C 8062
C 8063
C 8064
C 8065
C 8066
C 8067
C 8068
C 8069
C 8070
C 8071
C 8072
C 8073
C 8074
C 8075
C 8076
C 8077
C 8078
C 8079
C 8080
C 8081
C 8082
C 8083
C 8084
C 8085
C 8086
C 8087
C 8088
C 8089
C 8090
C 8091
C 8092
C 8093
C 8094
C 8095
C 8096
C 8097
C 8098
C 8099
C 80100
C 80101
C 80102
C 80103
C 80104
C 80105
C 80106
C 80107
C 80108
C 80109
C 80110
C 80111
C 80112
C 80113
C 80114
C 80115
C 80116
C 80117
C 80118
C 80119
C 80120
C 80121
C 80122
C 80123
C 80124
C 80125
C 80126
C 80127
C 80128
C 80129
C 80130
C 80131
C 80132
C 80133
C 80134
C 80135
C 80136
C 80137
C 80138
C 80139
C 80140
C 80141
C 80142
C 80143
C 80144
C 80145
C 80146
C 80147
C 80148
C 80149
C 80150
C 80151
C 80152
C 80153
C 80154
C 80155
C 80156
C 80157
C 80158
C 80159
C 80160
C 80161
C 80162
C 80163
C 80164
C 80165
C 80166
C 80167
C 80168
C 80169
C 80170
C 80171
C 80172
C 80173
C 80174
C 80175
C 80176
C 80177
C 80178
C 80179
C 80180
C 80181
C 80182
C 80183
C 80184
C 80185
C 80186
C 80187
C 80188
C 80189
C 80190
C 80191
C 80192
C 80193
C 80194
C 80195
C 80196
C 80197
C 80198
C 80199
C 80200
C 80201
C 80202
C 80203
C 80204
C 80205
C 80206
C 80207
C 80208
C 80209
C 80210
C 80211
C 80212
C 80213
C 80214
C 80215
C 80216
C 80217
C 80218
C 80219
C 80220
C 80221
C 80222
C 80223
C 80224
C 80225
C 80226
C 80227
C 80228
C 80229
C 80230
C 80231
C 80232
C 80233
C 80234
C 80235
C 80236
C 80237
C 80238
C 80239
C 80240
C 80241
C 80242
C 80243
C 80244
C 80245
C 80246
C 80247
C 80248
C 80249
C 80250
C 80251
C 80252
C 80253
C 80254
C 80255
C 80256
C 80257
C 80258
C 80259
C 80260
C 80261
C 80262
C 80263
C 80264
C 80265
C 80266
C 80267
C 80268
C 80269
C 80270
C 80271
C 80272
C 80273
C 80274
C 80275
C 80276
C 80277
C 80278
C 80279
C 80280
C 80281
C 80282
C 80283
C 80284
C 80285
C 80286
C 80287
C 80288
C 80289
C 80290
C 80291
C 80292
C 80293
C 80294
C 80295
C 80296
C 80297
C 80298
C 80299
C 80300
C 80301
C 80302
C 80303
C 80304
C 80305
C 80306
C 80307
C 80308
C 80309
C 80310
C 80311
C 80312
C 80313
C 80314
C 80315
C 80316
C 80317
C 80318
C 80319
C 80320
C 80321
C 80322
C 80323
C 80324
C 80325
C 80326
C 80327
C 80328
C 80329
C 80330
C 80331
C 80332
C 80333
C 80334
C 80335
C 80336
C 80337
C 80338
C 80339
C 80340
C 80341
C 80342
C 80343
C 80344
C 80345
C 80346
C 80347
C 80348
C 80349
C 80350
C 80351
C 80352
C 80353
C 80354
C 80355
C 80356
C 80357
C 80358
C 80359
C 80360
C 80361
C 80362
C 80363
C 80364
C 80365
C 80366
C 80367
C 80368
C 80369
C 80370
C 80371
C 80372
C 80373
C 80374
C 80375
C 80376
C 80377
C 80378
C 80379
C 80380
C 80381
C 80382
C 80383
C 80384
C 80385
C 80386
C 80387
C 80388
C 80389
C 80390
C 80391
C 80392
C 80393
C 80394
C 80395
C 80396
C 80397
C 80398
C 80399
C 80400
C 80401
C 80402
C 80403
C 80404
C 80405
C 80406
C 80407
C 80408
C 80409
C 80410
C 80411
C 80412
C 80413
C 80414
C 80415
C 80416
C 80417
C 80418
C 80419
C 80420
C 80421
C 80422
C 80423
C 80424
C 80425
C 80426
C 80427
C 80428
C 80429
C 80430
C 80431
C 80432
C 80433
C 80434
C 80435
C 80436
C 80437
C 80438
C 80439
C 80440
C 80441
C 80442
C 80443
C 80444
C 80445
C 80446
C 80447
C 80448
C 80449
C 80450
C 80451
C 80452
C 80453
C 80454
C 80455
C 80456
C 80457
C 80458
C 80459
C 80460
C 80461
C 80462
C 80463
C 80464
C 80465
C 80466
C 80467
C 80468
C 80469
C 80470
C 80471
C 80472
C 80473
C 80474
C 80475
C 80476
C 80477
C 80478
C 80479
C 80480
C 80481
C 80482
C 80483
C 80484
C 80485
C 80486
C 80487
C 80488
C 80489
C 80490
C 80491
C 80492
C 80493
C 80494
C 80495
C 80496
C 80497
C 80498
C 80499
C 80500
C 80501
C 80502
C 80503
C 80504
C 80505
C 80506
C 80507
C 80508
C 80509
C 80510
C 80511
C 80512
C 80513
C 80514
C 80515
C 80516
C 80517
C 80518
C 80519
C 80520
C 80521
C 80522
C 80523
C 80524
C 80525
C 80526
C 80527
C 80528
C 80529
C 80530
C 80531
C 80532
C 80533
C 80534
C 80535
C 80536
C 80537
C 80538
C 80539
C 80540
C 80541
C 80542
C 80543
C 80544
C 80545
C 80546
C 80547
C 80548
C 80549
C 80550
C 80551
C 80552
C 80553
C 80554
C 80555
C 80556
C 80557
C 80558
C 80559
C 80560
C 80561
C 80562
C 80563
C 80564
C 80565
C 80566
C 80567
C 80568
C 80569
C 80570
C 80571
C 80572
C 80573
C 80574
C 80575
C 80576
C 80577
C 80578
C 80579
C 80580
C 80581
C 80582
C 80583
C 80584
C 80585
C 80586
C 80587
C 80588
C 80589
C 80590
C 80591
C 80592
C 80593
C 80594
C 80595
C 80596
C 80597
C 80598
C 80599
C 80600
C 80601
C 80602
C 80603
C 80604
C 80605
C 80606
C 80607
C 80608
C 80609
C 80610
C 80611
C 80612
C 80613
C 80614
C 80615
C 80616
C 80617
C 80618
C 80619
C 80620
C 80621
C 80622
C 80623
C 80624
C 80625
C 80626
C 80627
C 80628
C 80629
C 80630
C 80631
C 80632
C 80633
C 80634
C 80635
C 80636
C 80637
C 80638
C 80639
C 80640
C 80641
C 80642
C 80643
C 80644
C 80645
C 80646
C 80647
C 80648
C 80649
C 80650
C 80651
C 80652
C 80653
C 80654
C 80655
C 80656
C 80657
C 80658
C 80659
C 80660
C 80661
C 80662
C 80663
C 80664
C 80665
C 80666
C 80667
C 80668
C 80669
C 80670
C 80671
C 80672
C 80673
C 80674
C 80675
C 80676
C 80677
C 80678
C 80679
C 80680
C 80681
C 80682
C 80683
C 80684
C 80685
C 80686
C 80687
C 80688
C 80689
C 80690
C 80691
C 80692
C 80693
C 80694
C 80695
C 80696
C 80697
C 80698
C 80699
C 80700
C 80701
C 80702
C 80703
C 80704
C 80705
C 80706
C 80707
C 80708
C 80709
C 80710
C 80711
C 80712
C 80713
C 80714
C 80715
C 80716
C 80717
C 80718
C 80719
C 80720
C 80721
C 80722
C 80723
C 80724
C 80725
C 80726
C 80727
C 80728
C 80729
C 80730
C 80731
C 80732
C 80733
C 80734
C 80735
C 80736
C 80737
C 80738
C 80739
C 80740
C 80741
C 80742
C 80743
C 80744
C 80745
C 80746
C 80747
C 80748
C 80749
C 80750
C 80751
C 80752
C 80753
C 80754
C 80755
C 80756
C 80757
C 80758
C 80759
C 80760
C 80761
C 80762
C 80763
C 80764
C 80765
C 80766
C 80767
C 80768
C 80769
C 80770
C 80771
C 80772
C 80773
C 80774
C 80775
C 80776
C 80777
C 80778
C 80779
C 80780
C 80781
C 80782
C 80783
C 80784
C 80785
C 80786
C 80787
C 80788
C 80789
C 80790
C 80791
C 80792
C 80793
C 80794
C 80795
C 80796
C 80797
C 80798
C 80799
C 80800
C 80801
C 80802
C 80803
C 80804
C 80805
C 80806
C 80807
C 80808
C 80809
C 80810
C 80811
C 80812
C 80813
C 80814
C 80815
C 80816
C 80817
C 80818
C 80819
C 80820
C 80821
C 80822
C 80823
C 80824
C 80825
C 80826
C 80827
C 80828
C 80829
C 80830
C 80831
C 80832
C 80833
C 80834
C 80835
C 80836
C 80837
C 80838
C 80839
C 80840
C 80841
C 80842
C 80843
C 80844
C 80845
C 80846
C 80847
C 80848
C 80849
C 80850
C 80851
C 80852
C 8
```

```

1 1.0) IF(CMPP .LT. 0.00000000001 .AND. CMPP .GT. -0.00000000001) G1507210
1 GO TO 46 G1507220
1 XDIAPT(G)=(-ZIY(G)/CMPP)*CKFP+AE G1507230
1 YDIAPT(G)=(-ZIY(G)/CMPP)*CLFP+YM(G) G1507240
1 GO TO 47 G1507250
46 CONTINUE G1507260
46 XDIAPT(G)=99999. G1507270
46 YDIAPT(G)=99999. G1507280
47 CONTINUE G1507290
1 IF(SQURAY(EQ.1) WRITE(6,500)G,RAYZ(G),RAY(Y(G),XDIAPT(G),YDIAPT(G)) G1507300
1 YIZIOPL(G),YM(G),NTRCY(G),NTRCY(G),XDIAPT(G),YDIAPT(G) G1507310
1 FLAG(G)=0 G1507320
48 CONTINUE G1507330
H=G G1507340
G=F+1 G1507350
NTACTY(G)=1.0 G1507360
RAYY(G)=RAY(H) G1507370
RAYZ(G)=RAY(H)+GRID G1507380
IF(FLAG(H).EQ.0) COUNT=COUNT+1 G1507390
GO TO 47 G1507400
C
C END OF FAY TRACE G1507420
C
C FLAG ALL FAILED RAYS G1507430
C
C NO INTERCEPT WITH 2ND SURFACE G1507440
C
C 50 NTACTY(G)=0.0 G1507450
C FLAG(G)=1 G1507460
C IF(SQURAY .EQ. 1) WRITE(6,600)G,RAY(Y(G),RAYZ(G) G1507470
C GO TO 45 G1507480
C INTERCEFT OUTSIDE BOUNDARY OF SECOND SURFACE G1507490
C NTACTY(G)=0.0 G1507500
C FLAG(G)=2 G1507510
C IF(SQURAY .EQ. 1) WRITE(6,700)G,RAY(Y(G),RAYZ(G) G1507520
C GO TO 45 G1507530
C TOTAL INTERNAL REFLECTION AT 2ND SURFACE E G1507540
C FLAG(G)=2 G1507550
C IF(SQURAY .EQ. 1) WRITE(6,800)G,RAY(Y(G),RAYZ(G) G1507560
C GO TO 45 G1507570
C TOTAL EXTERNAL REFLECTION G1507580
C NTACTY(G)=0.0 G1507590
C FLAG(G)=4 G1507600
C IF(SQURAY .EQ. 1) WRITE(6,802) G,RAY(Y(G),RAYZ(G) G1507610
C GO TO 45 G1507620
C RAY(Y(G))=LENS DIAMETER G1507630
C NTACTY(G)=0.0 G1507640
C 53
C 54
C 55

```

```

C150 7690
C150 7700
C150 7710
C150 7720
C150 7730
C150 7740
C150 7750
C150 7760
C150 7770
C150 7780
C150 7790
C150 7800
C150 7810
C150 7820
C150 7830
C150 7840
C150 7850
C150 7860
C150 7870
C150 7880
C150 7890
C150 7900
C150 7910
C150 7920
C150 7930
C150 7940
C150 7950
C150 7960
C150 7970
C150 7980
C150 7990
C150 8000
C150 8010
C150 8020
C150 8030
C150 8040
C150 8050
C150 8060
C150 8070
C150 8080
C150 8090
C150 8100
C150 8110
C150 8120
C150 8130
C150 8140
C150 8150
C150 8160
C150 8170
C150 8180
C150 8190
C150 8200
C150 8210
C150 8220
C150 8230
C150 8240
C150 8250
C150 8260
C150 8270
C150 8280
C150 8290
C150 8300
C150 8310
C150 8320
C150 8330
C150 8340
C150 8350
C150 8360
C150 8370
C150 8380
C150 8390
C150 8400
C150 8410
C150 8420
C150 8430
C150 8440
C150 8450
C150 8460
C150 8470
C150 8480
C150 8490
C150 8500
C150 8510
C150 8520
C150 8530
C150 8540
C150 8550
C150 8560
C150 8570
C150 8580
C150 8590
C150 8600
C150 8610
C150 8620
C150 8630
C150 8640
C150 8650
C150 8660
C150 8670
C150 8680
C150 8690
C150 8700
C150 8710
C150 8720
C150 8730
C150 8740
C150 8750
C150 8760
C150 8770
C150 8780
C150 8790
C150 8800
C150 8810
C150 8820
C150 8830
C150 8840
C150 8850
C150 8860
C150 8870
C150 8880
C150 8890
C150 8900
C150 8910
C150 8920
C150 8930
C150 8940
C150 8950
C150 8960
C150 8970
C150 8980
C150 8990
C150 9000
C150 9010
C150 9020
C150 9030
C150 9040
C150 9050
C150 9060
C150 9070
C150 9080
C150 9090
C150 9100
C150 9110
C150 9120
C150 9130
C150 9140
C150 9150
C150 9160
C150 9170
C150 9180
C150 9190
C150 9200
C150 9210
C150 9220
C150 9230
C150 9240
C150 9250
C150 9260
C150 9270
C150 9280
C150 9290
C150 9300
C150 9310
C150 9320
C150 9330
C150 9340
C150 9350
C150 9360
C150 9370
C150 9380
C150 9390
C150 9400
C150 9410
C150 9420
C150 9430
C150 9440
C150 9450
C150 9460
C150 9470
C150 9480
C150 9490
C150 9500
C150 9510
C150 9520
C150 9530
C150 9540
C150 9550
C150 9560
C150 9570
C150 9580
C150 9590
C150 9600
C150 9610
C150 9620
C150 9630
C150 9640
C150 9650
C150 9660
C150 9670
C150 9680
C150 9690
C150 9700
C150 9710
C150 9720
C150 9730
C150 9740
C150 9750
C150 9760
C150 9770
C150 9780
C150 9790
C150 9800
C150 9810
C150 9820
C150 9830
C150 9840
C150 9850
C150 9860
C150 9870
C150 9880
C150 9890
C150 9900
C150 9910
C150 9920
C150 9930
C150 9940
C150 9950
C150 9960
C150 9970
C150 9980
C150 9990
C150 9999
C56
      COUNT2=COUNT2+1
      FLAG(G)=5
      IF (SQRAY .EQ. 1) WRITE(6, 804) G, RAYZ(G), RAYZ(G)
      GU TO 45
      FAILED INTER2 SUBRCLINE
      NINCY(G)=0.0
      IF (SQRAY .EQ. 1) WRITE(6, 806) G, RAYZ(G), RAYZ(G)
      GU TO 45
C
C MIRROR IMAGE RAY MATCHING FOLLOWS
C
C 6C CONTINUE
      IF (SQRAY .EQ. 1) WRITE(6,401)
      Q=G-1
      S=G-T
      61 COUNT1NE
      IF (RAYZ(S)-Q) .EQ. 0.0) S=S+1
      IF (S .GT. Q) =FLAG(G)=FLAG(S) 0) COUNT=COUNT+1
      IF (FLAG(G)=RAYZ(S))
      RAYZ(G)=RAYZ(S)
      IF (FLAG(S) .GE. 1) GU TO 63
      IF (XIAP(G) .EQ. XIAP(S))
      YIAP(G) =YIAP(S)
      YIM(G)=YIM(S)
      ZIM(G)=ZIM(S)
      CFLAG(G)=OPL(S)
      INACTY(G)=INACTY(S)
      INACTY(G)=INACTY(S)
      IF (SQRAY .EQ. 1) WRITE(6,501) G, RAYZ(G), RAYZ(G), OPL(G),
      1 COUNT1NE
      YIM(G), ZIM(G), INACTY(G)
      S=S+1
      G=G+1
      GU TO 61
      62 COUNT1NE
      FLAG ALL MIRROR IMAGE RAYS
C
C 63 NO INTERFACE WITH 2ND SURFACE
      IF (FLAG(S) .GT. 1) GO TO 64
      IF (SQRAY .EQ. 1) WRITE(6,601) G, S, RAYZ(G), RAYZ(G)
      COUNT2=2
      INTERFACE OUTSIDE BOUNDARY OF 2ND SURFACE
      IF (FLAG(S) .GT. 2) GO TO 65
      IF (SQRAY .EQ. 1) WRITE(6,701) G, S, RAYZ(G), RAYZ(G)
      COUNT2=2
      TOTAL EXTERNAL REFLECTION
      IF (FLAG(S) .GT. 2) GU TO 66

```

```

C IF (SQUAREY .EQ. 1) WRITE(6,801) G,S,RAYX(G),RAYZ(G)
GO TO 64
CONTINUE
IF (FLAG(S) .EQ. 4) GO TO 67
IF (SQUAREY .EQ. 1) WRITE(6,803) G,S,RAYX(G),RAYZ(G)
GO TO 64
RAY SIDE LENS DIAMETER
IF (SQUAREY .EQ. 1) WRITE(6,805) G,S,RAYX(G),RAYZ(G)
COUNT2=CLNT2+1
GO TO 64
C
C 66 CONTINUE
RAYSS=RAYS-G
WRITE(6,135G) OSYMB,RZERO
WRITE(6,600) RAYS,COUNT2,COUNT
XI=1.0
YT=1.0
ZI=1.0
FORMAT(4.127) X1,Y1,ZI,CKPP,CLPP,CMPP
FORMAT(4.128)
FORMAT(1,*)
C
C 67 GENERATE OBJECT PLANE ELLIPSES:
IF (ELLIPS .EQ. 1) WRITE(6,1000) ENUM
NUMBER=1
NUMBER=1
CONTINUE
COCRD=-Y1(NUMBR)
ELZ(NUMR,COORD)=COCRD
CONTINUE
ELZ(NUMR,COORD)=(X1(NUMBR)+AB)*SIN(ALFAP)+DSQRT((Y1(NUMBR))**2-
1*ELZ(NUMR,COORD)*#2)*COS(ALFAP)
1 ELZ=ELZ(NUMR,COORD)
IF (ELLIPS .EQ. 1) WRITE(6,1100) NUMBER,COORD,ELY(NUMR,COORD),
1 COORD=CCRC+1
ELZ(NUMR,COORD)=ELZZ+ELL
IF (ELZ(NUMR,COORD) .GE. Y1(NUMBR)) GO TO 73
IF (ELZ(NUMR,COORD) .LT. -Y1(NUMBR)) GO TO 74
CONTINUE
ELZ=ELZ(NUMR,COORD)
IF (ELZ(NUMR,COORD)=(X1(NUMBR)+AB)*SIN(ALFAP)-DSQRT((Y1(NUMBR))**2-
1*(ELZ(NUMR,COORD)*#2)*COS(ALFAP))
1 ELZ=ELZ(NUMR,COORD)
CONTINUE
ELZ=ELZ(NUMR,COORD)

```

```

EL22=ELL2(NUMB,CCRC)
IF(EL22.EQ.1) WRITE(6,100) NUMBER,CORD,ELY(NUMB,CORD),
  CUCR(CALC)=COORD
  CORD=CCRD+1
  GO TO 74
75  COUNTLE
  NUMBER=NUMBER+(K-1)/ELLNLM
  NUMBER=NUMBER+1
  IF (NUMBER .GT. K) GO TO 76
  GO TO 71
76  COUNTLE
  IF(EL22.EQ.1) WRITE(6,1200)
  NUMBER=NUMBER-1

```

C IMAGE PLANE SPOT DIAGRAM STATISTICAL ANALYSIS:

```

SUM1=0.C
DO 77 G=1 RAYS
  IF(FLAG(G).GT.SUM1) GC TO 77
  SUM1=YIM(G)+SUM1

```

C 77 CONTAINE
 REFERENCE EACH ITERATION TC INCIDENT ANGLE & THICKNESS BY:

```

  IANGLE=ALFAP*10+
  THICK=(1/R)*100
  CENTER(CCF,SPOT):
  YCENTRA(IANGLE,THICK)=SUM1/COUNT
  STANDARDE(DEViations):
  SUM2=0.C
  SUM3=0.C
  DU 78 G=1 RAYS
  IF(FLAG(G).GT.0) GO TO 78
  SUM2=IM(G)*#2+SUM2
  SUM3=(CENTR(IANGLE,THICK)-YIM(G))**2+SUM3

```

C 78 CONTAINE
 SIGMAZ(IANGLE,THICK)=SUM2/COUNT
 SIGMAY(IANGLE,THICK)=SUM3/COUNT
 ROCT_MEAN_SQUARE(SPECT_SIZE):
 RMSRAD(IANGLE,THICK)=SQRT(SIGMAZ(IANGLE,THICK)+SIGMAY(IANGLE,
 THICK))
 WRITE(6,1300) I*U,ALFAP,R,YCENTR(IANGLE,THICK),RMSRAD(IANGLE,THICK),
 1SIGMAY(IANGLE,THICK),SIGMAZ(IANGLE,THICK)-YIM(G)**2+SUM2
 SP CT DIAGRAM ENERGY DENSITY VS. RADIUS FROM CENTRO ID:

```

DO 79 G=1 RAYS
  IF(FLAG(G).GT.0) GC TU 79
  SQR(G)=DSQRT((YCENTR(IANGLE,THICK)-YIM(G))**2+SUM2)

```



```

SC CUNTINLE
91 WRITE(1,14)
14 FORMAT(1X,14,7F10.7)
DO 56 NMB=1,NUMBT
56 WRITE(1,S2) CDR (NUMB)
92 FORMAT(1X,13)
CD S2 CCRD=1,CDRT
DC S2 CCRD=1,CDRT,NMB,COORD,EZL(NUMB,CCRD)
94 WRITE(1,94) ELY(NMB,COORD),EZL(NUMB,CCRD)
95 FORMAT(1X,14)
96 CONTINUE
97 FORMAT(1X,14,*)
C FORMAT STATEMENTS
10C FORMAT(1X,14,7F10.7//5X,14,7F10.7)
11C BETA = 1.9*2X,1ITERATION = 15/5X,INCIDENT ANGLE = 0,
11F9*6X,1ITERATION = 15/5X,EDGE THICKNESS = 0,F9.7,2X;
11C INDICES OF REFRACTION: N1 = F7*5/5X,N3 = F7.5,2X;
11F7*5/2X,1REFRACTION FROM STATION ZERO = F7.5,2X,
11DELTA UCP = F7.5//,1TOTAL LENS SURFACE LENGTH = 12P
11X, J 12//25X,1LP 11P 11 Y2 YDXT//,12P
200 FORMAT(1X,14,7F10.7//20X4F10.7//)
30C FORMAT(1C/1X,1NOSE SECTION DATA: //2X,1NOSE HALF ANGLE = 0,
11F7*5/2X,1OPACUE SURFACE LENGTH = 0,F7.5/2X,1TOTAL LENS SURFACE LENGTH
11TRANSFAREN T SURFACE LENGTH = F7.5/2X,1
11FORMAT(1X,1SKIN RAY TRACE PARAMETERS: //5X,1ALFAP = 0,F9.7,2X,
11GRID=0,F9.7,2X,1SEE LENS PARAMETERS ABOVE: //2X,1RAY
11RAY X0 YG XI YI ZIM NTNCY XCIAPT
1PL 400 FORMAT(1X,1MIRROR IMAGE SKIN RAYS FULLCW//1X,1IMAGE//2X,1RAY
1Y RAY RAY ZIM NTNCY XCIAPT
1Y,1RAY ZIM NTNCY XCIAPT
50C FORMAT(1X,14,7F10.7/8X,F13.9,3F10.7,2E13.3//)
50C FORMAT(14,1X,14,2F10.7,1C INTERCEPT WITH 2ND SURFACE//)
60C FORMAT(1X,14,2F10.7,1C INTERCEPT WITH 2ND SURFACE//)
60C FORMAT(1X,14,2F10.7,1C INTERCEPT OUTSIDE BOUNDARY OF 2ND SURFACE//)
70C FORMAT(1X,14,2F10.7,1C INTERCEPT OUTSIDE BOUNDARY OF 2ND SURFACE//)
70C FORMAT(1X,14,2F10.7,1C INTERCEPT CUTSIDE BOUNDARY OF 2ND SURFACE//)
800 FORMAT(1X,14,2F10.7,2X,1TOTAL INTERNAL REFLECTION AT 2NL SURFACE//)
801 FORMAT(1X,14,2F10.7,1TOTAL INTERNAL REFLECTION//)

```

SUBROUTINE INDEX CALCULATES THE INDEX OF REFRACTION AS A FUNCTION OF RADIALS FROM THE CENTER OF SYMMETRY. THE VALUES OF THE INDEX CONSTANTS AND THE ARE USER INPUTS.

SUBROUTINE INDEX(R,N,A,B,RZERO)

```

DOUBLE PRECISION R,N,A,B,RZERO
N=DSQR(1.0+B*(R/RZERO))**2
RETURN
END

```

```

C SUBROUTINE TRANSMIT(XM1,N1,FACE,XM2,N2,SQRT,COS
EACH RAY AT BOTH THE OUTSIDE AND INSIDE SURFACES USING THE
FRESNEL EQUATIONS.


```

```

SUBROUTINE XM1(N1,N2,FACE,XM1,N1,N2,SQRT,COS
REAL PHI,N3,XM1,N1,FACE,XM2,N2,SQRT,COS
INTEGER N1,N2,N3
IF(FACE.EQ.-2)N1=N3/N2
IF(FACE.EQ.-2)-(SIN(PHI)**2)
IF(VALUE.LT.0.0)GOTO 10
SQ=SQR(1.0-VALLE)
CUPR=CCSP/(PHI)
RPAR=((N1**2)*(COSr-SQ)/(N1**2)*(CCSP+SQ))
RPAR=((N1**2)*(COSr-SQ)/(N1**2)*(CCSP+SQ))
XN1=1.0-15*(RPER**2+RPAR**2)
RE TURN
1C CONTINUE
FACE=3
RE TURN
END

```

```

CCCCCCC

```

92

```

C SUBROUTINE RADYUS CALCULATES THE RADIAL DIMENSION FROM THE CENTER
RADYUS TO THE RAY AT THE ANGLE SPECIFIED.
RADYUS ALSO FINDS DR(D(THETA)) FOR SURFACE FILTER.
SUBROUTINE RADYUS(A,E,ARG,RSINC,ANGLE,R,DR,FILTER,EPSON)
REAL EPSON
COLEBLER(FRECIION ANGLE,R,DR,ARG,RSINC,FRACTN,A,E
INTEGER J,FILTER
FRACTN=ESIN(-2.0*EPSLN)
IF((A+AFG**FRACTN).LE.0.0)GOTO 10
R=SQRT((0.0*DABSN(E)/DARG*FRACTN)
DR=(EFFSLCN*R**3)/(2.0*E**2)*DCOS(-2.0*EPSON*ANGLE+K SINU)*ARG
1C CONTINUE
FILTER=0
IF((A+AFG*FRACTN).LT.0.0) FILTER=1
RE TURN
END

```

```

C SUBROUTINE RADUS CALCULATES THE RADIUS TO THE FRONT SURFACE AT

```

C THE SPECIFIED ANGLE AND ALSC FINDS ITS DERIVATIVE WITH RESPECT
C TO ANGLE.

```
C SUBROUTINE RADUS(X1,X1,Y1,Y1,U,CSYME,THEETAP,RADD,RDCT,PI,PI2,CSYMB
C DOUBLE PRECISION X1,Y1,U,CSYME,THEETAP,RADD,RDCT,PI,PI2,CSYMB
C PI2=PI/2
C S=DCOTAN((1+U)
C B=Y1-S*(X1+CSYMB)
C RADD=B/(DCOS(THETAP)-S*DCOS(THETAP))
C RUG=B*(DCOS(THETAP)+S*DSIN(THETAP))/(
C ((CSIN(THETAP)-S*DCCS(THETAP))*#2)
C RETURN
C END
```

C SUBROUTINE INTERCEP PERFORMS ITERATION TO FIND R AND THE TAP
C OF THE INTERCEPT OF THE GRINSKEW-RAY AND THE INSIDE CONICAL
C SURFACE USING THE NEWTON-RAPHSON ITERATION PROCEDURE.

```
C SUBROUTINE INTERSIGN THETA,R,THEETAP,FILTER,A,E,ARG,K,SINO,
1EPSLON,C,TCRIT,NPOXY,NPOZ,PSIO,XO,YC,ZO,RO,CKKP,CLLP,
1CMMP,ALFFACSYMB,FLUG
INTEGER LCCPFILTER,FLUG
REAL REALSEGMENTEPSILON
DOUBLE PRECISION THETA,R,THEETAP,A,E,ARG,K,SINO,RO,CSYMB,
1ALPHA,RADD,FX,FDCT,RDCT,DX,NEWDF,C,FACTR,PSIO,
1FACTOR,EXIT,THEETAP,PI,XO,YU,ZC,NPOX,NFOY,NPOZ,CKKP,CLLP,CMMPP
```

```
C LOCPE=0
C FILTER=(141592653589793
C PI=3.141592653589793
1C CONTINUE
C THEET=THEETAP
C IF (THEETA-GT-TCRIT) THEET=THEET-A
C IF (THEETA-GT-TCRIT) EPSLON=+1.0
C CALL RACEYUS(A,E,ARG,K,SINO,THEET,RADG,RDCT,FILTER,EP SLUN)
C IF (FILTER-EQ.1) RETURN
C IF (FILTER-EQ.2) RETURN
C CALL SURF(THEETA,RAEYH,RDCTS,SIGN,FILTER,NPOX,NPOY,NPOZ,PSIO,XU,
1YO,ZO,CSYMB,RO,CKKP,CLLP,CMMPP,ALPHA)
C IF (FILTER-EQ.3) RETURN
C FX=RADG-RDH
C FXCCT=FLCTG-RDOTS
C FACTOR=1.7/(DABS(P1-PS10))**.5
C IF (CSYME-GT.0) FACTR=1.3
C XNEW=THEETA-(FX/FDCT)/FACTOR
C DIFF=DAB*(THEET-XNEW)
C EXIT=0.00001*DABS(P1-PS10)
C IF (CSYME-GT.0) EXIT=0.0000001
```

```

IF (DIF .GT. EXIT) GO TO 20
THE TAP = TETAP
R=RADS
RETURN
2C CONTINUE
IF (LLOCF .GE. 90) GO TO 30
LLOCF=LCCP+1
THE TETAP=XNEW
GO TO 1C
30 CONTINUE
IF (LLOCF .GE. 90) FILTER=3
IF (LLOCF .LT. 64) FILTER=1
IF (LLOCF .EQ. 64) FILTER=0
IF (LLOCF .EQ. 90) FILTER=3
IF (LLOCF .LT. 1X) SOLUTION NOT FOUND
RETURN
ENC

C SUBROUTINE INTERCEPT2 PERFORMS ITERATION TO FIND THE ANGLE IN
C THE GRIN RAY AND THE INSIDE SURFACE USING THE ANGLE IN
C TERMS OF RADII PROCEDURE.
C
C SUBROUTINE INTER2(RPTTETAP, RPP, THETAP, E, ARG, RSIN, EP SLN,
1 SIN, NPCX, NPOY, NPOZ, PSIO, X0, Y0, Z0, CSYMB, RO, CKKP, CLLP, CMMMP,
1 INTEG, ERTR, FILTER, FLUG)
REAL SIGN, EPSLN
DOUBLE PRECISION RP, THETAP, RPP, A, E, ARG, RSIN, OSYMB
1PS10, RCALPHA, RSIN, CHECK1, CHECK2, THETA, THATF, RDOT, ARSH,
1XU, Y0, ZC, NPCX, NPOY, NP0Z, CKKP, CLLP, CMMPP, ALPHAD,
FILTER=C
TK1P=0
TK2P=TRIP+1
ARG=(E*#2/RP*#2-A)/ARG
IF (DAB(LARGH).GT.1.0) GC TC 50
RSIN=CAFSIN(ARGH)
THETP=-EPSLN/2*(RSIN-RSIN0)
CHECK1=TETPP-THETAP
CALL SURF(TETPP, RPP, RDOT, SIGN, FILTER, NPOX, NPOY, NP0Z, PS10, XU,
1Y0, Z0, CSYMB, RO, CKKP, CLLP, CMMPP, ALPHAD)
CHECK2=ABS(IRP-RPP)
RP=RPP
THE TAP = TETPP
IF (TRIP.GT.100) GO TO 20
IF (CHECK2.LT..000001) GO TO 20
GO TO 1C
THE TAP = TETAP
RETURN
ENC
C
20
50

```

SUBROUTINE SURF CALCULATES BOTH THE RADIUS TO THE LOCUS OF THE INTERCEPT OF THE RAY PLANE AND THE INSIDE SURFACE AND THE DERIVATIVE OF THE RADIUS WRT THETA GIVEN THE ANGLE THETA. SURF IS DESIGNED PRIMARILY FOR USE WITH SUBROUTINES INTERCEPT1 AND INTERCEPT2.

```

SUBROUTINE SURF(THETA,R,ROOT,SIGN,FILTER,NPCX,NPOY,NPOZ,PS10,X0,
  1 YU120E,YN120E,B120E,CKKP,CCKP,CMP,CMPP,ALPHA)
  1 INTEGER FILTER
  REAL XC,YC,ZO,NPOX,NPOY,NPOZ,CCKP,CCKP,CMP,CMPP,SIGN
  DOUBLE PRECISION THETA,R,ROOT,PS10,CSYME
  DRO,ALFA,DRC,DC,DZ,A1,A2,A3,B1,B2,B3,C1,C2,C3
  ICAL,DBE,DSIN,(THETA)-DCSIN(PS10)
  ALFA=DSIN((THETA)/DSIN(PS10))
  A=ALFA*(XC+CSYMB)/R+Beta*CKKP
  B=ALFA*(YC+CSYMB)/R+Beta*CCKP
  C=ALFA*2C/R+Beta*CMPP
  A2=B*#2+C*#2-#2*(A*#2)*(DTSIN(ALPHA)*#2)
  B2=BE*NP_C*#2+C*#2*(NP_OZ+A*#2*(O*A#2)*SYMB*(DTAN(ALPHA)*#2)
  C2=CSYME*#25*(B2/A2)*#2+C2/A2
  SQUARE=C*#25*(B2/A2)*#2+C2/A2
  IF(SQUARE=0) FILTER=3
  IF(FILTER=0) RETURN
  R=-B2/(4#*A2)+SIGN*DSQRT(SQUARE)
  CALCUL4TE(THETA)-DCSIN(PS10)
  DALE=DCSIN(THETA)/DSIN(PS10)
  DBE=DCSIN((THETA)-DCSIN(PS10))
  DA=DALE*(XC+CSYMB)/R+CEE*CKKP
  DB=DAL #2C/R+DBE*CLLP
  DC=DAL #2C/R+DBE*CMMP
  DA=2#C*B*DB#2-O*C*DC-2#0*A*DA*(DTAN(ALPHA)*#2)
  CB2=DB #1FOY+UC*NPOZ+DA*NPOX+2#0*DA*CSYMB*(DTAN(ALPHA)*#2)
  A3=-0#5*(A2#DB#2-B2#CA2)/(A2#*2)
  B3=S1#5*(B2#DSQRT(0#25*(B2/A2)*#2*(C2/A2))
  C3=0#2*(A2#*2)*(A2#*2)*#2.0#B2*D#2-(B2#*2)*#2.0#A2*(CA2)/(A2**4)-#
  1IC2*CA2/(A2#*2)
  RDCT=A2+B3*C3
  RETURN
END

SUBROUTINE SURF(THETA,R,ROOT,SIGN,FILTER,NPCX,NPOY,NPOZ,PS10,X0,
  1 YU120E,YN120E,B120E,CKKP,CCKP,CMP,CMPP,ALPHA)
  1 INTEGER FILTER
  REAL XC,YC,ZO,NPOX,NPOY,NPOZ,CCKP,CCKP,CMP,CMPP,SIGN
  DOUBLE PRECISION THETA,R,ROOT,PS10,CSYME
  DRO,ALFA,DRC,DC,DZ,A1,A2,A3,B1,B2,B3,C1,C2,C3
  ICAL,DBE,DSIN,(THETA)-DCSIN(PS10)
  ALFA=DSIN((THETA)/DSIN(PS10))
  A=ALFA*(XC+CSYMB)/R+Beta*CKKP
  B=ALFA*(YC+CSYMB)/R+Beta*CCKP
  C=ALFA*2C/R+Beta*CMPP
  A2=B*#2+C*#2-#2*(A*#2)*(DTSIN(ALPHA)*#2)
  B2=BE*NP_C*#2+C*#2*(NP_OZ+A*#2*(O*A#2)*SYMB*(DTAN(ALPHA)*#2)
  C2=CSYME*#25*(B2/A2)*#2+C2/A2
  SQUARE=C*#25*(B2/A2)*#2+C2/A2
  IF(SQUARE=0) FILTER=3
  IF(FILTER=0) RETURN
  R=-B2/(4#*A2)+SIGN*DSQRT(SQUARE)
  CALCUL4TE(THETA)-DCSIN(PS10)
  DALE=DCSIN(THETA)/DSIN(PS10)
  DBE=DCSIN((THETA)-DCSIN(PS10))
  DA=DALE*(XC+CSYMB)/R+CEE*CKKP
  DB=DAL #2C/R+DBE*CLLP
  DC=DAL #2C/R+DBE*CMMP
  DA=2#C*B*DB#2-O*C*DC-2#0*A*DA*(DTAN(ALPHA)*#2)
  CB2=DB #1FOY+UC*NPOZ+DA*NPOX+2#0*DA*CSYMB*(DTAN(ALPHA)*#2)
  A3=-0#5*(A2#DB#2-B2#CA2)/(A2#*2)
  B3=S1#5*(B2#DSQRT(0#25*(B2/A2)*#2*(C2/A2))
  C3=0#2*(A2#*2)*(A2#*2)*#2.0#B2*D#2-(B2#*2)*#2.0#A2*(CA2)/(A2**4)-#
  1IC2*CA2/(A2#*2)
  RDCT=A2+B3*C3
  RETURN
END

```

```

EP S=1.0E-06
SIGN=+1.0
IF ((DAB<=(NPFX)) .GT. EPS) GO TO 50
IF ((DAB<=(NPFY)) .LT. EPS) GO TO 30
IF ((DAB<=(RRY)) .LT. EPS) GO TO 25
CMP=C*C
AP=1.0*(FRX/RRY)**2
BP=DCCS((PSIR)*RRX/RRY**2-1.0
CP=P*(BPF/APP+SIGN*DSQRT(BPP**2-APP*CPP))/APP
CLP=(LCCS((PSIR)-RRX*CKP))/RRY
RETURN
25 CONTINUE
CLP=C*(CS((PSIR)/RRX
CLP=SIGN*DSQRT(1.0-CKP**2))
RETURN
3 C CONTINUE
IF ((DAE<=(NPFZ)) .GT. EPS) GO TO 40
IF ((DAE<=(RRZ)) .LT. EPS) GO TO 35
CLP=C*C
AP=1.0*(RRX/RRZ)**2
BP=DCCS((PSIR)*RRZ/RRZ**2-1.0
CP=P*(BPF/APP+DSQRT(BPP**2-APP*CPP))/APP
CLP=(LCCS((PSIR)-RRX*CKP))/RRZ
RETURN
35 CONTINUE
CLP=C*(CS((PSIR)/RRX
CLP=SIGN*DSQRT(1.0-CKP**2))
RETURN
40 CONTINUE
IF ((DAB<=(RRX)) .GT. EPS) GO TO 45
CLP=C*(CS((PSIR))/RRY-NPY/NPFZ*RRZ)
CMP=-NPFY/NPFZ*CLP
CLP=SIGN*DSQRT(1.0-CLP**2-CMP**2)
RETURN
45 CONTINUE
IF ((DAB<=(NPFY/NPFZ)) .GT. EPS) GO TO 47
CLP=C*(CS((PSIR))/RRX
CMP=-SIGN*DSQRT((1.0-CKP**2)/(1.0+(NPFY/NPFZ)**2)))
CLP=-NPFY/NPFZ*CLP
RETURN
47 CONTINUE
SIGN=-1.C
IF (RRY .LT. 0.0 .OR. RRX .LT. 0.0) SIGN=+1.C
IF (RRY .LT. 0.0 .AND. RRX .LT. 0.0) SIGN=-1.C

```

```

APP = ((RFFY-NPFY/NPFZ*RRZ)/RRX)**2+1.0*(NPFY/NPFZ)**2
BP = Q*DCCS(P$IR)/(RRX)**2-1.0
CP = P=EFF/(2.0*APP)+SIGN*DSQRT(BPP**2-4.0*APP*CPP)/(2.0*APP)
CNP = -NPFY/NPFZ*CLP
CKP = (LCCS(P$IR)-(RRY-NPFY/NPFZ*RRZ)*CLP)/FRX
RETURN
CONTINUE
5 C SIGN=-1.0
IF(RRY-LT.0.0)SIGN=+1.0
IF(RRY-LT.0.0*AND. NPFZ .LT. 0.0) SIGN=-1.0
AA=NPFY*FRY-NPFY*RRX
BB=NPFY*RRZ-NPFZ*RRX
CC=NPFY*CCD(S(P$IR)
IF((DAE<(EB)) .GT. EPS) GO TO 60
CLP=CC/AA
AP=(NPFZ/NPFX)**2+1.0
BP=NPFY*NPFZ/NPFX**2*CLP
CP=(NFFY/NPFY/NPFX)**2+1.0*(CLP**2-1.0*DSQRT(BPP**2-4.0*APP*CPP))/APP
CKP=(-EFP/APP+SIGN*DSQRT(BPP**2-4.0*APP*CPP))/NPFX
RETURN
CONTINUE
6 C
IF(EB .GT. C.0) SIGN=-1.0
AP=(NPFY/NPFX)**2+1.0
BP=(NPFZ/NPFX)**2+1.0
CP=2.0*NPFY*NPFZ/NPFX**2
APP=AP*EF*(AA/BB)**2-CP*AA/BB
BPP=2.0*C*AA*CC*BP/BB**2-CP*CC/BB
CP=BP*(CC/EB)**2-1.0
CLP=EFF/(2.0*APP)+SIGN*DSQRT(BPP**2-4.0*APP*CPP)/(2.0*APP)
CKP=(C/BB*AA/BB*CLP-NPFZ*CMP)/NPFX
RETURN
END

```

APPENDIX B

```

***** C H E C K *****

***** THIS PROGRAM IS DESIGNED TO CHECK THE ACCURACY OF
***** THE TRACE FROM THE MIDPOINT OF EACH SET OF POINTS THAT
***** DEFINE THE FRONT SURFACE THROUGH THE LENS AND TUMARUS
***** THE FOCAL POINT. DEVIATIONS IN THE Y-COORDINATE AT
***** THE FOCAL POINT ARE RECORDED. *****

MAJOR VARIABLE DEFINITIONS:
***** X0,YC : COORDINATES OF MIDPOINT AT FRONT SURFACE
***** THE1AO : INITIAL ANGLE
***** RO : INITIAL RADIUS BETWEEN RADIUS AND RAY DIRECTION
***** PSIC : RAY MATCHING CONSTANT
***** THE1AC : ANGLE OF MINIMUM RADIUS
***** XI,YI : FIRST GUESS COORDINATES AT INNER SURFACE
***** XF,YF : SOLUTION POINT COORDINATES
***** THE1AP : ANGLE AT INNER SURFACE
***** RAD : RADII AT INNER SURFACE
***** PSIF : ANGLE BETWEEN RADIUS AND RAY DIRECTION AT
*****           INNER SURFACE
***** YS : Y-COORDINATE ON IMAGE PLANE

SPECIFICATION STATEMENTS
INTEGER K,I,L,TRIP,EXIT2
DOUBLE PRECISION DIFF,THETAN,THETAP1,THETAH1,P12,BF,RZERO,
1F,ALPHA,RL,N1,N2,N3,N4,SYMB,A,B,P1,P2,Y2,X2,X1,Y1,
1X1(1010),Y1(1010),X2(1010),Y2(1010),X1(1010),Y1(1010),
1I1,1I1P1,I2P,THETAH1,RO,ARG,RSIN,TCRIT,P,SIO,E,PLSUN,
1S,S1,S2,S3,XF,YSIPSIP,ZETA,UP,YSC1010,SIN,EUN,EONR,RP,RPP,BE,
1SL,RSIN,THETA,CHECK1,CHECK2

C REAL INPUT FROM PROGRAM GISL
C READ(5,100)A,B,USY,B,K,ALPHA,N3,F,RL
C DO 5 J=1,K
C READ(5,100)X1(J),Y1(J),X2(J),Y2(J)
C CONTINUE

```

```

C SET CONSTANTS
C
P1=2*PI/2
P12=P1/2
N1=1.0
N3=1.0
EF=F/R
RZERO=(X2(1)+OSYMB)**2+Y2(1)**2+(R**2+CSYMB**2)
IF(OSYMB.LT.-0.6) RZERO=DSCRT(R**2+CSYMB**2)

C START RAY TRACE
C
DO 10 n=2,K
L=J-1
TRIP=0

C CALCULATE MIDPOINT
C
S=(Y1(J)-Y1(L))/(X1(J)+X1(L))/2.
XU=(X1(J)+X1(L))/2.
YU=(Y1(J)+Y1(L))/2.

C CALCULATE LINE CONSTANTS
C
L1=PI2-LATAN(S)
THETAO=LATAN(Y0/(X1+OSYMB))
IF(THETAO<LT.0) THETAO=PI+THETAO
RO=DCSRJ(Y0**2+(X0+LCSYMB)**2)
CALL INRECT(RO,N20,A,B,RZERO)
L1P=DASIN((N1/N20)*DSIN(L1))
PS10=P1-THTAO-N1+T1P
EPSLN=1.0*CT*PI2*QR*PSI0.LT.0.0) EPSLN=-1.0
E=RO*N2C*CSIN(PSI0)
ARG=DSCRT(LA**2+4*B*(E**2)/(RZERO**2))
RSINC=CARSLN((2*(E**2)/(RO**2)-A)/ARG)
C=PI2-FCINC
TCRIT=PI2-(EPSLN/2.)*(PI2-RSINC)
IF(PSI0.LT.FI2) C=0.0

```

C FIND FIRST GUESS COORDINATES, RADIUS AND ANGLE

```

S1=-DTAN(L1-T1P)
S2=DTAN(ALPHA)
X1=(YO-S1*X0)/(S2-S1)
Y1=(S2*X1)
THETAP=LATAN(Y1/(X1+OSYMB))

```

```

IF (THETAP .LT. 0.0) THETAP=THETAP+PI
RP=CSQR((Y1**2+(X1+OSYM)*2))
EE=-OSYME
SL=1.0

C GL TO THETA IN TERMS OF RADIUS ITERATION IF ANGLE LARGE
C
C IF (THETAP .GT. 2.0) GO TC 25

C NEWTON-RAPSON ITERATION
C
C 2 CONTINUE
TRIP=TRIP+1
IF (THETAP .GE. TCRIT) THETP=THETAP-C
IF (THETAP .LT. TCRIT) THETP=THETAP
IF (THETAP .GE. TCRIT) EPSLN=+1.0
THETA=THETP-THETAO
CALL RADYUS(ARGRSNO,THETAH,RAD,RDG) FILTER,A,EPSLON,E
CALL RADCLS(CSYM,S2,THETAP,RADD,RDGG)
RDF=RAD-RADD
RCT=FCG-RDG
FACTCR=1.7/(DABS(PS10))
FACTCR=1.0/10.0 FACTCR=10.0
IF (CSYM .GT. 0.0) FACTCR=1.3
THETAN=THETP-THETAO
DIFF=DABS(THETAN-THETAO)
EXIT=0.00001*DABS(PS10)
IF (CSYM .GT. 0.0) EXIT=0.000001
EXIT=200
IF (TRIP .LT. EXIT) GO TO 30
IF (TRIP .GT. EXIT) GO TO 20
THETA=THETP
GO TC 20

C THETA IN TERMS OF RADIUS ITERATION
C
C 25 TRIP=TRIP+1
RSIN=CARSLN((2*E**2/RP**2-A)/(ARG))
THETA=THETAO-EPSLN/2*(RSIN-RSINC)
CHECK1=THETA-THETAO
RPP=E/(CSIN(THETA)-SL*D COS(THETA))
CHECK2=DABS(RP-RPP)
THETAF=THETA
RP=RFF
IF (TRIP .GT. 100) GO TO 26
IF (CHECK2.LT.0.000001) GO TU 26
GO TC 25
RAD=RFF

```

```

C CALCULATE FINAL POINT AT INNER SURFACE COORDINATES AND ANGLES
C
3C XF=RAD*(COS(THETAP))-OSYMB
3C YF=RAD*(CSIN(THETAP))
CALL INCEX(RAD)N2,A,B,RZERO)
EONR=E/(N2*RAD)
IF(EONR.GT.1.0) WRITE(6,630)
IF(EONR.LT.-1.0) EUNR=1.0
PSIP=DAFSIN(EUNR)
IF(THETAP.LT.TCRIT.AND.PS10.GT.0.0) PSIP=PI-PSIP
ZETA=P1-THETAP-PSIP
I2=F12-ZETA-TALPHA
EON=(N2/A3)*DSIN(12)
IF(EON.GT.1.0) WRITE(6,640)
IF(EON.LT.-1.0) ECN=1.0
I2P=DAFSIN(EUN)
UP=P12-ALPHA-I2P

C CALCULATE Y-COORDINATE AT FOCAL PCINT
S3=-DTAN(I2P)
YS(J)=S3*(F-XF)+YF
WRITE CUTFIT
1C CONTINUE
1C STCP

C FORMAT STATEMENTS
10C FURMAT(1X,3F11.7)15,F10.7,3F5.3)
20C FURMAT(1X,4F10.7)
50C FURMAT(1X,16.2F16.8)16)
63C FURMAT(1X,'WHOOPS PSIP ARSIN')
64C FURMAT(1X,'WHOOPS AGAIN I2P ARSIN')

C END

C SUBROUTINE INDEX CALCULATES THE INDEX OF REFRACTION AS A FUNCTION
C OF RADIALS FROM THE CENTER OF SYMMETRY. THE VALUES OF THE INDEX
C CONSTANTS ARE USER INPUTS.
SUBROUTINE INDEX(R,N,A,B,RZERO)
DOUBLE PRECISION N,A,B,R,RZERO
N=LSQRT((A+B*(R/RZERO))**2)
RETURN

```

END

SUBROUTINE RADYUS(ARG,R,SING,ANGLE ,R ,DR ,FILTER ,A ,EPSLON ,E)
THE SPECIFIED ANGLE AS WELL AS ITS DERIVATIVE WITH RESPECT TO
ANGLE .

```
      SUBROUTINE RADYUS( ARG,R,SING,ANGLE ,R ,DR ,FILTER ,A ,EPSLON ,E )
      INTEGER FILTER
      DOUBLE PRECISION ANGLE ,R ,DR ,FILTER ,A ,EPSLON ,E ,FRACTN
      DOUBLE PRECISION(-2.0*EPSLON*ANGLE +R*SING)
      FRACTN = C
      IF ((A+ARG)*FRACTN <= 0.0) GOTO 10
      R = SQR((2.0)*DABS(E)/DABS(A+ARG*FRACTN))
      IF (FRACTN <= -0.989) GOTO 10
      DR = ((EPSLON*R#*3)/(2.0*E#*2))*DCOS((-2.0*EPSLON*ANGLE +R*SING)
      1C CONTINUE
      FILTER = C
      IF ((A+ARG)*FRACTN <= -0.989) FILTER = 2
      IF ((A+ARG)*FRACTN) .LT. 0.0) FILTER = 1
      RETURN
      END
```

SUBROUTINE RADYUS CALCULATES THE RADIALS TO THE FRONT SURFACE AT
THE SPECIFIED ANGLE AND ALSO THE DERIVATIVE WITH RESPECT TO
ANGLE .

```
      SUBROUTINE RADYUS(SYMB ,S ,THETAP ,RACC ,RDGG )
      DOUBLE PRECISION THETAP ,SYMB ,S
      RACC = -C*SYMB #S/(DSIN(THETAP))-S*DCCS(THETAP))/_
      RDGG = S*(SYMB *(DCOS(THETAP)+S*D SIN(THETAP))-
      1((DSIN(THETAP)-S*DCCS(THETAP))#2))
      RETURN
      END
```

APPENDIX C

```

DETECTOR FORTRAN
*****
THIS PROGRAM IS DESIGNED TO COMPLETE THE RAY TRACE OF
A MIRROR AND DETECTOR SYSTEM. RAYS THAT LEAVE THE LENS
ARE TRACED TO THE MIRROR, THEN REFLECTED OFF AND TRACED
TO THE DETECTOR. THIS PROCESS IS REPEATED FOR EACH
INCREMENT OF MIRROR ANGLE. THE NUMBER OF RAYS STRIKING
THE BUFFER AND LOWER HALF OF THE DETECTOR ARE STORED AT
EACH ANGLE AND THEN THIS INFORMATION IS OUTPUT SO THAT
APPROPRIATE PLOTS MAY BE MADE.

VARIABLE DEFINITIONS
BF : DISTANCE FROM FOCAL POINT TO CONE APEX
ALPHA : CONE ANGLE OF BACK LENS SURFACE
ALFAP : ANGLE OF RADIATION INCIDENT TO LENS
DETP : DETECTOR POSITION
DETS : DETECTOR RADIAL SIZE
MIRP : MIRROR PIVOT POSITION
XC,YC,ZC : COORDINATES OF RAY EXITING LENS
XM,YM,ZM : COORDINATES OF RAY AT MIRROR SURFACE
XC,ZD : COORDINATES OF RAY AT DETECTOR (XD=DETP)
CK,CLL,CMM : DIRECTION COSINES OF RAY FROM MIRROR TO DETECTOR
CKK,CLL,CMM : DIRECTION COSINES OF RAY FROM MIRROR TO DETECTOR
COUNT1 : RAY COUNT ON UPPER DETECTOR
COUNT2 : RAY COUNT ON LOWER DETECTOR

SPECIFICATION STATEMENTS
INTEGER JK,L,OUT1,OUT2(500),COUNT1(500),COUNT2(500),
1TERM1,TERM2
REAL BF,ALPHA,P1,P12,DETP,DETS,MIRP,THETM(200),XU(500),YU(500),
1ZU(500),CKL(500),CL(500),CM(500),DL(500),FL(500),YL(500),ZL(500),
1CKK,CLL,CMM,YD(500),ZD(500),ALFAP,THETD(500)

READ IN LENS CONSTANTS
READ (5,100) BF,ALPHA,ALFAP

```

۲۰۰

103

```

C SET CONSTANTS
P1=3.14159
P12=P1/2.
DETIP=0.4
MIRP=1.4
THETC=66.6*PI/180
DETIP*TAN(ALPHA)
DETJM(1)=THETC-0.20404040
J=C
L=1
CUT1=0
TERM1=C
TERM2=0

C READ IN RAY DATA REJECTING RAYS BLOCKED BY DETECTOR
10 J=J+1
    REAC(SQR1(YC(J)*Z0(J)*Z0(J)*Z0(J)),YC(J),CL(J),CL(J))
    IF(SQR1(YC(J)*Z0(J)*Z0(J)*Z0(J))<=DET) GO TO 11
    IF(X0(J).EQ.-1.0.AND.Y0(J).EQ.1.0.EQ.1.0.AND.Z0(J).EQ.1.0) TERM1=J
    GU TO 12
11 J=J-1
    CUT1=0
    GO TO 12
12 CONTINUE

C INCREMENT MIRROR ANGLE AND CHECK FOR COMPLETE SHEEP
20 L=L+1
    K=L-1
    THETM(L)=THETM(K)+0.00404040
    THETD(L)=THETM(L)+180/P1
    IF(THETM(L)>180) GT THETC+20,TERM2=L-1
    IF(WRITE(200)) THETM(L)=OUT1; TERM1=TERM2
    IF(THETM(L).LT.0) OUT1=TERM1; TERM1=TERM2
    CUT2(L)=0
    CUT3(L)=C
    COUNT1(L)=0
    COUNT2(L)=0

C C RAY TRACE FROM BACK LENS SURFACE TO MIRROR AND THEN TO DETECTOR
30 J=C+1

```

```

C IF(J.EEQ.JERM1) GC TC 20
C FIND MIRROR INTERSECTION POINT DISCARD RAYS OUTSIDE MIRROR
D1=(TAN(THETM(L))*((XO(J)-MIRP)-YC(J))/((CL(J)-CK(J))*TAN(THETM(L)),)
XM(J)=CL*CK(J)+XC(J)
YM(J)=CL*CK(J)+ZC(J)
ZM(J)=CL*CK(J)+YC(J)
WRITE(*,1000) XM(J),YM(J),ZM(J)
IF(SQRT((2M(J)*#*2+(CCS(THETM(L))*YM(J))*#*2)) .GT.1.0)
1 CUT2(L)=CUT2(L)+1
IF(SQRT((2M(J)*#*2+(CCS(THETM(L))*YM(J))*#*2)) .GT.1.0) GO TO 30
C FIND DIRECTION OF RAY REFLECTED FROM MIRROR SURFACE
CKK=+CCS(2*THETM(L))*CK(J)+SIN(2*THETM(L))*CK(J)
CLL=-CCS(2*THETM(L))*CL(J)+SIN(2*THETM(L))*CK(J)
CMY=CM(1)
WRITE(6,1010) CK(J),CL(J),CM(J),CKK,CLL,CMY
C FIND INTERSECTION WITH DETECTOR DISCARD RAYS MISSING DETECTOR
D2=(DET1F-XM(J))/CKK
YD(J)=E2*CLL+YM(J)
ZD(J)=E2*CMY+ZM(J)
IF(SQRT((YD(J)*#*2+ZD(J)*#*2)) .GT. DETS) CUT2(L)=CUT3(L)+1
IF(SQRT((YD(J)*#*2+ZD(J)*#*2)) .GT. DETS) GO TO 3C
C COUNT RAYS HITTING UPPER AND LOWER PARTITIONS OF DETECTOR
IF(YD(J)>0.0) COUNT1(L)=COUNT1(L)+1
IF(YD(J)<0.0) COUNT2(L)=COUNT2(L)+1
GO TO 2C
C WRITE OUTPUT
C 40 CON1INE(6,1005) ALFAP
DO 50 L=2 TERM2
WRITE(6,101C) THETD(L),COUNT1(L),COUNT2(L)
50 CON1INE
STCP
C FORMAT STATEMENTS
C 100 FORMAT(1X,3F10-7)
C 200 FORMAT(1X,6F10-7)
C100C FORMAT(1X,3F10-6)

```

DET01450
DET01460
DET01470
DET01480
DET01490
DET01500

C101C FORMAT(1X,6F10.6)
C200C FORMAT(1X,F10.7,3I10)
C200C FORMAT(1X,F10.6)
C201C FORMAT(1X,F10.6,2I5)
C ENCL

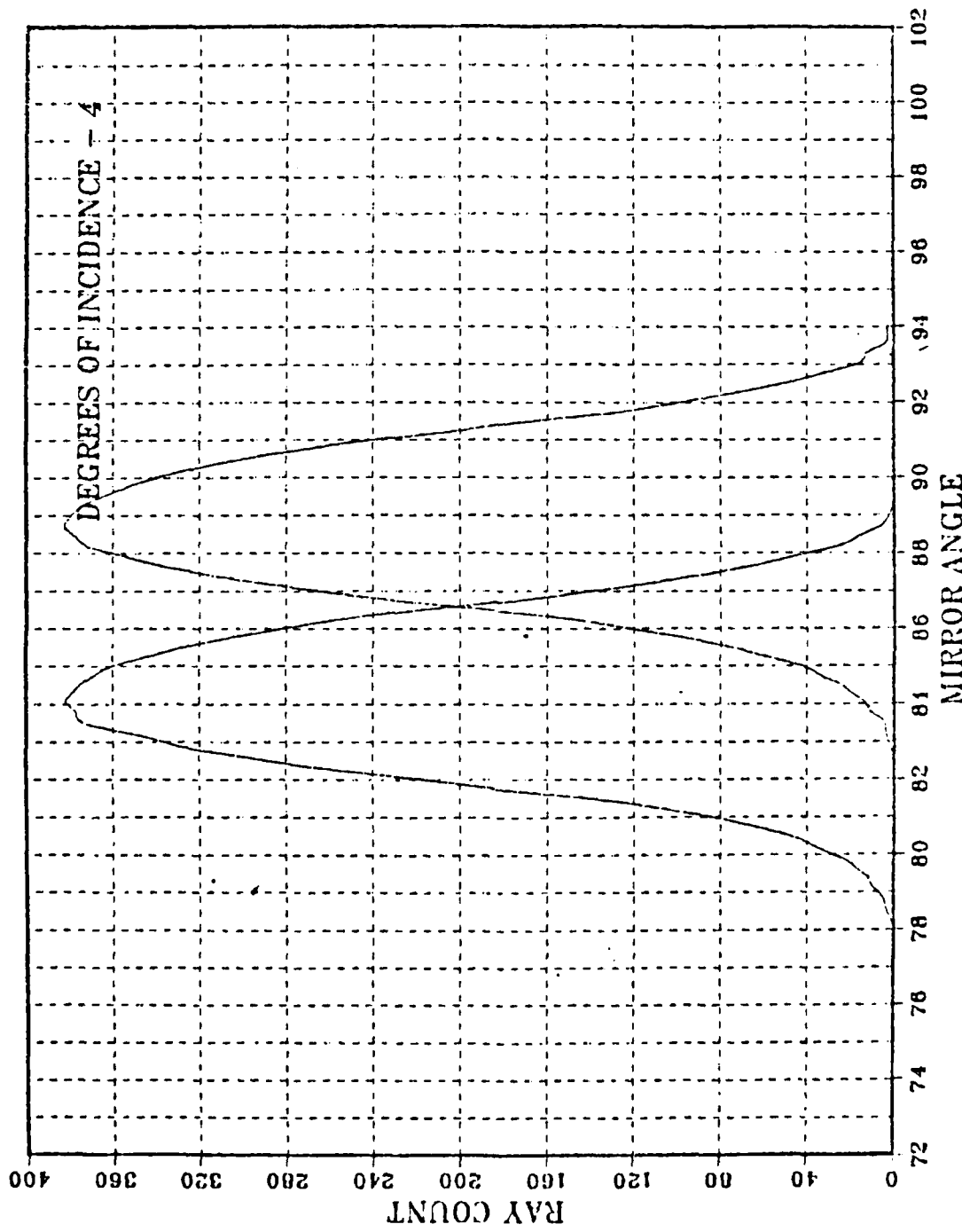


Figure D-1. Detector Signal at 4 Degrees Incidence.

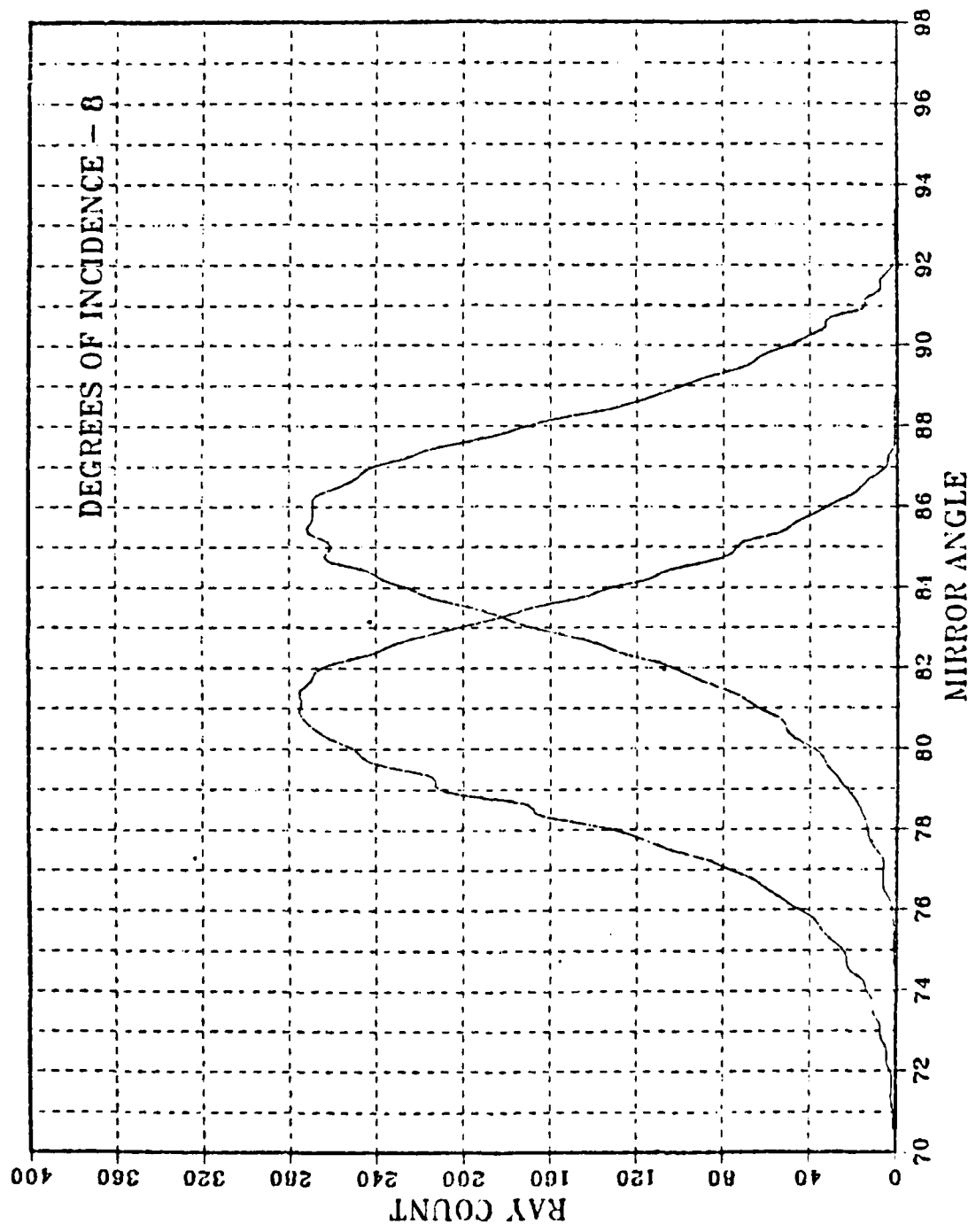


Figure D-2. Detector Signal at 8 Degrees Incidence.

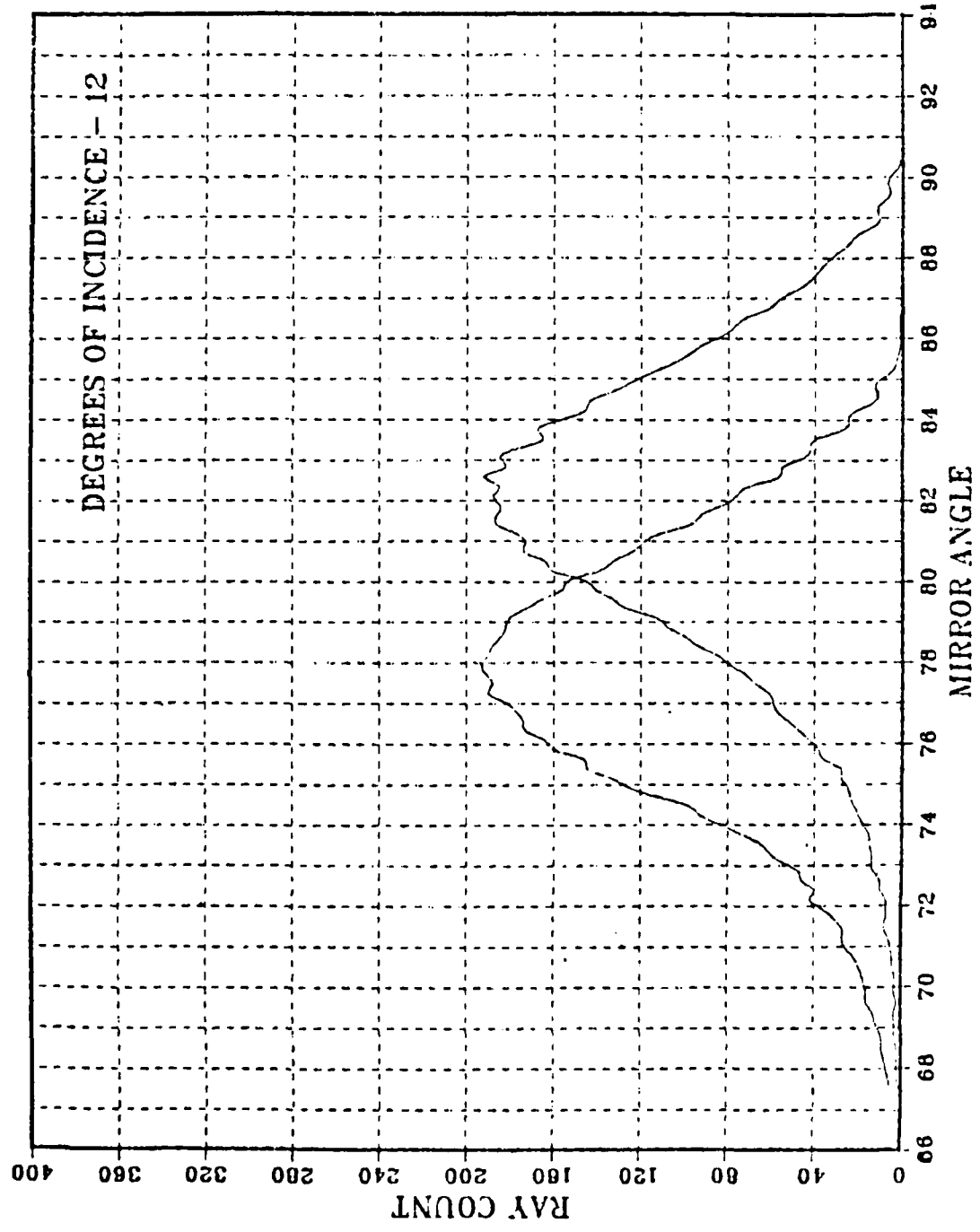


Figure D-3. Detector Signal at 12 Degrees Incidence.

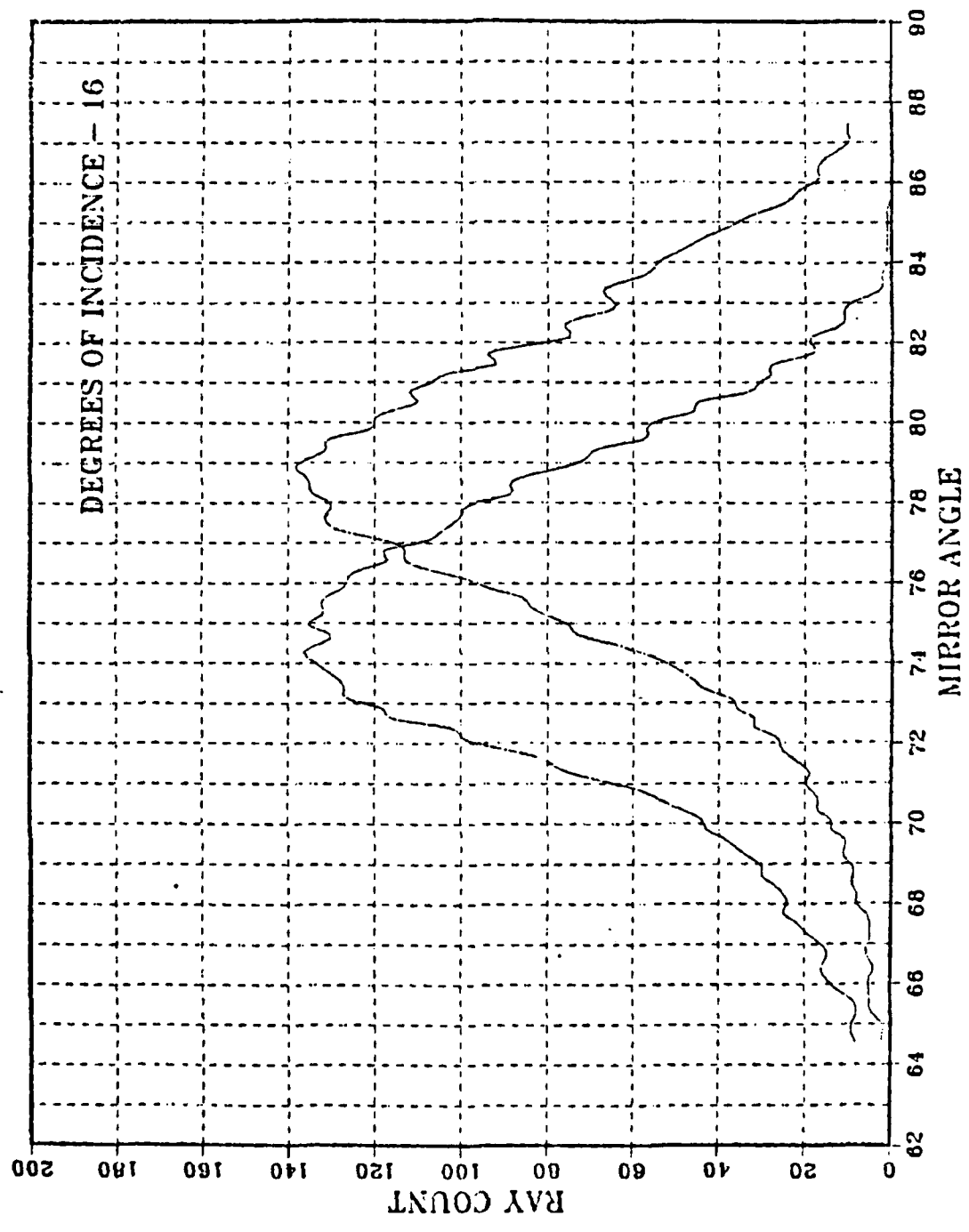


Figure D-4. Detector Signal at 16 Degrees Incidence.

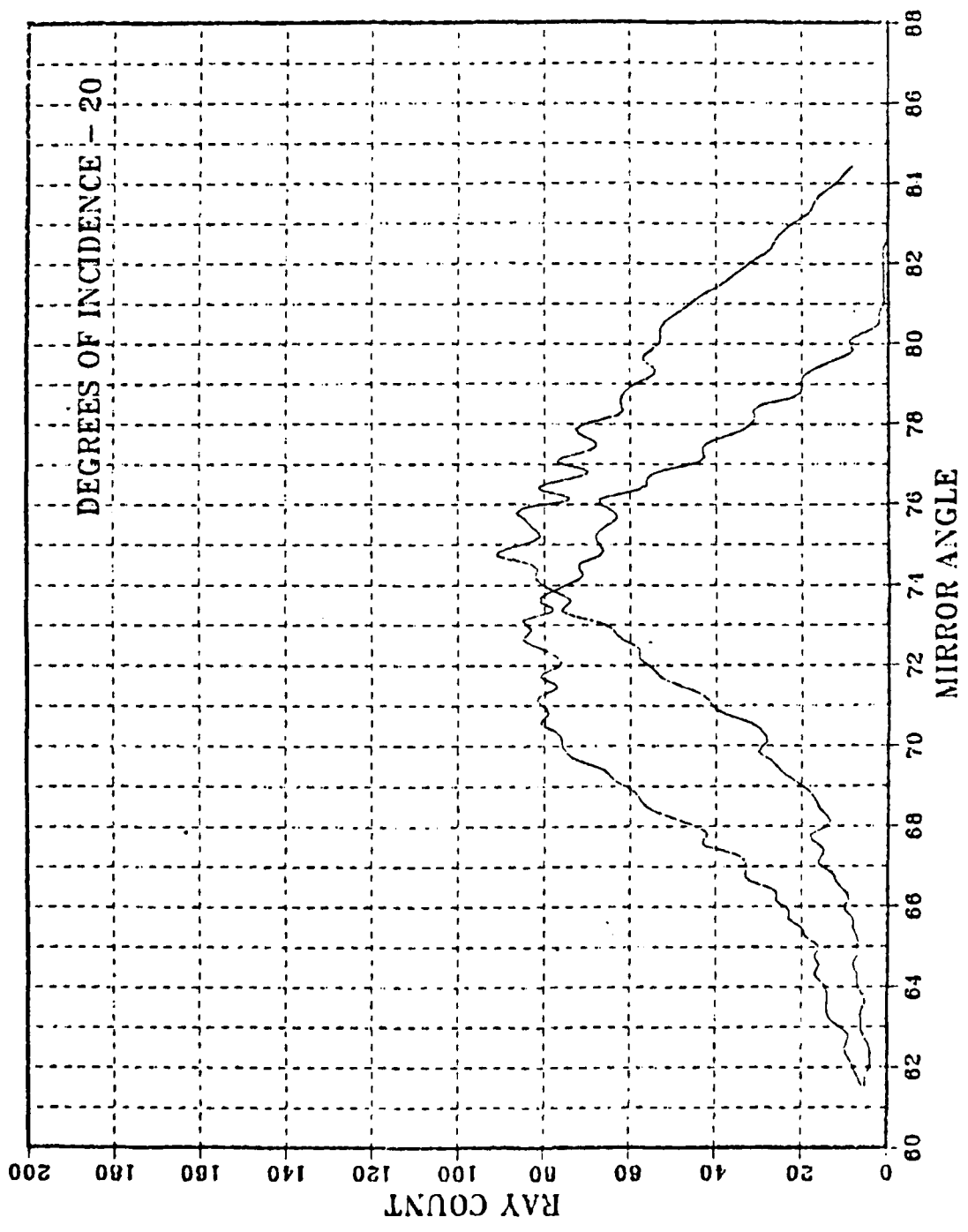


Figure D-5. Detector Signal at 20 Degrees Incidence.

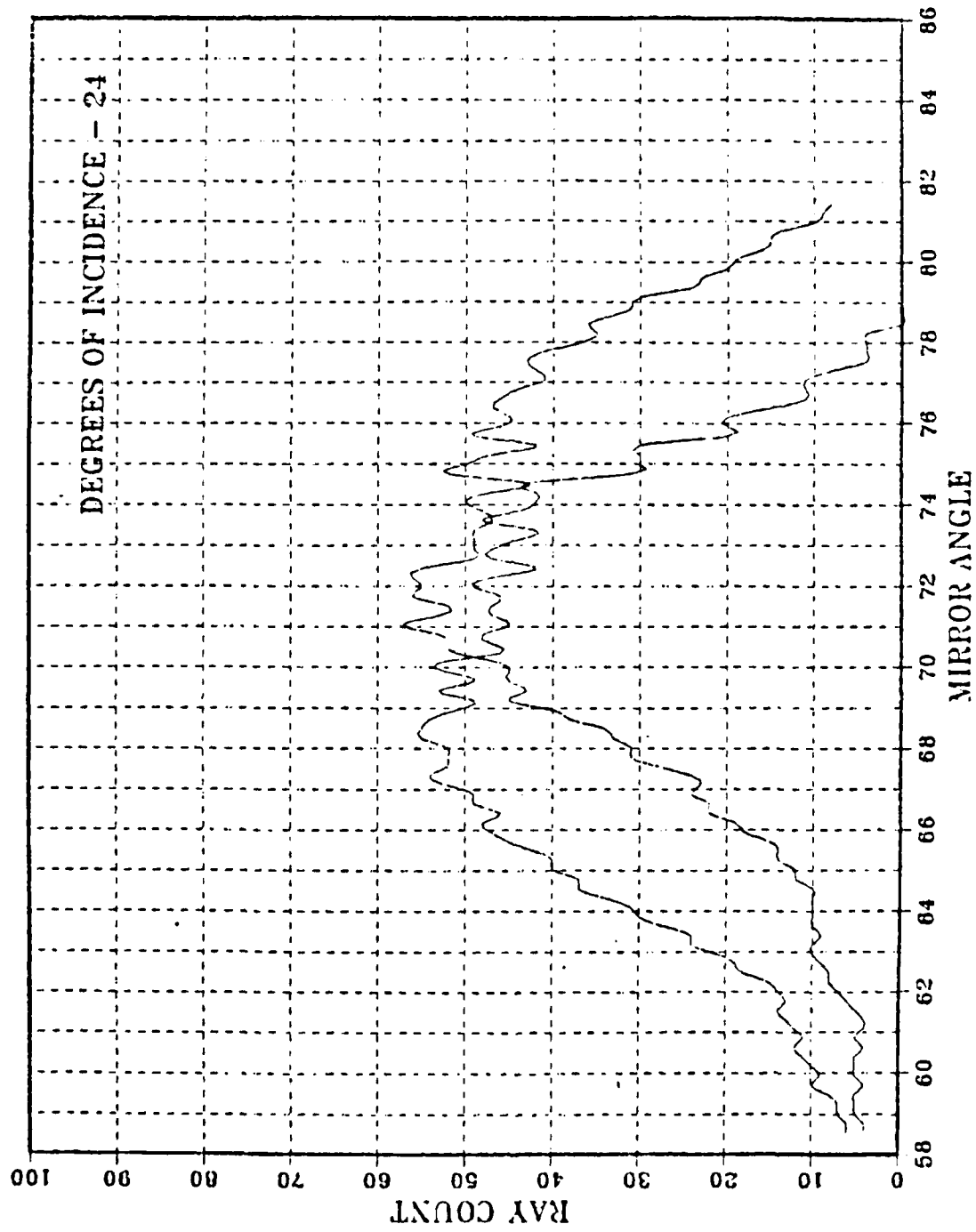


Figure D-6. Detector Signal at 24 Degrees Incidence.

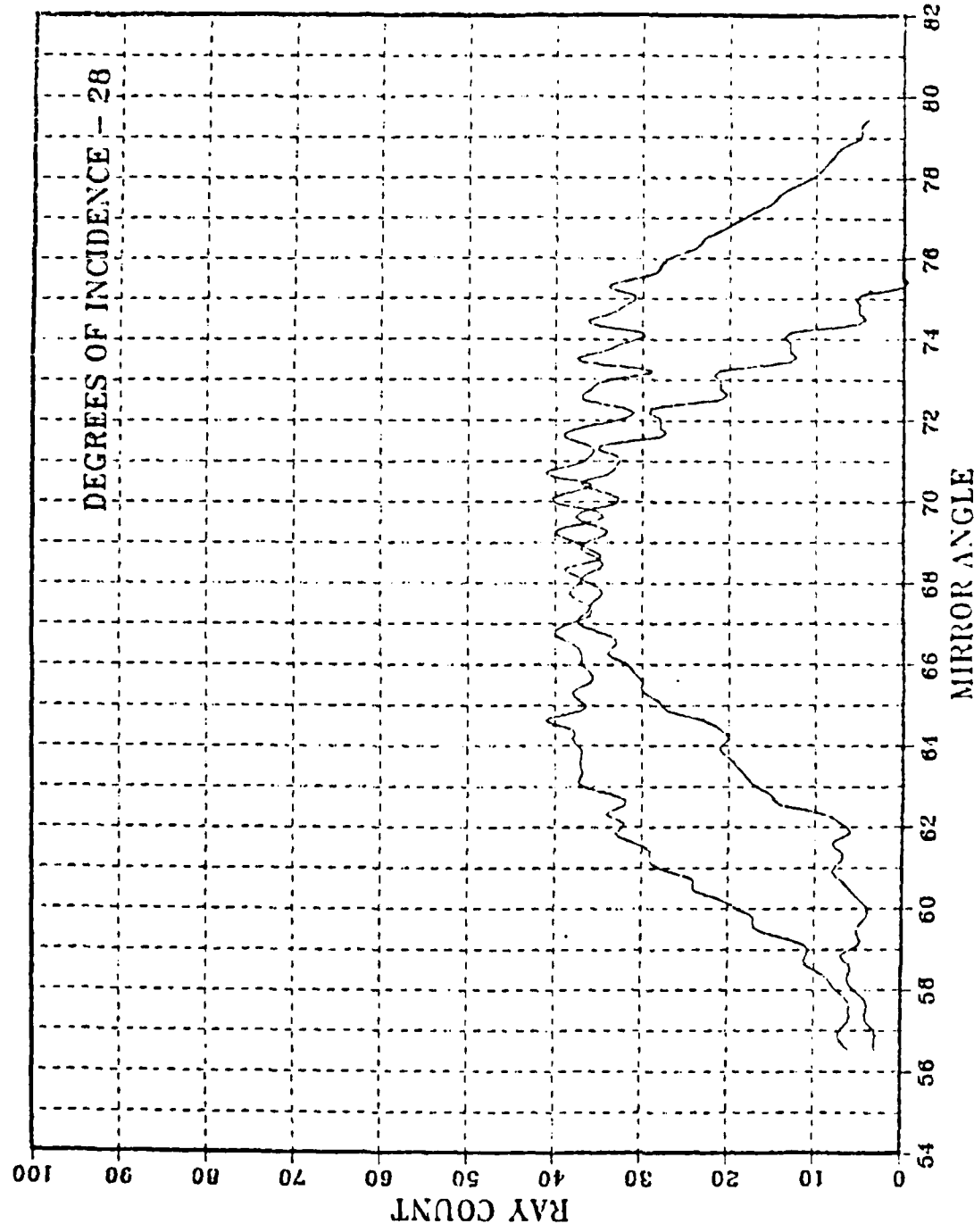


Figure D-7. Detector Signal at 28 Degrees Incidence.

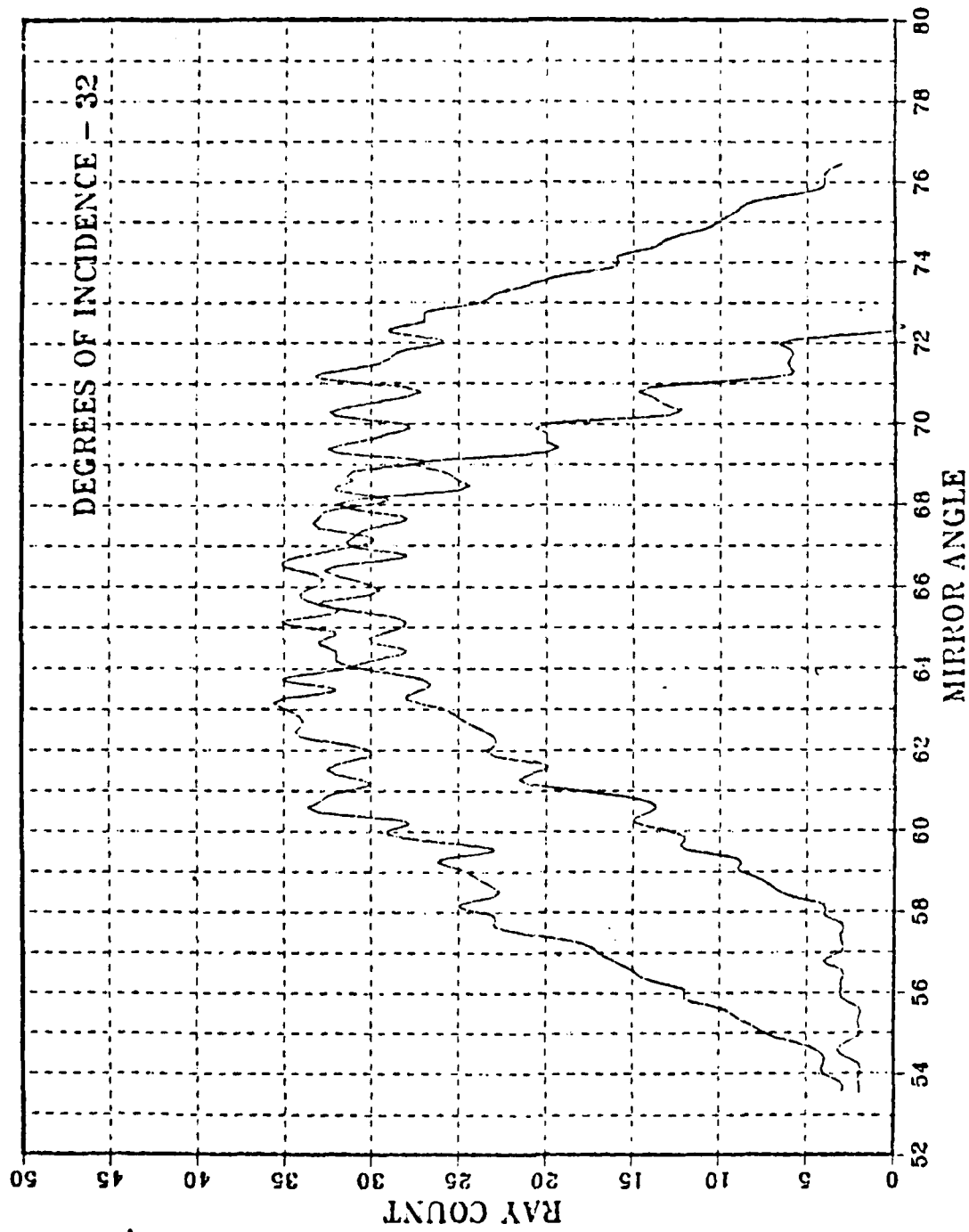


Figure D-8. Detector Signal at 32 Degrees Incidence.

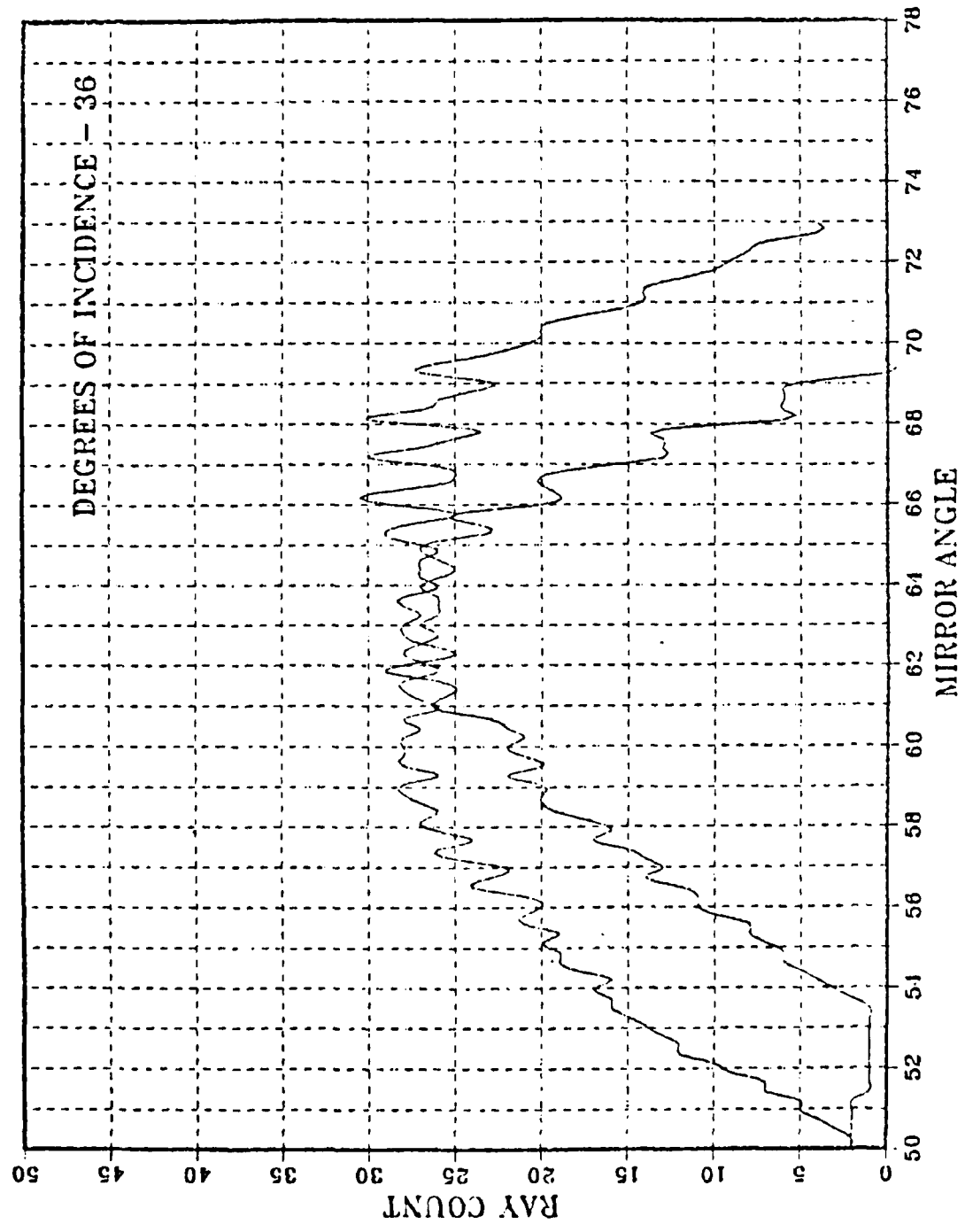


Figure D-9. Detector Signal at 36 Degrees Incidence.

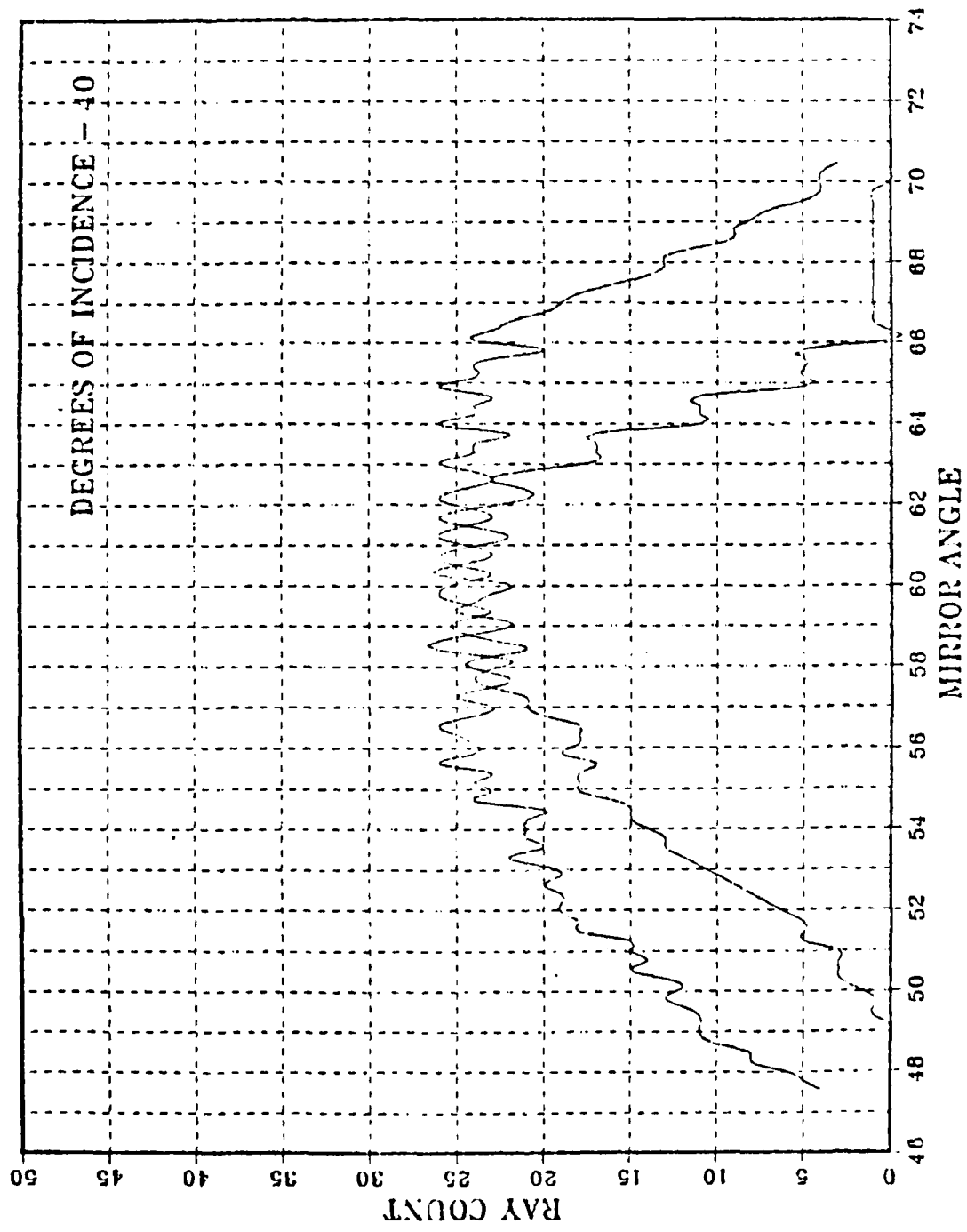


Figure D-10. Detector Signal at 40 Degrees Incidence.

LIST OF REFERENCES

1. Frazier, Robert L., Exterior Ballistics, Guidance Laws and Optics for a Gun-Launched Missile, M. S. Thesis, Naval Postgraduate School, Monterey, California, December 1980.
2. Terrell, James M., Conical Lens for a 5"/54 Gun Launched Missile, M. S. Thesis, Naval Postgraduate School, Monterey, California, June 1981.
3. Amichai, Oded, Sharp Nose Lens Design Using Refractive Index Gradient, Naval Postgraduate School Contractor Report NPS67-82-003CR, Monterey, California, June 1982.
4. Carr, Herbert M., Aerodynamically Efficient Gradient Refractive Index Missile Seeker Lens, M. S. Thesis, Naval Postgraduate School, Monterey, California, October 1982.
5. Marchand, Erich W., Gradient Index Optics, Academic Press, 1978.
6. U. S. Army Missile Command Technical Report RG-CR-32-6, Gradient Index Lens Research-Final Report, by D. T. Moore, p. 36, 19 October 1981.
7. U. S. Army Missile Command Technical Report H8 3-3-BO20-1, Gradient Index Optics Application by R. L. Light, 30 September 1983.
8. D. S. Davidson and A. E. Fuhs, Tracing Nearly Radial Lines in a Spherically Symmetric Gradient Index Lens, Applied Optics, Letter to Editor (in press).

INITIAL DISTRIBUTION LIST

	No. Copies
1. Defense Technical Information Center Cameron Station Alexandria, Virginia 22314	2
2. Library, Code 0142 Naval Postgraduate School Monterey, California 93943	2
3. Directorate of Land Armament and Electronics Engineering and Maintenance Attn: Colonel B. L. Code National Defense Headquarters Ottawa, Ontario, Canada K1A 0K2	2
4. Distinguished Professor A. E. Fuhs Code 67Fu Department of Aeronautics Naval Postgraduate School Monterey, California 93943	4
5. Col. R. Larriva, USMC Defense Advanced Research Projects Agency 1400 Wilson Boulevard Arlington, Virginia 22209	2
6. Charles R. Christensen Research Directorate U. S. Army Missile Command (DRSMI-RRO) Redstone Arsenal, Alabama 35898	1
7. Commander, U. S. Army Missile Command (DRSMI-ROA) Redstone Arsenal, Alabama 35898 Attn: CAPT H. Carr	1
8. Professor A. E. Milne Code 61Mn Naval Postgraduate School Monterey California 93943	1
9. Professor D. T. Moore University of Rochester Rochester, New York 14627	1

- | | | |
|-----|--|---|
| 10. | Dr. Lloyd Smith
Code 3205
Naval Weapons Center
China Lake, California 93555 | 1 |
| 11. | Directorate of Land Armament and Electronics
Engineering and Maintenance
Attn: Capt. D. Davidson
National Defense Headquarters
Ottawa, Ontario, Canada K1A 0K2 | 2 |
| 12. | Directorate of Personnel Education
and Development (DPED)
National Defense Headquarters
Ottawa, Ontario, Canada K1A 0K2 | 1 |